SYSTEM IDENTIFICATION OF A GENERAL AVIATION AIRCRAFT USING A PERSONAL ELECTRONIC DEVICE

A Dissertation
Presented to
The Academic Faculty

by

Michael Nothem

In Partial Fulfillment
of the Requirements for the Degree
Master of Science in the
Daniel Guggenheim School of Aerospace Engineering

Georgia Institute of Technology
May 2019

SYSTEM IDENTIFICATION OF A GENERAL AVIATION AIRCRAFT USING A PERSONAL ELECTRONIC DEVICE

Approved by:

Dr. Dimitri Mavris, Advisor
Daniel Guggenheim School of Aerospace Engineering
Georgia Institute of Technology

Dr. Simon Briceno
Daniel Guggenheim School of Aerospace Engineering
Georgia Institute of Technology

Dr. Kyle Collins
Daniel Guggenheim School of Aerospace Engineering
Georgia Institute of Technology

Date Approved: April 15, 2019

TABLE OF CONTENTS

LIST OF TABLES

LIST OF FIGURES

LIST OF SYMBOLS AND ABBREVIATIONS

6-DOF	6-Degree-of-Freedom
AC	Advisory Circular
AFM	Aircraft Flight Manual
AHRS	Attitude and Heading Reference System
ANN	Artificial Neural Network
AoA	Angle of Attack
ASIAS	Aviation Safety Information Analysis and Sharing
CFD	Computational Fluid Dynamics
CG	Center of Gravity
DCM	Direction Cosine Matrix
EEM	Equation Error Method
EFB	Electronic Flight Bag
EKF	Extended Kalman Filter
FAA	Federal Aviation Administration
FAR	Federal Aviation Regulations
FDM	Flight Data Monitoring
FDR	Flight Data Recorder
FDX	Flight Data Exchange
FGDS	FlightGear Desktop Simulator
FOQA	Flight Operational Quality Assurance
GA	General Aviation
GAARD	General Aviation Airborne Recording Device

GPS	Global Positioning System
LTI	Linear Time Invariant
LOC	Loss of Control
MLE	Maximum-Likelihood Estimation
NED	North-East-Down Reference Frame
NGAFID	National General Aviation Flight Information Database
NTSB	National Transportation Safety Board
OEM	Output Error Method
PED	Personal Electronic Device
PFD	Primary Flight Display
POH	Pilot's Operating Handbook
SA	Situational Awareness
SysID	System Identification
UAV	Unmanned Aerial Vehicle

SUMMARY

System Identification (SysID) is the process of obtaining a model of system dynamics by analyzing measurement data. SysID is often used in flight testing to obtain or refine estimates for aircraft stability and control derivatives and performance. Recent applications have shown that SysID can also be used to monitor and update models of dynamics and performance during routine operations.

General Aviation (GA) continues to see higher accident rates than other aviation sectors. To combat this, research into accident mitigation strategies, especially loss of control (LOC) accidents, has led to the development of energy-based or envelope-based safety metrics that can be used to monitor and improve the safety and efficiency of GA operations. However, these methods depend on the existence of an accurate aircraft model to predict the performance and dynamics of the aircraft. The diversity of the aging GA fleet has established the need to calibrate existing models using flight data. SysID therefore has the potential to improve these methods by monitoring and updating aircraft models for each individual GA aircraft.

Any SysID process depends on the type and quality of measurement data available as well as the nature of the aircraft model (what parameters are being identified) and the method of SysID being used. As opposed to flight test SysID, availability of flight data can be limited in GA. However, flight data recording using Personal Electronic Devices (PEDs) or low-cost Flight Data Recorders (FDRs) is becoming common. The capabilities of SysID methods using data from these devices has yet to be explored.

This work demonstrates a process for evaluating SysID techniques for GA aircraft using data from a PED. A simulator environment was created that allowed testing of a variety of SysID and estimation methods. An observability condition was developed and used to inform decisions regarding model parameters and necessary assumptions. The results of this process provide a proof for existence and uniqueness of a solution to the minimization problem that SysID aims to solve. Local observability and global identifiability were also used to divide the "blind" SysID process into two estimations: an online estimation of aircraft states and unknown controls, and an offline identification of model parameters. Two SysID methods were then compared: Output Error Method (OEM), and Filter Method using an Extended Kalman Filter (EKF). It was shown that OEM outperformed EKF at the expense of increased computational burden. Potential improvements to both OEM and EKF SysID in this context are discussed. However, using OEM resulted in improved estimates of performance and dynamics over an assumed *a priori* model. These improvements were robust to both sensor quality and assumptions in the model, therefore demonstrating the potential of SysID using PED data to improve GA safety and efficiency.

CHAPTER 1. INTRODUCTION AND MOTIVATION

System Identification (SysID) is the process of obtaining a mathematical model of a system using measurement data. Systems of interest can be modelled as correlations between measurements or between known inputs and outputs. SysID aims to obtain this correlation which is a parameterized mathematical model of the system. In aerospace engineering and aviation, SysID is often used to obtain the stability and control derivatives of an aircraft model. The physics governing aircraft motion are parameterized in terms of these derivatives and the SysID process obtains the values of these parameters that matches the aircraft model to measured flight data. The resulting parameters define the 6-degree-of-freedom (6-DOF) model of the aircraft.

SysID is a powerful tool for obtaining an aircraft's dynamic model in flight test. Aircraft manufacturers use stability and control derivatives to assess handling qualities, compute performance for the creation of charts in a Pilot's Operating Handbook (POH) or Aircraft Flight Manual (AFM), design controllers, and other related tasks. SysID is the last step in the refinement of these models; Computational Fluid Dynamics (CFD) and/or wind tunnel tests may also be conducted to estimate the aircraft model, but SysID is used to refine and update these estimates using actual flight data.

Outside of flight test, SysID has received interest in applications such as health and performance monitoring and adaptive control. Active SysID can be used to detect changes in aircraft dynamics which can be used to update control architecture in real-time [1] [2] [3]. Active SysID can also be used to estimate unmeasured quantities besides aircraft parameters, such as angle of attack, sideslip, and wind direction [4] [5]. The capability of

SysID to solve these problems, and many others, make it a potentially useful tool for General Aviation.

General Aviation (GA) refers to any flight that does not fall under the category of commercial, airline, cargo, or military flights. Civil aviation refers to all non-military flights and includes operations governed under Federal Aviation Regulations (FAR) parts 121 and 135. The remaining portion of civil aviation is encompassed by GA. Included in GA are such operations as personal and recreational flying, flight instruction, emergency medical services, inspection flights, and many more. As seen below in Figure 1, GA accounts for roughly half of all aviation operations in the United States [6].

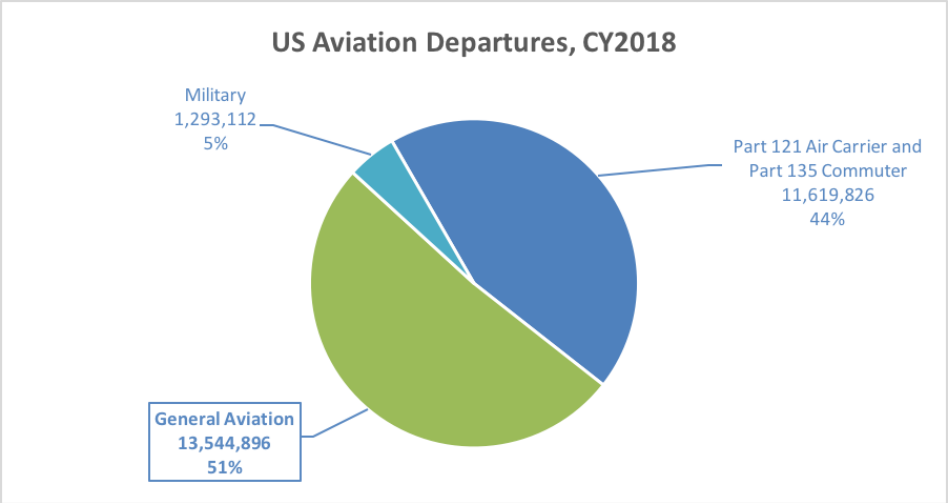

Figure 1. FAA Traffic Flow Statistics, 2018

Even though GA makes up only half of aviation activity by flight, these operations accounted for 95% of all civil aviation accidents in 2015. Specifically, personal and recreational flying accounted for 65% of all accidents and 85% of fatal accidents. NTSB accident statistics for 2015 are displayed below in Figure 2 [7].

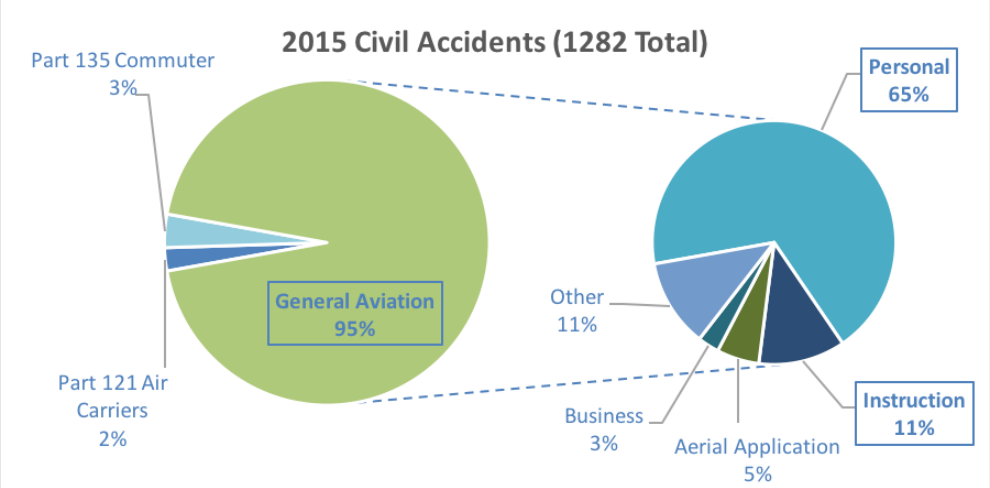

Figure 2. NTSB Accident Statistics, 2015

The above figures clearly show that GA accident rates are higher than in other aviation operations. As such, many research efforts and studies have been undertaken to try to understand how the accident rate might be reduced. One such initiative is called "data-driven safety". In 2004, the FAA published Advisory Circular (AC) 120-82: Flight Operational Quality Assurance (FOQA) [8]. FOQA (also referred to as Flight Data Monitoring or FDM) encourages operators to use flight data recorders (FDR) to obtain data about each flight and to use that data to identify risk areas in their operation. Mitigations to these risk areas can then be identified and applied, and the effectiveness of these mitigations can be quantified by continuing to record and analyze flight data. AC 120-82 was published as a resource for operators to implement FOQA and identifies potential safety metrics to use.

FOQA has been shown to have a significant impact in reducing safety exceedances on many operations [9]. However, FOQA as described in AC 120-82 is mainly a tool for large commercial operators such as part 121 and 135; the infrastructure and data analysis

necessary to successfully implement a FOQA program can be inhibiting to smaller, low-budget operations [10] [11]. As a result, the Aviation Safety Information Analysis and Sharing (ASIAS) program was created to offload data-storage and data-analysis and allow operators to more directly access the safety information they need. ASIAS is a voluntary FAA sponsored effort that allows operators to upload the data from their flight data recording devices to the ASIAS database [12]. This data exists in a de-identified format such that each operator can see their own data in comparison with that of all ASIAS participants. Along with ASIAS, other programs such as Flight Data Exchange (FDX) [13] are working to provide similar services. However, small GA operators and personal or recreational aviation continues to not be well represented in ASIAS [12]. Unfortunately, the accident statistics shown above in Figure 2 demonstrate that these sectors see the highest accident rates.

Research has been conducted to determine the best way to bring FOQA and FDM into GA. Mitchell et. al. [11] and Lau [14] discuss the benefits of FOQA in GA including improved training and safer and more efficient operations and maintenance. One of the primary barriers to FOQA implementation in GA is limited access to low-cost FDRs that do not require significant installation or interface with the existing aircraft's electrical system. Unlike Part 121 and 135 operations, acquisition and installation costs for high-fidelity FDRs can be extremely inhibitive for GA operators. Additionally, the diversity of GA aircraft renders such devices impractical for widespread use. However, low-cost and non-intrusive FDRs are becoming more available. Kuo et. al. [15] echoes the importance of such systems and provides experimental data for a possible candidate: Appareo Systems' Vision 1000, a self-contained unit (except for power and cockpit audio, which still need to

wire into the aircraft) which measures linear position, velocity, and acceleration, and angular position and velocity. It also uses a camera to visually capture the flight instruments. In [15], this system is used to provide FOQA-level data for both a fixed wing and rotary wing aircraft.

Investigations have also been conducted on using smartphones and tablets as FDRs. Called Personal Electronic Devices (PEDs), these systems are becoming ubiquitous in both commercial and general aviation [16]. Gocha [17] explored the use of a smartphone as a flight test data acquisition unit for a university test aircraft and compared it to a Garmin GPS unit. Although the author concluded that a smartphone was not a viable measurement device, no quantitative error analysis was performed. Additionally, no filtering was done on either system [18] [19]. Despite the possible limitations on sensor quality from PEDs, applications have been developed that use sensor data to assist pilots and operators with a variety of tasks, including data-driven safety. One such example is Mitre's General Aviation Airborne Recording Device (GAARD) app, which records data from a PED and uploads it to the National General Aviation Flight Information Database (NGAFID) [10]. NGAFID is similar to ASIAS but specifically targets GA. CloudAhoy [20] provides a similar service.

Applications like ForeFlight [21], Gyronimo [22], and AVPlan EFB [23] can be used to predict aircraft flight performance from user-input data from a pilot's operating handbook (POH). These apps aid flight planning by calculating glide distances to airports near the planned route in the case of an engine failure. Applications like Xavion [24] provide the pilot with glide paths and distances to alternate airports during flight by using an aircraft model, and provide synthetic vision that allows the pilot to fly cues to a safe

landing in the case of an emergency [25]. These functions are provided using the sensors, processing, and display of a PED (addition of an external GPS is recommended) [24]. One notable limitation to the above applications is the reliance on *a priori* data about aircraft performance, which may not be accurate for several reasons (see below) [16]. In addition, these performance calculations are given for zero wind, whereas winds aloft are not always negligible. As processing power of these devices continues to increase, the capabilities of these devices as FDRs will only continue to grow [26].

Aside from data collection, another challenge for FOQA implementation in GA is the development of relevant safety metrics. As previously discussed, GA encompasses a wide variety of operations, each with individual considerations for safety. Additionally, the aircraft flown by GA pilots are diverse, as shown below in Figure 3 [27].

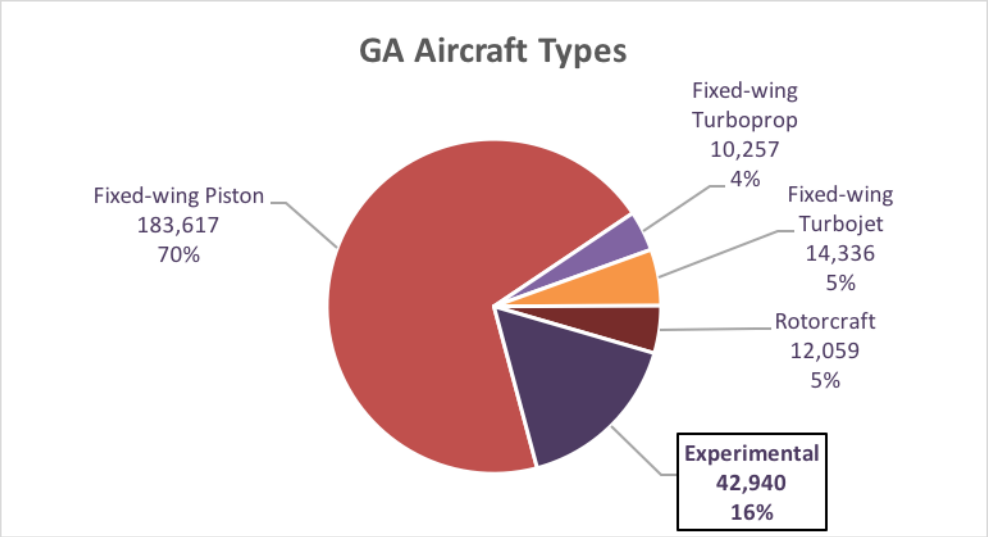

Figure 3. GA Fleet by Aircraft Type

Puranik [16] and Min [18] have studied possible metrics for data-driven safety that could be applied to a wide range of GA operations. They explore detection of exceedances and anomalies, which are discussed in AC 120-82 FOQA, as well as energy based methods, which detect performance envelope exceedance. Energy based methods rely on the use of a performance model to generate a flight envelope and analyze flight data with respect to how close the aircraft is to escaping the safe envelope [16] [18]. Performance models can sometimes be obtained *a priori* from a POH or AFM. However, this is not always possible. For example, Figure 3 shows that 16% of the GA fleet is experimental aircraft. These aircraft often require that the data in a POH or AFM be acquired by the pilot through flight test. As a result, pilots who fly these aircraft are 350% more likely to have a fatal accident within the first 40 hours of flight [28]. Bonadonna et. al. [28] discuss how FDRs and SysID can be used to obtain better estimates for the performance characteristics of these aircraft and obtain models for aircraft in which no *a priori* data exists. Additionally, the edges of the performance envelope can be more accurately estimated without requiring potentially risky envelope expansion test flights [29].

In cases where POH or other data is available, both Puranik [16] and Min [18] highlight the importance of "calibrating" these models using flight data. POH data only represents a subset of possible flying conditions, and is also published with data for brand-new aircraft flown by test pilots [30]. However, as shown below in Figure 4, the average age of a GA aircraft is 35 years [27]. Performance changes are known to take place as aircraft age, and therefore data in a POH may not accurately represent the performance of the aircraft [30]. Perhaps more influential are the flying conditions for a particular flight. In their work, Puranik states: "The deterioration of the airplane components with use,

piloting skill, variations in aircraft model, modifications/maintenance that might have been made to that aircraft, actual gross weight of operations on that particular day, environmental conditions, and noise in recorded parameters are just some of the factors that might cause uncertainty in estimates obtained from [an *a priori*] model" [16].

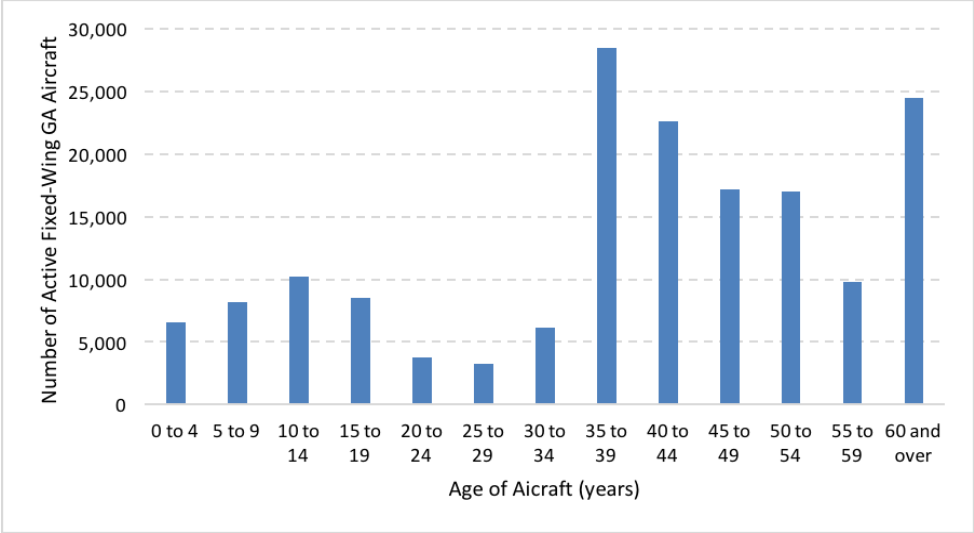

Figure 4. General Aviation Fleet by Age (2016)

In both [16] and [18], calibration and filtering routines were used to adapt *a priori* performance models to data from a specific flight to accurately identify safety metrics for GA operations. These calibration routines are an application of SysID. As discussed earlier, SysID is the process of obtaining a mathematical model of a system from measured data. While Puranik [16] and Min [18] identified performance parameters, such as lift and drag coefficients, Krajcek et. al. [30] used SysID of a 6-DOF aircraft model to achieve the same goal. The authors were interested in assessing performance changes of an aircraft using SysID by developing and monitoring an aircraft 6-DOF model. SysID therefore provides a

means for obtaining performance models when no *a priori* data exists (as in the case of experimental aircraft) or calibrating existing performance models. In addition, SysID can be used to provide more than just performance data: The stability and control derivatives can also be identified and monitored. This additional stability information is useful not only for analyzing flight safety based on performance and energy methods, but also for Loss of Control (LOC) prevention and mitigation.

Loss of Control, both on the ground and in flight, is one of the leading accident causes in aviation, especially in personal use aviation. A well-accepted definition of LOC in flight comes from the Civil Aviation Safety Team (CAST) and International Civil Aviation Organization (ICAO) Common Taxonomy Team (CICTT), which defines LOC as: "an extreme manifestation of a deviation from intended flightpath. The phrase "loss of control" may cover only some of the cases during which an unintended deviation occurred" [31]. Some common flight scenarios that are included in this category include stalls and spins, pilot-induced oscillations, and autorotation or loss of tail-rotor effectiveness (LTE) for helicopters. The NTSB uses the CICTT definitions of occurrence categories to label accident data. 2016 accident statistics by occurrence category can be seen below in Figure 5 [7]. Although only personal flying accidents are shown, other GA operations show similar trends. Additionally, as stated previously and shown in Figure 2, personal flying accounts for most accidents in GA.

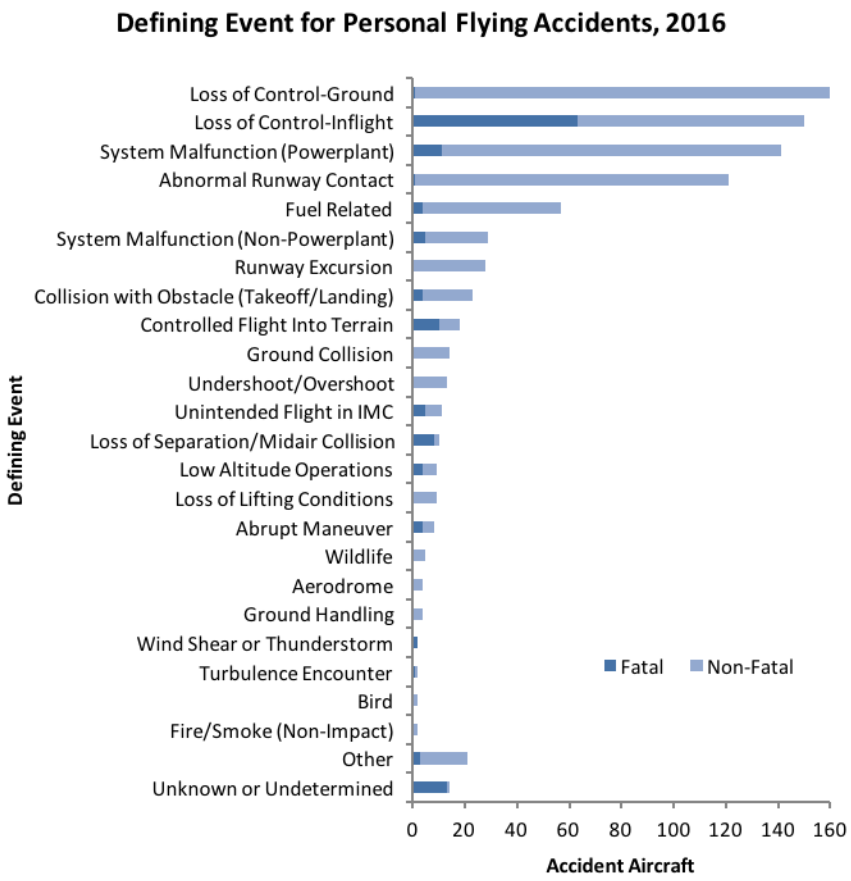

Figure 5. Accidents by Occurrence Category

Reducing LOC related accidents is therefore a priority for the aviation community, and has been the focus of many research efforts. Chambers and Stough [32] summarize NASA research into stall/spin aerodynamics. The authors describe how increased understanding of stall/spin aerodynamics could enable a reduction in LOC events through stall/spin resistant design, development of mitigation procedures for exiting LOC events, and improved simulations for training. Regarding simulation training, simulators must be able to accurately represent the dynamics that occur during a LOC event. Foster et. al. [33]

discusses the importance of gathering data for LOC events to enable simulation in these regimes. Figure 6 below, taken from [33], shows the discrepancy between manufacturer-provided aerodynamic data and the aerodynamic characteristics of a LOC event. Simulators based only on data provided from a manufacturer would be unable to capture the dynamics in upset conditions such as these.

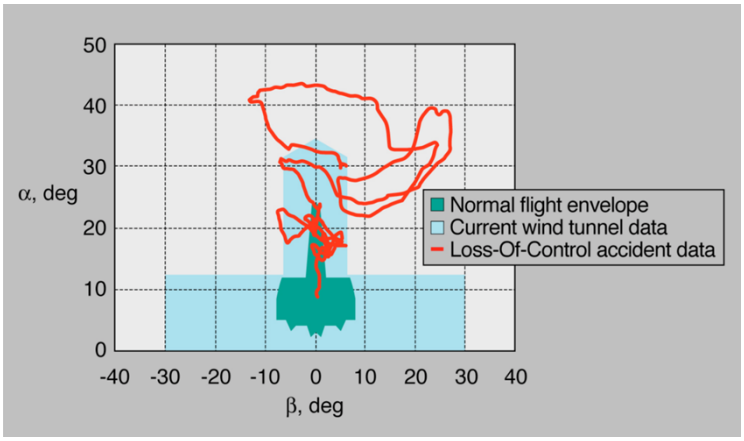

Figure 6. LOC Accident Flight Data for a Transport Aircraft

Chambers and Stough [32] used a combination of wind-tunnel testing and flight tests to gain insight into stall/spin aerodynamics. However, wind tunnel testing is limited by applicability to full-scale vehicles, and flight testing of these conditions is difficult and dangerous. Foster et. al. [33] used wind tunnel testing on transport aircraft to expand the envelope of available data (shown in blue in Figure 6) and therefore provide a means for increasing simulator fidelity in upset conditions. However, Lichota and Lasek [34] and Hamel and Jategaonkar [35] discuss the potential of SysID to accomplish the same task. SysID applied to accident data, such as that shown in red in Figure 6, could provide insight for accident investigation as well as increase the knowledge of LOC dynamics and enable

simulators and other interventions to be developed without the need for additional testing. While it is unfortunate that these accidents occur, making use of the data already available from these accidents to better understand LOC events can help prevent future accidents from occurring. Even in wind-tunnel testing, SysID can be used to investigate less-understood dynamics such as transient aerodynamic characteristics or aeroelastic effects [35] [36].

Other LOC mitigations have been aimed at increasing the pilot's situational awareness. While most aircraft are equipped with stall warning indicators or alarms, visual Angle of Attack (AoA) indicators can provide better understanding of the aircraft's conditions and energy state before reaching the point at which stall warnings are activated. This knowledge may also help in upset recovery after a LOC event has been entered. Therefore, AoA indicators have potential for reducing the fatal accident rate in GA, and the FAA is encouraging retrofitting the entire GA fleet with AoA indicators [37]. However, similar to FDRs, these systems incur acquisition and installation costs which can be inhibiting to many GA operations [5] [11]. On the other hand, Sembiring et. al. [4] and Morelli [5] demonstrated that models developed form SysID could be used to estimate unmeasured parameters, such as AoA, in real-time, without having to install additional measurement devices.

One of the downfalls of the AoA indicator is its additional demand on pilot situational awareness (SA). Active warning systems, such as stall-warning horns, can provide instantaneous warnings of impending stall or LOC. However, depending on the aircraft configuration and phase of flight, these warnings can come too late [38]. Active LOC warning systems that consider not only current aircraft state, but also projected state and

time until LOC, have been proposed in [38] and [39]. Scherer [38] posits the use of a constant-time warning. Kinematic equations are used to determine the rate at which the aircraft is approaching stall or other LOC indicators. The warning is activated if the "time-to-LOC" is calculated as less than some threshold value. However, this approach is limited in its use of kinematic equations; while kinematics may be a decent approximation to aircraft motion, increased accuracy could be obtained using a more refined aircraft physics model. Harrison [39] defined a LOC envelope using upper and lower limits for AoA, angle of sideslip, and velocity, as well as defining safe sets, or the set of all initial conditions for which the resulting trajectory would not exceed this envelope. Harrison also investigates the development of control strategies for mitigating LOC if the vehicle trajectory exits the safe set. Both the calculation of the safe set and mitigation strategies require an aircraft 6-DOF model. In Harrison's work, this model is assumed accurate and known. However, as discussed above, *a priori* models and data for GA aircraft may either not exist or be inaccurate. In these cases, SysID provides a means of obtaining or calibrating aircraft 6-DOF models, thereby enabling LOC analysis and mitigation.

SysID also has potential applications in navigation and performance monitoring. As previously discussed, several applications for PEDs have been developed to assist pilots with flight and performance planning. Many of these apps use the sensor data and display of the PED to offer pilots a backup of their flight instruments [40] [41]. Called "synthetic vision", this function provides the pilot with a secondary display, much like a Primary Flight Display (PFD) in a glass cockpit, with the aircraft's speed, orientation, and location. Because not all these values are measured directly, and may contain noise and uncertainty, a state estimation and filtering process is used to obtain the data necessary for simulating

the aircraft instruments [16] [18] [19]. Perhaps the most-used filter for these state estimation and navigation problems is the Kalman filter and its variants [19] [42]. However, Kalman filters require a model of system dynamics to perform the estimation, and inaccuracies in the model can degrade the performance of these filters [43] [44]. Using active SysID to refine the model used in state estimation could increase the fidelity of these applications and others.

When coupled with state estimation, SysID can also provide estimates for unmeasured parameters, such as AoA and sideslip, as previously discussed. State estimates can also be obtained for center of gravity using accelerometer measurements [45], which can be used in conjunction with an aircraft model to estimate fuel burn. Using SysID to develop the aircraft model and monitor fuel burn may help mitigate fuel-related accidents, which are one of the top 5 accident occurrence categories shown in Figure 5.

GA could therefore benefit from SysID application to flight data recorded with low-cost FDRs or PEDs. SysID provides a means of obtaining aircraft 6-DOF models when *a priori* information does not exist, refining or calibrating existing models, and monitoring changes in dynamics. Potential uses for the resulting models in GA are summarized below:

- Assist data-driven safety efforts in GA by using identified models to increase fidelity in the definition and detection of relevant safety metrics for a wide range of operations and aircraft types
- Increase understanding of LOC events through application to accident data

- Assist efforts for LOC mitigation by providing models that can be used in the definition of safe sets, investigation of mitigation strategies, and increased simulator fidelity for upset conditions and upset recovery
- Increase pilot situational awareness by providing estimates of unmeasured parameters such as AoA and fuel burn
- Improve state-estimation, navigation, and performance calculations currently in-use on PEDs by increasing model fidelity used by such applications

Several barriers to SysID implementation in GA exist and must be overcome before these potential benefits can be realized. While low-cost FDRs and PEDs in the cockpit are becoming more available, the amount and quality of data provided by these systems may not be enough to obtain accurate models through SysID. Limited knowledge of control inputs can make SysID especially challenging, and is referred to as "blind" SysID. Specifically, for PEDs, processing power may also pose limitations. Additionally, several methods of SysID exist that could be applied to this problem, and may have varying degrees of success. Therefore, an investigation is needed to determine the suitability of existing methods of SysID to obtain GA vehicle models from FDR or PED data. This leads to the formulation of the research objective below:

Research Objective:

Determine the requirements, capabilities, and limitations of existing System Identification methods and their application to General Aviation aircraft flight data obtained through a low-cost Flight Data Recorder or Personal Electronic Device.

The rest of this thesis is organized as follows:

- Chapter 2 presents literature review on existing SysID methods and their applications in aircraft SysID from flight data
- Chapter 3 formulates important research questions that must be answered to address the research goal and develops hypotheses and experiments to answer these questions
- Chapter 4 presents the methodology that was used to conduct the experiments
- Chapter 5 presents the results of the studies conducted and their implication for GA
- Chapter 6 summarizes the work and its potential impact as well as recommendations for future research

CHAPTER 2. BACKGROUND AND LITERATURE REVIEW

This chapter will provide a background and literature review of topics necessary for the formulation of specific research questions, hypotheses, and experiments. Specifically, Section 2.1 discusses aircraft dynamics, common formulations of the aircraft equations of motion (EOM), and discussion of the dynamics formulation used in this study. Section 2.2 will provide background on SysID methods and examples of their use for aircraft SysID. Section 2.3 discusses observability and identifiability of nonlinear systems, and Section 2.4 discusses the role of control inputs in SysID, control input design, and "blind" SysID in which control inputs are unknown.

2.1 Aircraft Dynamics

Aircraft dynamic models for this work were developed from standard aircraft equations of motion in [46] as well as FlightGear Desktop Simulator (FGDS) [47] [48] [49] which provides a specific parameterization of the aerodynamic and propulsive forces in these equations. These sources use standard flight dynamics coordinate systems as described in Figure 7 below (Images from [46]). Figure 7(a) shows the earth coordinate systems, with O_E representing the Earth-fixed North-East-Down (NED) coordinate system. Figure 7(b) shows the aircraft body-fixed reference frame. The origin is at the aircraft's center of gravity. Positive x-axis points out the aircraft nose, positive z-axis down out of the aircraft belly, and positive y-axis follows right-hand rule and points out of the right

wing. Figure 7(c) shows the wind coordinate system, with positive angle of attack (AoA), α, and positive angle of sideslip, β.

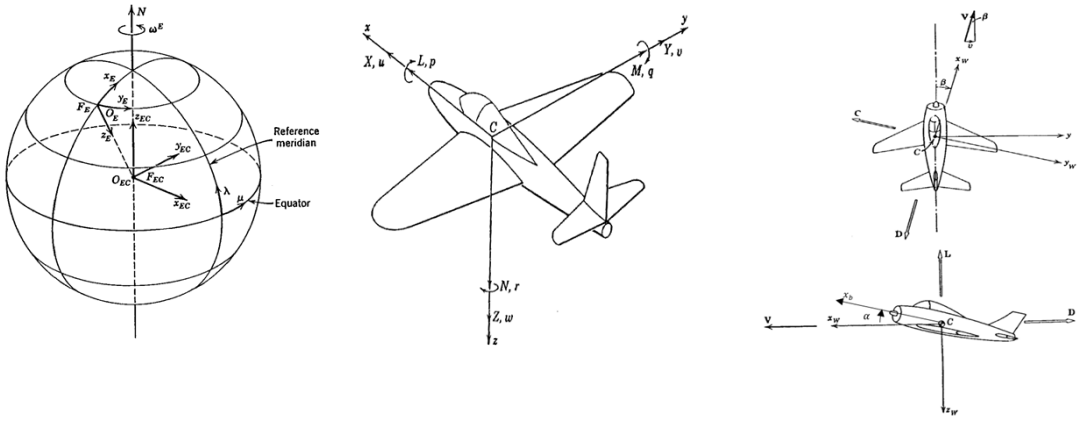

(a) (b) (c)

Figure 7. Flight Dynamics Coordinate Systems

Throughout this work, the stationary flat-earth assumption will be utilized, such that ω_e and O_{EC} are negligible. Coordinate systems considered will be only NED, aircraft body-fixed, and wind. This is an adequate assumption for short time-scales in which the Earth's Coriolis acceleration is negligible [46]. Table 1 below summarizes the nomenclature used in the aircraft equations of motion and the equations themselves expressed in aircraft-fixed body coordinates follow the table:

Table 1. Aircraft EOM Nomenclature

Vector	Component	Description
-	x_N x_E x_D	Position in NED coordinates
V	u v w	Inertial velocity in aircraft-fixed body coordinates
$\dot{V}$	$\dot{u}$ $\dot{v}$ $\dot{w}$	Inertial acceleration in aircraft-fixed body coordinates
-	ϕ θ ψ	Euler-angles
ω	p q r	Rotational velocity in aircraft-fixed body coordinates
$\dot{\omega}$	$\dot{p}$ $\dot{q}$ $\dot{r}$	Rotational acceleration in aircraft-fixed body coordinates
$F_{aeroprop}$	X Y Z	Aerodynamic and propulsive forces in aircraft-fixed body coordinates
-	g m $DCM_{e2b}(...)$ $DCM_{w2b}(...)$ α $\dot{\alpha}$ β	Acceleration due to gravity Mass Direction-cosine matrix from NED coordinates to aircraft-fixed body coordinates Direction-cosine matrix from wind coordinates to aircraft-fixed body coordinates Angle of attack Rate of change of angle of attack Angle of sideslip
F_{aero}	D Y L	Drag force Side force Lift force (not to be confused with roll moment)
-	T C_{X_Y} ρ S_w b_w c_w	Thrust Derivative of coefficient C_X with respect to Y Air density Wing reference area Wingspan Wing mean aerodynamic chord

Table 1 (continued). Aircraft EOM Nomenclature

-	δ_a δ_e δ_r	Aileron control deflection Elevator control deflection Rudder control deflection
M	L M N	Roll moment (not to be confused with lift force) Pitch moment Yaw moment
-	I $\vec{r}_{cg2ac}$	Inertia Matrix Moment arm between CG and aerodynamic center
V_w	u_w v_w w_w	Three-component wind velocity in aircraft-fixed body coordinates
V_∞	u_∞ v_∞ w_∞	Three-component airspeed in aircraft-fixed body coordinates

$$F_{aeroprop} + F_{grav} = m(\dot{V} + \omega \times V)$$

$$\begin{bmatrix} X \\ Y \\ Z \end{bmatrix} + DCM_{e2b}(\phi, \theta, \psi)\begin{bmatrix} 0 \\ 0 \\ g \end{bmatrix} = m\left(\begin{bmatrix} \dot{u} \\ \dot{v} \\ \dot{w} \end{bmatrix} + \left(\begin{bmatrix} p \\ q \\ r \end{bmatrix} \times \begin{bmatrix} u \\ v \\ w \end{bmatrix}\right)\right) \tag{1}$$

$$\begin{bmatrix} X \\ Y \\ Z \end{bmatrix} = DCM_{w2b}(\alpha, \beta)\begin{bmatrix} D \\ Y \\ L \end{bmatrix} + \begin{bmatrix} T \\ 0 \\ 0 \end{bmatrix} \tag{2}$$

$$\begin{bmatrix} D \\ Y \\ L \end{bmatrix} = \begin{bmatrix} C_D \\ C_Y \\ C_L \end{bmatrix}\left(\frac{1}{2}\rho V_\infty^2\right)S_w \tag{3}$$

$$M = I\dot{\omega} + \omega \times I\omega$$

$$\begin{bmatrix} L \\ M \\ N \end{bmatrix} = \begin{bmatrix} I_{xx} & -I_{xy} & -I_{xz} \\ -I_{xy} & I_{yy} & -I_{yz} \\ -I_{xz} & -I_{yz} & I_{zz} \end{bmatrix}\begin{bmatrix} p \\ q \\ r \end{bmatrix} + \begin{bmatrix} p \\ q \\ r \end{bmatrix} \times \begin{bmatrix} I_{xx} & -I_{xy} & -I_{xz} \\ -I_{xy} & I_{yy} & -I_{yz} \\ -I_{xz} & -I_{yz} & I_{zz} \end{bmatrix}\begin{bmatrix} p \\ q \\ r \end{bmatrix} \tag{4}$$

$$\begin{bmatrix} L \\ M \\ N \end{bmatrix} = \begin{bmatrix} L \\ M \\ N \end{bmatrix}_{aero} + \vec{r}_{cg2ac} \times \begin{bmatrix} D \\ Y \\ L \end{bmatrix} \tag{5}$$

$$\begin{bmatrix} L \\ M \\ N \end{bmatrix}_{aero} = \begin{bmatrix} C_L b_w \\ C_M c_w \\ C_N b_w \end{bmatrix} \left(\frac{1}{2} \rho V_\infty^2 \right) S_w \tag{6}$$

$$V_\infty = V + V_w$$

$$\begin{bmatrix} u_\infty \\ v_\infty \\ w_\infty \end{bmatrix} = \begin{bmatrix} u \\ v \\ w \end{bmatrix} + DCM_{e2b}(\phi, \theta, \psi) \begin{bmatrix} V_{w_n} \\ V_{w_e} \\ V_{w_d} \end{bmatrix} \tag{7}$$

$$\alpha = \tan^{-1}\left(\frac{w_\infty}{u_\infty} \right) \tag{8}$$

$$\dot{\alpha} = \left(\frac{1}{1 + \left(\frac{w_\infty}{u_\infty} \right)^2} \right) \left(\frac{u_\infty \dot{w} - w_\infty \dot{u}}{u_\infty^2} \right) \tag{9}$$

$$\beta = \sin^{-1}\left(\frac{v_\infty}{V_\infty} \right) \tag{10}$$

Equations (1) through (3) describe the force equations, whereas (4) through (6) describe the moment equations. It is also necessary to relate the aircraft inertial states to airspeed, AoA, and angle of sideslip to calculate aerodynamic forces. This relationship is described in equations (7) through (10). The rate of change of angle of attack, $\dot{\alpha}$, must also be calculated, which is done by taking the time derivative of equation (8), as shown in equation (9), with the assumption that $\dot{u}_\infty = \dot{u}$ and $\dot{w}_\infty = \dot{w}$, taken from [48].

The aerodynamic coefficient buildup used in this work uses the assumption of linear air reactions discussed in [46]. The basis behind this formulation of aerodynamics is a

Taylor series expansion for the derivatives of the coefficients with respect to parameters. An example for lift-coefficient with respect to AoA is given below:

$$C_L = C_{L_0} + C_{L_\alpha}\alpha + \frac{1}{2}C_{L_{\alpha\alpha}}\alpha^2 + \ldots \tag{11}$$

It is often sufficient to truncate the higher-order terms and assume linear aerodynamic derivatives [46]. The aerodynamic coefficient buildups utilized in this work are a combination of those found in [48] and [49], and are shown below in equations (12) through (17). Note that flap deflection is not accounted for; only aileron, elevator, and rudder are considered. Note also that the damping terms (derivatives with respect to p, q, and r) are normalized by the terms $\left(\frac{c_w}{2V_\infty}\right)$ for longitudinal coefficients, and $\left(\frac{b_w}{2V_\infty}\right)$ for lateral coefficients. This is standard for flight dynamics formulations and can be found in [46] [47] [48].

Drag
$$C_D = C_{D_0} + K_{C_L}(C_L - C_{L_0})^2 + C_{D_\beta}\beta + C_{D_{\delta_e}}\delta_e \tag{12}$$

Side-force
$$C_Y = C_{Y_\beta}\beta + C_{Y_p}p\left(\frac{b_w}{2V_\infty}\right) + C_{Y_r}r\left(\frac{b_w}{2V_\infty}\right) + C_{Y_{\delta_r}}\delta_r \tag{13}$$

Lift
$$C_L = C_{L_0} + C_{L_\alpha}\alpha + C_{L_{\dot\alpha}}\dot\alpha\left(\frac{c_w}{2V_\infty}\right) + C_{L_q}q\left(\frac{c_w}{2V_\infty}\right) + C_{L_{\delta_e}}\delta_e \tag{14}$$

Roll
$$C_L = C_{L_\beta}\beta + C_{L_p}p\left(\frac{b_w}{2V_\infty}\right) + C_{L_r}r\left(\frac{b_w}{2V_\infty}\right) + C_{L_{\delta_a}}\delta_a + C_{L_{\delta_r}}\delta_r \tag{15}$$

Pitch
$$C_M = C_{M_0} + C_{M_\alpha}\alpha + C_{M_{\dot\alpha}}\dot\alpha\left(\frac{c_w}{2V_\infty}\right) + C_{M_q}q\left(\frac{c_w}{2V_\infty}\right) + C_{M_{\delta_e}}\delta_e \tag{16}$$

Yaw
$$C_N = C_{N_\beta}\beta + C_{N_p}p\left(\frac{b_w}{2V_\infty}\right) + C_{N_r}r\left(\frac{b_w}{2V_\infty}\right) + C_{N_{\delta_a}}\delta_a + C_{N_{\delta_r}}\delta_r \tag{17}$$

2.2 System Identification Methods

System Identification (SysID) is the process of matching some model of system behavior to measurement data from the real system. General forms of the system model, f, and measurement model, h, are shown below in Equations (18) and (19) as functions of time, t, state variables, x, controls or other inputs, u, and the unknown parameters, Θ:

$$x_{k+1} = f(t, x_k, u_k, \Theta) \tag{18}$$

$$y_k = h(t, x_k, u_k, \Theta) \tag{19}$$

The SysID problem then becomes one of finding the parameters, Θ, that best match the model to the observations. This is often done by formulating some cost function and performing a minimization routine. This cost function is often a form of the sum of squares formula shown below, where z_k represents the k-th measurement:

$$J(\Theta) = \sum (z_k - y_k)^T (z_k - y_k) \tag{20}$$

Depending on the form of the model f, this minimization can take different forms. Hamel and Jategaonkar [35] published a literature review of existing SysID methods. The following sections discuss this comparison of methods for SysID of aircraft and provide some recent examples of their application.

2.2.1 Equation Error Method

Equation error methods (EEM) utilize least-squares regression for linear systems to minimize the error between the measured data and the output of a linear time-invariant (LTI) system [35]. The system model in Equations (18) and (19) is simplified as an LTI system:

$$x_{k+1} = A(\Theta)x_k + B(\Theta)u_k \tag{21}$$

$$y_k = C(\Theta)x_k + D(\Theta)u_k \tag{22}$$

where A, B, C, and D are all constant matrices that depend on the parameters Θ. Rewriting the output equation system as an explicit function of Θ yields:

$$Z = X\Theta \tag{23}$$

$$X = \begin{bmatrix} x_0^T & u_0^T \\ x_1^T & u_1^T \\ \vdots & \vdots \\ x_k^T & u_k^T \end{bmatrix}, \qquad Z = \begin{bmatrix} z_0 \\ z_1 \\ \vdots \\ z_k \end{bmatrix} \tag{24}$$

where X is a matrix of the system outputs at each time step, and Z is a matrix of the measurements of the system. The cost function in Equation (20) can then be written:

$$J(\Theta) = \frac{1}{2}(Z - X\Theta)^T(Z - X\Theta) \tag{25}$$

and the least-squares solution $\hat{\theta}$ that minimizes this cost is given as:

$$\hat{\Theta} = (X^T X)^{-1} X^T Z \tag{26}$$

This minimization will result in the set of parameters that most closely maps the system described in Equations (21) and (22) to the measured system outputs.

In aircraft SysID, these parameters represent the stability and control derivatives of the linearized aircraft model. This linearization is only valid near an equilibrium condition, and therefore the SysID process must be repeated over sets of data obtained near different equilibrium conditions. An example of this is given in Cetin [50], in which the author performs EEM SysID on a Cessna 172 simulation model at 12 distinct trim points scheduled by dynamic pressure. After obtaining the models through SysID, closed-loop controllers are developed to meet certain handling qualities requirements. The author demonstrated that the obtained SysID models were accurately able to reproduce the simulator behavior, and the designed controllers could meet the requirements.

In Berger et. al. [29] the authors develop a "stitched" model of a transport aircraft in which a full-envelope model is obtained by applying EEM SysID at set intervals defined by a chosen scheduling parameter. In this study, the authors chose the aircraft body u-velocity, which closely approximates the true airspeed. The stability and control derivatives then become a function of the u-velocity, allowing a full-envelope model to be developed from the LTI models obtained during each EEM SysID process. The authors demonstrated that this model could be extrapolated to points outside the original data used for SysID (other points in the envelope) without significant error.

In both cases above, the SysID process was applied at trim conditions that were specified either by simulation [50] or by flight test [29]. In less-controlled environments, other techniques may be needed to determine when the linearized model is valid for system ID [3]. Noriega [2] used EEM to develop linear models for a UAV using discrete "batches" of data. This resulted in a semi-real-time application of EEM, the results of which were monitored and used to develop confidence for the stability and control derivative estimates as well as monitor for actuator failures by detecting large changes in the derivatives between batches. However, no knowledge was assumed about the maneuver in each batch; data may have come from conditions near trim, in which a linear model is applicable, or from more nonlinear flight conditions. EEM was applied to each batch, and the resulting covariance was used to determine if a linear model was valid. If the residual error from the model was too high, it could be concluded that a linear model was not applicable, and that batch would be excluded from the monitoring of stability and control derivatives.

In the above applications, the aircraft equations are formulated in the time-domain, but many studies have used EEM in the frequency domain using recursive Fourier transforms. The system model remains the same linear model as described in Equations (21) and (22) with the exception that the states and controls have all been transformed into the frequency domain. The discrete Fourier transform of a signal is given by:

$$X(\omega) = \sum_{i=0}^{N-1} x_i e^{-j\omega t_i} \tag{27}$$

$$\tilde{x}(\omega) \approx X(\omega)\Delta t \tag{28}$$

The transformed system then takes the form:

$$j\omega\tilde{x}(\omega) = A(\Theta)\tilde{x}(\omega) + B(\Theta)\tilde{u}(\omega) \tag{29}$$

$$y_k(\omega) = C(\Theta)\tilde{x}(\omega) + D(\Theta)\tilde{u}(\omega) \tag{30}$$

A recursive Fourier transform can be used to relate the discrete Fourier transform at time i to time $i-1$ by:

$$X_i(\omega) = X_{i-1}(\omega) + x_i e^{j\omega i\Delta t} \tag{31}$$

The recursive Fourier transform for a given frequency or range of frequencies can be computed at each time-step with relatively low computational effort and without the need to store large batches of data to perform the regression. Additionally, excluding the zero frequency helps remove the effect of trim and steady-state values on the perturbation dynamics. The result is a real-time SysID process that continuously updates the estimates for the stability and control parameters.

Examples of successful implementation of real-time EEM using recursive Fourier transform are given in [1] [5] [51]. Morelli [5] successfully determined the stability and control derivatives for an F-16 nonlinear simulation and a T-2 flight test aircraft. Despite the simulation and true aircraft having nonlinear dynamics, the application of EEM (which assumes linear dynamics) was shown to be accurate for the flight regimes tested. Additionally, this analysis was done without measured air data such as angle of attack or sideslip; these values were reconstructed from inertial data. Accurate results were obtained from the SysID process in both cases.

In another study by Morelli [51], real-time EEM using recursive Fourier transform was used to design flight test maneuvers for system identification during a flight test. System dynamics were used to design the maneuvers, SysID using EEM applied to the results, and the updated model used to update the design of the maneuver. Several studies have been conducted on the topic of maneuver design for aircraft SysID and are discussed in more detail in Section 2.4.

DeBusk et. al. [1] used the recursive Fourier transform method on an autonomous vehicle to monitor changes in dynamics for future implementation of adaptive control algorithms. Both frequency and time domain methods were used and showed good correlation with measured data. Like the above studies, it was found that a linear model using EEM was sufficient to capture the dynamics of the aircraft, despite the possible presence of nonlinear dynamics.

The benefits of EEM in either frequency or time domain are in its simplicity and low computational burden. This makes it an ideal method for implementations in which on-board processing power is severely limited. However, due to its linear nature, EEM suffers from an inability to characterize nonlinear dynamics or coupling between lateral and longitudinal states. It also relies on the knowledge of trim points about which the linear perturbation model is valid [3]. Therefore, other methods, such as Output Error Method, are often used to characterize nonlinear models and remove the amount of *a priori* knowledge required to perform SysID.

2.2.2 Output Error Method

Output Error Method (OEM) utilizes standard optimization techniques, such as Gauss-Newton, to minimize some cost function for a nonlinear dynamical model [35]. This cost function is often formulated as a Maximum Likelihood Estimation (MLE) such as the following:

$$J(\Theta) = \sum_{k=1}^{N} [z_k - y_k]^T R^{-1} [z_k - y_k] + \frac{N}{2} \ln |R| \tag{32}$$

In Equation (32) above, z_k represents the measurement data, y_k represents the predicted measurements obtained through the system model (Equations (18) and (19)) and R is some weighting or probability matrix, often the measurement covariance matrix. This allows the SysID process to account for probabilistic distributions of parameters and not just the values themselves as in EEM. Note that if R is taken as the identity matrix this cost function reverts to total sum of squares. However, even in this case, there exists no simple linear algebra result for the minimization like there is for EEM. Therefore, some other minimization routine must be used to find the error, such as Gauss-Newton method.

Gauss-Newton is a gradient-based minimization method that results in obtaining a local minimum if one exists. Therefore, attention must be paid to the initial guess at which the minimization is initialized. Lichota and Lasek [34] used FDR data to perform SysID of a linearized model in post-flight analysis. The cost function in this study was simplified to a matrix norm of the covariance matrix R in Equation (32). The authors used Levenberg-Marquardt algorithm for the minimization, which is an interpolation between Gauss-

Newton and Steepest Descent methods, both gradient-based. As part of their study, an analysis was conducted on the effect of inaccurate initial guesses. Unsurprisingly, inaccurate initial guesses resulted in longer computational times and less-accurate final results for system parameters. To offset this, many applications will use analytical relationships or known data for a similar aircraft to initialize the SysID process.

Tanner and Montgomery [52] also used a linear model with OEM to obtain the system matrices for a modified Beech-99 test aircraft. Although no *a priori* information was assumed to begin the OEM process, stability and control derivatives showed good agreement with the manufacturer's estimates. For the inaccuracies that were found, it was unclear whether these differences were due to the modified aircraft, poor SysID results, or inaccurate manufacturer estimates. Additionally, although a linear model was used, this model was obtained at a variety of flight conditions, and correlations between the coefficients and flight conditions (angle of attack for example) could be seen, hinting at the existence of nonlinearities.

Neither of the above studies used nonlinear dynamics; however, one of the benefits of OEM is the ability to characterize nonlinearities. For example, Murphy and Klein [36] demonstrated the use of OEM SysID to characterize the dynamics of unsteady nonlinear aerodynamics for a transport aircraft using wind-tunnel test data. Models for aerodynamic derivatives were posited, and OEM in the time-domain was used to obtain the parameters in those models. The results matched both the data used for SysID as well as predicted the aerodynamics of other cases, validating the accuracy of the models. In this case, SysID provided a means to obtain knowledge about aerodynamic characteristics that were previously unknown.

Similarly, Marwaha et. al. [53] used OEM to identify a system model that consisted of both linear and nonlinear dynamics for an F-16 simulation and flight data form an Extra-300 aircraft. Nonlinear polynomials were used to model the dynamics, and the SysID process identified the coefficients for the nonlinear terms. Accuracy was determined to depend on the order of the polynomials used. Despite a lack of *a priori* knowledge on control influences in the model, the results showed the capability to accurately model the nonlinear dynamics of both aircraft.

OEM, especially MLE as described by Equation (32), have the advantage of accounting for nonlinear models and/or probability distributions of parameters. However, this necessitates an additional computational burden, and as such, the applications discussed above performed SysID offline. Additionally, no explicit treatment of noise in the data used for OEM is discussed; noise is implicitly minimized through the minimization of the likelihood cost function. Maine and Iliff [54] discuss an adaptation of OEM that accounts for both sources of uncertainty; however, computational burden was higher than that of standard output error method. Filter methods, on the other hand, can filter both the state data, measurement data, and estimated parameters, and are relatively computationally inexpensive, making them ideally suited for SysID applications in real-time in the presence of turbulence and/or noisy measurements [35].

2.2.3 Filter Method

Filter method for SysID is commonly implemented using some variant of a Kalman filter [35]. Kalman filters are optimal estimators for linear systems with noise, and use a blend of predicted states from a system model updated using system measurements [42] [55]. This allows the SysID process to explicitly account for noise and disturbances in measured data and the posited model. The resulting estimation is equivalent to maximum likelihood estimation (MLE) for a linear system with only zero-mean Gaussian probability distributions [35]. Extended Kalman filters (EKF) are a variant of the linear Kalman filter that can be applied to a nonlinear system. In an EKF, the system is linearized at each time step using Taylor series expansion and the Jacobian of the process and measurement models (see Equation (42) below). The standard linear Kalman filter equations are then used on the linearized system. Because the system is not truly linear, the EKF is a near-optimal estimator; this method does not perform well in the presence of highly nonlinear or noisy systems. The algorithm for the EKF is described in the following paragraphs [55].

The system model can be formulated as the adaptation of Equations (18) and (19) shown below in Equations (33) and (34) where the $w_i(t)$ terms represent zero-mean uncorrelated normal distributions with standard deviation equal to one. E and G are matrices that scale these distributions to approximate the noise in the system model, f, and measurement model, h, respectively. In general, these matrices can be functions of time, state variables, and controls; for simplicity, these arguments are not represented below:

$$x_{k+1} = f(t,x_k, u_k) + E_k w_1(t) \tag{33}$$

$$\hat{z}_k = h(t,x_k,u_k) + G_k w_2(t) \tag{34}$$

The process noise covariance matrix can be calculated as $Q_k = E_k E_k^T$ and similarly, the measurement noise covariance is $R_k = G_k G_k^T$. The EKF algorithm is then shown below in Equations (35) through (41) [55]. The subscripts for $\hat{x}_{k|k-1}$ can be interpreted: "state estimate at time-step k constructed from estimates at time-step $k-1$".

Predict:

Predicted State Estimate $$\hat{x}_{k|k-1} = f(\hat{x}_{k-1|k-1}, u_k) \tag{35}$$

Predicted Covariance Estimate $$P_{k|k-1} = F_k P_{k-1|k-1} F_k^T + Q_k \tag{36}$$

Update:

Measurement Residual $$y_k = z_k - h(\hat{x}_{k|k-1}) \tag{37}$$

Residual Covariance $$S_k = H_k P_{k|k-1} H_k^T + R_k \tag{38}$$

Near-Optimal Kalman Gain $$K_k = P_{k|k-1} H_k^T S_k^{-1} \tag{39}$$

Updated State Estimate $$\hat{x}_{k|k} = \hat{x}_{k|k-1} + K_k y_k \tag{40}$$

Updated Covariance Estimate $$P_{k|k} = (I - K_k H_k) P_{k|k-1} \tag{41}$$

The EKF handles non-linear dynamics by linearizing around each current time-step using the Jacobian of the state transition function f and the measurement function h computed with the current state estimate such that:

$$F_k = \left.\frac{\partial f}{\partial x}\right|_{\hat{x}_{k|k-1},\, u_k} \qquad \text{and} \qquad H_k = \left.\frac{\partial h}{\partial x}\right|_{\hat{x}_{k|k-1},\, u_k} \tag{42}$$

The predicted state estimate (Equation (35)) is obtained using the previous state estimate $\hat{x}_{k-1|k-1}$ and the state transition function, f. The predicted covariance (Equation (36)) is calculated using the Jacobian of the state transition function F_k, the previous covariance, $P_{k-1|k-1}$, and the process noise Q_k which represents the unknown noise in the dynamics. The measurement residual (Equation (37)) is the difference between the actual measurement, z_k, and the expected measurements, $\hat{z}_k$, using the predicted state estimate $\hat{x}_{k|k-1}$ and Equation (34). The residual covariance (Equation (38)) is computed using the Jacobian of the measurement function H_k, the predicted covariance $P_{k|k-1}$, and the measurement noise R_k. The near-optimal Kalman gain (Equation (39)) takes the measurement Jacobian H_k, the predicted covariance $P_{k|k-1}$, and the residual covariance S_k , to obtain the weighting for the measurements. A higher Kalman gain causes the measurements to be "trusted more" than the predicted state from the dynamics, and vice-versa. This is represented in Equation (40). Finally, the updated covariance estimate is computed and the updated state estimate and covariance estimate are passed to the next iteration.

The formulation above is for a generic state estimation problem. Typically, the aircraft states (position, velocity, etc.) are estimated from sensor measurements using this approach

[19]. The SysID problem can be transformed into a state estimation problem by appending the unknown parameters as additional states in the state vector. This is the basis for the filter method of SysID. This method has been shown to be effective for aircraft SysID, especially in the presence of turbulence and noisy measurement data [35].

Valasek and Chen [3] utilized a standard linear Kalman filter to develop linear models for a nonlinear aircraft by performing SysID around trim points. To ensure validity of the linear model, the Kalman filter was enabled only when the aircraft had properly trimmed in a desired state. However, uncertainty in this trimmed state must be accounted for by the filter when it initializes. The authors also explored the effect of wind gusts (disturbances) on the SysID process. It was determined that the performance of the filter was relatively insensitive to moderate gusts and turbulence, but performance was degraded as gust magnitude and duration increased.

Grillo and Montano [56] applied the EKF approach to a nonlinear UAV model for online SysID during UAV flights. Stability and control derivatives were appended to the aircraft states, and the implication of filter tuning using the process noise Q_k was discussed. Accurate estimates for the system parameters were obtained at notably less computational expense compared to OEM. Similarly, Evans et. al. [57] compared the EKF method and OEM on computational burden and accuracy. EKF produced comparable results to that of OEM, was computationally cheaper, and was less sensitive to *a priori* information. Chowdhary and Jategaonkar [58] investigated both EKF and unscented Kalman filter (UKF) for parameter estimation of longitudinal dynamics of fixed wing and rotary wing aircraft. UKFs are another variant of Kalman filters that work with nonlinear systems, but avoid the linearization technique used by EKFs, and are therefore computationally cheaper

for large-dimension problems. Output accuracy of both filters was comparable for the parameter estimation problem, and as such, only EKFs will be considered in this work.

The main limitation in the filtering approach to SysID is in filter tuning. Performance of Kalman filters is highly dependent on the provided covariance matrices Q_k and R_k. The measurement covariance, R_k, can often be determined by testing and measuring the accuracy of the sensors used. However, the process covariance Q_k is generally unknown. While tuning procedures have been developed to try to estimate Q_k [59] [60] [61], these methods are computationally expensive, and rely on accurate simulation of the posed filtering problem in order to optimize the filter [1]. These tuning procedures are discussed in more detail in Section 4.3.

2.2.4 Artificial Neural Networks

Artificial Neural Network (ANN) methods perform system identification by modelling the input-output relationship of the system with an ANN. The ANN uses a flexible network of nodes, or neurons, to model any input-output relationship without *a priori* knowledge of the system dynamics or even the form of the model [35]. The main benefit and limitation of ANNs is the same: the resulting model is purely mathematical. The weightings of the nodes in the ANN do not necessarily have any physical meaning. However, this also allows models to be created for dynamics that are of an unknown form. For example, Roudbari and Saghafi [62] utilized an ANN to identify the dynamics of a highly-maneuverable and nonlinear aircraft from simulation data. Results of this study demonstrated the feasibility of using ANNs for SysID, especially in cases where limited *a priori* information about the dynamics exists. However, another limitation of the ANN

approach is the dependency on a relatively large dataset and computation time for creating and training the model. This dependency prevents ANN method from being applicable to online SysID [35].

2.3 Identifiability of Parameters

An important consideration in SysID is identifiability of the parameters. Identifiability is closely related to observability, which dictates that the states of a system can be uniquely determined from the measured outputs [63]. In other words, for a given measured output, z_k, there exists a unique set of parameters that minimizes the error between z_k and the model-predicted measurement y_k. If the parameters are not identifiable, there exists at least two parameters that are correlated, or indistinguishable from one another. A simple example of this is illustrated below in Equation (43):

$$C_L = C_{L_0} + C_{L_\alpha}\alpha \tag{43}$$

In the above example, assume that C_L and α are measured outputs (a normalized accelerometer measurement and an AoA vane, for example), and C_{L_0} and $C_{L_\alpha}$are the parameters of interest. The estimation and SysID problem is to accurately estimate the values of all four parameters. This system is therefore nonlinear due to the $C_{L_\alpha}\alpha$ term. It is also unobservable: for a measured value of $[\alpha_1, C_{L_1}]^T$, there are infinitely many possibilities for $C_{L_0}$and C_{L_α} that satisfy this relationship (if one value increases, the other

can decrease to result in the same relationship). Therefore, there is no way to uniquely determine these parameters; either more data or more equations would be needed.

Observability/Identifiability for an *n*-dimensional LTI system (see Equations (21) and (22)) is easily quantifiable by examining the rank of the observability matrix given by:

$$Q_o = \begin{bmatrix} C \\ CA \\ CA^2 \\ \vdots \\ CA^{n-1} \end{bmatrix} \tag{44}$$

If this matrix has rank *n*, then the system is locally observable, and since the system is time-invariant, also globally observable for all time [64] [65]. For the example above, it can be shown that this matrix is rank deficient. We can translate the system described in Equation (43) into state-space form:

$$\begin{bmatrix} C_{L_0} \\ C_{L_\alpha} \\ \alpha \\ C_L \end{bmatrix} = \begin{bmatrix} C_{L_0} \\ C_{L_\alpha} \\ \alpha \\ C_{L_0} + C_{L_\alpha}\alpha \end{bmatrix} \tag{45}$$

$$\begin{bmatrix} \alpha \\ C_L \end{bmatrix} = \begin{bmatrix} 0 & 0 & 1 & 0 \\ 0 & 0 & 0 & 1 \end{bmatrix} \begin{bmatrix} C_{L_0} \\ C_{L_\alpha} \\ \alpha \\ C_L \end{bmatrix} \tag{46}$$

For a given measurement, $[\alpha_1, C_{L_1}]^T$, this system can be linearized into:

$$\begin{bmatrix} C_{L_0} \\ C_{L_\alpha} \\ \alpha \\ C_L \end{bmatrix} = \begin{bmatrix} 1 & 0 & 0 & 0 \\ 0 & 1 & 0 & 0 \\ 0 & 0 & 1 & 0 \\ 1 & \alpha_1 & C_{L_\alpha} & 0 \end{bmatrix} \begin{bmatrix} C_{L_0} \\ C_{L_\alpha} \\ \alpha \\ C_L \end{bmatrix} \tag{47}$$

$$\begin{bmatrix} \alpha \\ C_L \end{bmatrix} = \begin{bmatrix} 0 & 0 & 1 & 0 \\ 0 & 0 & 0 & 1 \end{bmatrix} \begin{bmatrix} C_{L_0} \\ C_{L_\alpha} \\ \alpha \\ C_L \end{bmatrix} \tag{48}$$

The observability matrix in Equation (44) can then be calculated as:

$$Q_o = \begin{bmatrix} 0 & 0 & 1 & 0 \\ 0 & 0 & 0 & 1 \\ 0 & 0 & 1 & 0 \\ 1 & \alpha & C_{L_\alpha} & 0 \\ 0 & 0 & 1 & 0 \\ 0 & 0 & 0 & 1 \\ 0 & 0 & 1 & 0 \\ 1 & \alpha & C_{L_\alpha} & 0 \end{bmatrix} \tag{49}$$

The rank of this matrix is 3 (rows 1-4 are identical to rows 5-8, and row 1 is identical to row 3), and therefore the system is not observable according to the rank condition given in Equation (44). Even in this simple example, the nonlinear system is unobservable; therefore, it cannot be expected, in general, that a nonlinear system is completely locally observable at any single time-step. However, intuition dictates that nonlinear systems may be completely observable over a set of data.

There is no standard criterion by which the observability of a nonlinear system can be determined. However, methods have been used to determine the identifiability of constant parameters in SysID by deriving an extension of this criteria to discrete measured systems [64] [66] [67]. The intuition behind this criterion can be explained with the example above. It was shown already that the system is not, in general, observable using the rank condition. However, under the assumption that C_{L_0} and C_{L_α} are constant over a certain batch of data, it can easily be seen that any two distinct measurements $[\alpha_1, C_{L_1}]$ and $[\alpha_2, C_{L_2}]$, will allow easy calculation of both $C_{L_0}$and C_{L_α}, making the system identifiable.

This is equivalent to examining the rank of a "stacked" observation matrix, in which each entry is an observation matrix as computed above in Equation (44), replacing the A

and B matrices of the linear system with the Jacobians F_k and H_k of the nonlinear system (see Equation (42)):

$$Q_{o_k} = \begin{bmatrix} H_k \\ H_k F_k \\ H_k F_k^2 \\ \vdots \\ H_k F_k^n - 1 \end{bmatrix} \tag{50}$$

$$Q_{o_{stack}} = \begin{bmatrix} Q_{o1} \\ Q_{o2} \\ \vdots \\ Q_{oN} \end{bmatrix} \tag{51}$$

Similar to the LTI case, if this matrix has rank *n,* then the constant parameters are identifiable. This validates the intuition in the example above; any two distinct values of α will result in $Q_{o_{stack}}$ having full rank. Additionally, each individual observability matrix Q_{o_k} can be used to determine local observability of the system. The linearization of the nonlinear system, F_k and H_k, is a local approximation to the true system; therefore, it's observability condition is also a local approximation to the true observability [66] [68] [69].

Southall et. al. [66] discussed the impact of the identifiability condition given by $Q_{o_{stack}}$ on an EKF. It was shown that for an example where several observations are obtained with regards to an agricultural model, this identifiability condition not only determines whether the system is identifiable but gives also a lower bound for the number of measurements necessary to fully observe the system. Anguelova [64] performed a similar analysis but for more general nonlinear systems with applications in biology. In addition, the author showed that the non-identifiable parameters could be determined and assumed known *a priori* to limit the parameter set to only identifiable parameters, therefore

resulting in an observable system. Zhen Yao et. al. [67] derived and used the same condition for the design of experiments related to polymerization. A method was also explored for characterizing the parameters from "most identifiable" to "least identifiable", and characterizing the observable and unobservable subspaces of the system. Experiments could then be designed to explore unobservable spaces.

The above condition describes only structural identifiability, but in real measured systems, practical identifiability is also a concern [63]. Practical identifiability can only exist if the system is structurally identifiable AND the amount and quality of measured data is sufficient for obtaining "low" uncertainty of parameters. In the simple example discussed in Equation (43), structural identifiability can be guaranteed by assuming two distinct measurements of α, but if these measurements are noisy, practical identifiability may require much more than two observations. Raue et. al. [63] discusses methods for improving identifiability (both structural and practical) by reducing the model (removing or constraining unidentifiable parameters) or adding additional measurements to the system. In general, however, there is no existing method for determining if a system/experiment is practically identifiable *a priori*.

The structural observability criteria for nonlinear systems is still a useful tool for SysID and allows an exploration of valid parametrizations of an aircraft model. Given a set of measurement devices and a set of desired parameters to estimate, this technique can be used to determine if the parametrization is observable and identifiable prior to any experimentation. In the case of an observable/identifiable system, this condition ensures that the problem is structurally sound and has a unique solution. However, no guarantee is given that this solution can easily be found. In the case of a non-identifiable system,

adjustments can be made by removing redundant parameterizations [64], adding additional measurements [63], or designing experiments to explore the unobservable subspace if possible [67]. Additionally, if it is impossible or impractical to obtain an observable system, maximum likelihood estimation (MLE) using OEM or filter method may produce satisfactory results by restricting the possible values of unidentifiable parameters using probability distributions [39]. However, this requires additional *a priori* information and will not result in a unique solution to the SysID problem.

2.4 Control Inputs for System Identification

The SysID process for obtaining estimates for aircraft dynamic derivatives necessitates that the aircraft dynamics are excited with control inputs. Therefore, an important consideration for the aircraft SysID process is the quality of control inputs used. Several studies have been conducted to investigate the role of control input and accuracy of SysID. Morelli [51] studied SysID as a means to design control inputs in flight. Input types considered were conventional doublets, 2-1-1, and 3-2-1-1 input types. These inputs are well understood and documented in flight test SysID. Doublet inputs are typically designed to match the frequency of the dominant oscillatory mode. 2-1-1 inputs are designed such that the 2-1 pulses bracket this frequency. For 3-2-1-1 design, the 2 pulse is scaled to match the frequency of the dominant oscillatory mode, and the others are scaled accordingly. In [51], designs were sequential; maneuvers would be designed and performed in sequence with each subsequent maneuver design relying on the model obtained from the

previous input. This process was shown to be effective for parameter identification, and computationally practical for real-time maneuver design during flight test.

Gupta and Hall [70] investigated the design of optimal control sequences for aircraft SysID. Several considerations for optimal control design were discussed including: pilot acceptability, instrumentation, identification technique, modelling assumptions, aircraft structural constraints, and output sensitivity. In their work, optimal inputs were designed by minimizing functions of the covariance of parameter estimates. Like the previous study, maneuver design and implementation was carried out sequentially. However, the optimal input was not limited to square waves. The results showed the covariance of the parameter estimates decreased with each subsequent maneuver, and remained lower than the covariance estimates obtained from a simple doublet input.

Morelli [71] performed a comparison of optimal square-wave inputs (designed using a similar method as above) and more conventional doublet and 3-2-1-1 inputs. Maneuvers were restricted to square waves to meet the pilot-acceptability criteria above (it is easier and more repeatable for a pilot to perform a full-deflection square wave than to track a sinusoidal input). It was found that the optimal square-wave input reduced parameter covariances by an additional 20% compared to the 3-2-1-1 input and an additional 64% compared to the doublet. It was determined that a properly designed 3-2-1-1 input sequence obtains adequate parameter identifiability while avoiding the computational expense of finding the optimal input and the complexity of accurately executing the optimal maneuver.

Similarly, Plaetschke et. al. [72] performed a comparison between several input types, including conventional doublet and 3-2-1-1 as well as more sinusoidal-type inputs

such as Mehra, Shulz, and DUT inputs. All inputs were designed to minimize the covariance of the parameter estimates. This study concluded that the high-frequency doublet and 3-2-1-1 inputs performed better for parameter identification for the aircraft considered. The research in these studies as well as others have led to the 3-2-1-1 input being widely used for the identification of aircraft parameters, especially when no *a priori* model is known to construct an optimal input [50] [56] [62].

In all studies discussed thus far, it is assumed that the control inputs are designed and known. An interesting challenge in SysID arises in cases where the inputs may not be known, or are measured imprecisely. This is closely related to the observability and identifiability of parameters discussed in the previous section. Linder [73] discusses this problem and its surrounding literature, which focuses on four main mitigations strategies:

1. Estimate the unknown input (known as "blind" SysID)
2. Neglect the input (treat inputs as noise or disturbances)
3. Reconstruct the input using other parameters (add relationships to the model)
4. Measure the input

These are similar to the mitigations for unobservable systems discussed in the previous section. In [73], Linder develops a unique approach that partitions the model into "direct" and "indirect" sub-models, which can be used in conjunction with one another to eliminate the unknown control input from the estimation problem. The result was that no single dataset could be used for parameter identification, but several sets of data could be used in conjunction to estimate the system dynamics. Harrison [39] discusses the use of maximum

likelihood estimation for estimating control inputs. If observable, unknown controls can be estimated in this manner, although additional computational expense may be required.

CHAPTER 3. PROBLEM FORMULATION

CHAPTER 1 discussed the usefulness of accurate aircraft models in GA and the potential of SysID methods for obtaining and updating these models. CHAPTER 2 discussed SysID methods and examples of their application to the aircraft SysID problem. This chapter will focus on the development of research questions, hypotheses, and experiments that must be addressed to complete the research objective, restated here:

Research Objective:

Determine the requirements, capabilities, and limitations of existing System Identification methods and their application to General Aviation aircraft flight data obtained through a low-cost Flight Data Recorder or Personal Electronic Device.

Given the diversity of GA aircraft, SysID methods, and possible sensors to consider, the scope of work needed to fully investigate this objective is rather large. As such, several assumptions have been made in this work to make the problem tractable:

- Focus will be placed on only small fixed-wing GA aircraft. In particular, the models developed are representative of a Cessna 172 airplane
- Equations of motion for simulated aircraft as well as SysID models will follow the dynamics formulation of Section 2.1. Note that this is not the only way to express the equations of motion, and that other parameterizations may be utilized. However, for the remainder of the work, the following parameters should be defined:

    - Aircraft State will include all inertial positions, velocities, and accelerations, both linear and rotational
    - Control Inputs will only include aileron, elevator, rudder, and throttle
    - Air Data will refer to four quantities: three components of wind velocity in NED axes, and ambient density
    - Weight and Balance data or Configuration Data will refer to the six point masses described in the aircraft model of Section 4.1.1: pilot, copilot, two passengers, baggage, and fuel
    - Aerodynamics will be represented as linear air reaction stability and control coefficients as discussed in Section 2.1
- Although all the SysID methods explored in CHAPTER 2 are applicable to both time-domain and frequency-domain models, only time-domain models are considered in this work
- Sensors considered will only be those that may be reasonably and inexpensively acquired or installed on a small fixed-wing aircraft

The overall research hypothesis with regards to the overall research objective can be stated as follows:

Research Hypothesis: *Existing System Identification methods applied to low-cost Flight Data Recorder or Personal Electronic Device data from a General Aviation aircraft will enable accurate 6-Degree-of-Freedom models of fixed-wing aircraft to be determined.*

To address this hypothesis, several research questions must be answered and are developed in the following sections.

3.1 Identifiability of Aircraft Model

As discussed in CHAPTER 2, one of the primary considerations for any SysID or state-estimation process is the observability or identifiability of the parameters. Identifiability requires that each estimated quantity produces a unique effect on the measured outputs of the system. Aircraft dynamics can be represented in potentially infinite ways, using any number of parameters. Deriving a parameterization of the aircraft dynamics that is identifiable and useful for the considerations discussed in CHAPTER 1 is therefore a necessary first step. Besides the structure of the model, identifiability also depends on the types of measurements considered. For GA aircraft, data may be limited to only a low-cost FDR or PED, and therefore an investigation is required to determine identifiable model-measurement pairs before SysID can be applied. In the case that a certain parameterization is not identifiable, methods for mitigating unidentifiable systems may be applied. These are discussed in Section 2.3, but are summarized here:

1. Remove redundant\unobservable parameters
2. Add measurements
3. Make additional assumptions to remove unknowns
4. Use MLE on non-identifiable system to restrict parameter values

There are several types of information that affect aircraft dynamics and may be included either explicitly or implicitly in the model. For this work, standard

parameterizations from Etkin [46] are used (these are discussed in more detail in CHAPTER 4). The dynamics are modelled using the following types of information:

- Aircraft State (position, velocity, orientation, etc.)
- Control inputs
- Air data (wind direction, air density)
- Weight and balance data (CG location, mass, moments of inertia)
- Stability and control derivatives

Aircraft state, controls, and air data are quantities that define the aircraft trajectory. These quantities can be considered to change rapidly (time-dependent) in comparison to weight and balance data and stability and control derivatives which may be assumed relatively constant over a given time (time-independent). In a blind SysID process using PED data, very few of the above quantities are measured directly. Instead, these values must be either estimated or assumed known. Estimation is only possible if the quantities are observable/identifiable. Specifically, quantities that are time-dependent such as aircraft state must be locally observable, whereas quantities that are time-independent must be at least globally identifiable if not locally observable. Ideally, all quantities would be measured or estimated to eliminate reliance on potentially inaccurate *a priori* information. In practice however, limited measurements, and therefore limited observability, make this impossible. Therefore, it is necessary to determine the set of observable quantities and identifiable parameters and the set which is not observable/identifiable. This prompts the formulation of Research Questions 1(a) and 1(b):

Research Question 1(a):

Which quantities in the parameterization of General Aviation aircraft dynamics are locally observable using measurements obtained from a low-cost Flight Data Recorder or Personal Electronic Device?

Research Question 1(b):

What parameterizations of General Aviation aircraft dynamics are globally identifiable using measurements obtained from a low-cost Flight Data Recorder or Personal Electronic Device?

In answering the research questions above, a parametrization (or multiple) of aircraft dynamics will be derived that can be used for SysID. The purpose of this exercise is to determine what subsets of the information of interest can be estimated, both locally and globally. Additionally, an investigation can be carried out to determine what sensors might be needed to increase the set of identifiable parameters. Lastly, the assumptions that are necessary to obtain an identifiable model can be examined and their effect on the SysID process explored. This is the basis for Experiment 4, which is discussed later in this chapter.

Research Question 1(a) examines the local observability of parameters. This is a necessary condition for online estimation or filtering using a standard Extended Kalman Filter (EKF) and is discussed in more detail in Section 2.3. For quantities that are never locally observable, the EKF will not converge to any meaningful result. However, globally identifiable parameters can be estimated using other techniques, such as regression, Output Error Method (OEM), or EKF variants that operate on "batches" of data instead of single

points [66]. In either case, answering Research Question 1(a) will reveal which quantities can be estimated online, whereas Research Question 1(b) will reveal which can be estimated using "batching" or post-processing.

As discussed above, the aircraft state, control inputs, and air data define the aircraft trajectory. It is therefore desirable that these quantities are locally observable. Inertial sensors are often used for navigation state estimation problems, and it is therefore highly likely that the aircraft states will be locally observable using inertial PED data. Harrison [39] discusses applications of successful control estimation, so it is likely also that control inputs will be locally observable. Studies such as Sembiring et. al. [4] and Morelli [5] have shown that angle of attack and sideslip can be estimated in real time without direct measurements of airflow. Therefore, Hypothesis 1(a) can be formulated below:

Hypothesis 1(a): *If only Personal Electronic Device sensor data is used, Aircraft State, Control Inputs, and Air Data will be locally observable.*

As discussed at the beginning of this chapter, aircraft state refers to the inertial position, velocity, and acceleration (both linear and rotational) of the aircraft body. Control inputs will refer to only aileron, elevator, rudder, and throttle. Air Data will refer to the three components of wind velocity in the NED frame and ambient air density.

Hypothesis 1(a) can be tested by applying the local observability condition given by Equation (50). For a given trajectory (from simulation), the system model can be linearized with respect to these parameters and the local observability matrix constructed for each point in the trajectory. The rank of this local observability matrix will determine how many

quantities are locally observable at each time step, therefore determining not only if the state, controls, and air data are observable, but at which points along the trajectory they are observable. This forms the basis for experiment 1(a), the results of which are given in Section 5.1.1. It is important to note the dependency on the trajectory itself. If a certain quantity appears to be nowhere locally observable, this could mean either that the variable is indeed unobservable given the measurement types available or that the trajectory for which this condition was computed is insufficient for estimating that parameter. Control input design for aircraft SysID problems as discussed in Section 2.4 often seek to maximize the observability of the parameters. However, no control design was conducted in this study beyond adopting typical SysID control input sequences as discussed in Section 4.1.3. However, these inputs have been shown to be successful for aircraft SysID and the resulting trajectory can therefore be considered adequate for the purposes of this experiment. Hypothesis 1(a) will therefore be validated if the state, controls, and air data are locally observable along at least a portion of the trajectory; if any quantities are nowhere locally observable, Hypothesis 1(a) will be invalidated.

Research Question 1(b) is parallel to 1(a) but for the globally identifiable case. Globally identifiable parameters may not be locally observable, but the reverse is guaranteed to be true. Therefore, state, controls, and air data in hypothesis 1(a) will not be duplicated in the discussion of global identifiability; if hypothesis 1(a) is correct, these quantities are guaranteed to be globally identifiable. Instead, only weight and balance data and stability and control parameters will be discussed.

The example observability problem in Section 2.3 illustrated that local observability for stability and control derivatives in a nonlinear model is likely never guaranteed. A

similar argument can be made for weight and balance data. However, for both categories, it is reasonable to assume that they remain constant over short periods and may therefore be globally identifiable without being locally observable. This assumption cannot be made for state variables, and in general is likely to be invalid for control inputs and air data as well, motivating the use of the local observability condition for these quantities in Experiment 1(a).

It is not likely that both the weight and balance data and the stability and control derivatives will be together globally identifiable. Rather, only one or the other may be observed at a given time. Aircraft motion is primarily governed by Newton's second law; at "bird's-eye" view, the stability and control derivatives characterize the forces, weight and balance characterizes the mass, and the accelerations are measured using the PED. Therefore, both increased force or decreased mass can cause the same output. In other words, neither produces a unique effect on the output, and they are therefore not together globally identifiable. However, if either is assumed known, the other can likely be estimated. This leads to the formulation of hypothesis 1(b) as follows:

Hypothesis 1(b): *If only Personal Electronic Device sensor data is used, weight and balance data and stability and control derivatives will not be together globally identifiable. However, if one is assumed known, the other will be globally identifiable.*

This hypothesis can be tested by applying the global identifiability rank condition for a given trajectory, as described by Equation (51) in Section 2.3. At each point in the trajectory, the local observability condition can be constructed for the given quantities. This

is a necessary step for creating the global observability matrix and can also validate or invalidate the assumption that these parameters are not locally observable. The global condition can be constructed by appending all local observability matrices. This identifiability condition can be constructed for the stability and control parameters alone, weight and balance alone, and both together, therefore exploring hypothesis 1(b). Hypothesis 1(b) will be validated if the stability and control parameters are identifiable under the assumption of known weight and balance data; otherwise, Hypothesis 1(b) will be invalidated.

The importance of the two experiments just discussed cannot be overstated. In a typical aircraft SysID process, these steps are often trivial and therefore overlooked. However, the GA SysID problem is much more limited by type and quality of data. In this case, the results of these experiments will provide insight into which quantities can be estimated in real time (locally observable), which must be estimated using post-processing or "batching" (globally identifiable but not locally observable), and which cannot be estimated at all (neither globally nor locally observable). For the latter, the mitigation strategies discussed at the beginning of this section must be employed until a fully observable and identifiable system is derived. If such a system is found (all quantities under estimation locally and/or globally identifiable), then the existence of a unique solution to the estimation problem (and SysID problem) is guaranteed. In other words, the local and global observability condition guide the construction of a SysID problem that is well posed with regards to available measurements, aircraft trajectory, control inputs, and model structure. Without this procedure, there would be no guarantee that SysID of GA aircraft using the proposed methods has a solution. However, even if the existence of this solution

is shown through the above experiments, there is no guarantee that the methods, measurements, and assumptions utilized will produce meaningful results. Therefore, additional research questions are needed to address the research objective.

3.2 Comparing System Identification Methods

Aside from the model structure, SysID is also dependent on the method utilized. As discussed in CHAPTER 2, several possible methods exist. Research Question 2 is therefore:

Research Question 2

Which method of System Identification is best suited for accurately determining a 6-Degree-of-Freedom model of a General Aviation aircraft from a low-cost Flight Data Recorder or Personal Electronic Device?

The research discussed in CHAPTER 2 included benefits and limitations of each method. These are summarized in Table 2 below:

Table 2. Comparison of System Identification Methods

Method	Benefits	Limitations
Equation Error	• Computationally inexpensive • Easy implementation	• Only linear models considered • Requires knowledge of trim conditions
Output Error	• Works for nonlinear models • Maximum likelihood estimation	• Computationally expensive • Not suited for online estimation
Filter	• Computationally inexpensive • Accounts for noise • Ideal for online estimation	• Requires tuning procedure • Can perform poorly for highly nonlinear systems
ANN	• No knowledge of model structure required	• Model parameters do not represent physical quantities

One of the primary motivations for this work is SysID's potential for increasing knowledge of LOC events, which are highly-nonlinear in nature. Therefore, Equation Error, which must use a linear model, will not be explored further in this work. Additionally, ANN methods do not provide any physical understanding of the system as they are a purely mathematical approach. Therefore, only Output Error Method (OEM) and filter method will be considered. Because nonlinear dynamics are of interest, the Extended Kalman Filter (EKF) will be the basis of filter method. Previous studies have shown successful aircraft SysID with both techniques. However, these methods have yet to be applied to the blind SysID problem for GA aircraft using PED data.

An investigation is therefore necessary to determine which of these methods is best applied to the current research objective. Research discussed in CHAPTER 2 indicates that

both OEM and EKF can be used on nonlinear systems and account for probability/noise. However, OEM is computationally more expensive, and is therefore typically not implemented in real-time. In cases where online estimation is required, such as estimation of control inputs or air data, EKF method seems like the obvious choice. However, because EKF is not an optimal estimator, and is known to produce poor results for highly nonlinear systems, it is likely that post-processing data using OEM will provide higher accuracy for estimates of model parameters.

Hypothesis 2: *Post-processing data using Output Error System Identification will provide higher accuracy for stability and control parameters than online estimation using Extended Kalman Filter System Identification*

The observability study from the previous section can give an initial indication of how these methods will perform by characterizing the locally observable and globally identifiable subspaces. However, the results of this experiment will demonstrate only structural observability; practical observability and the accuracy of the results of these processes cannot be determined from the observability conditions alone. Therefore, an additional experiment is needed to address Hypothesis 2. Using data from the simulated aircraft trajectory and simulated measurements, both OEM and EKF SysID methods can be applied and the results of the two methods compared. Several metrics can be used for the comparison of these methods to address Hypothesis 2.

The stability and control parameters of the aircraft are the parameters that describe the aerodynamic forces and moments, and therefore the accelerations, that act upon the aircraft. Using a simulator environment, the true accelerations along a trajectory can be

compared to those predicted by the identified models from OEM and EKF SysID. The accuracy of these predicted accelerations should improve using both methods (both are minimizing the error in these exact states) but the amount of improvement can be compared to determine which method performs better. However, this metric does not provide enough information to fully address the hypothesis; other comparisons must also be conducted.

The second comparison is a direct parameter-to-parameter comparison for the stability and control derivatives. These values are known for the "true aircraft" (simulated aircraft), and are being estimated by the SysID process using data produced by the "true aircraft". Therefore, a direct comparison is possible and can be used to assess SysID performance. The third and fourth metrics pertain to the "usefulness" of the SysID results for predicting aerodynamic performance (lift and drag polars) and stability characteristics (longitudinal and lateral modes for a given trim point). Once again, the true values from the simulated aircraft can be compared to the estimated values from both SysID methods.

Hypothesis 2 can be addressed by comparing the performance (described by the above metrics) of OEM and EKF SysID for the same set of data. Hypothesis 2 will be validated if OEM outperforms EKF in most metrics, and invalidated if the reverse is true or if the two methods appear to perform nearly equivalently. Addressing this hypothesis will then answer Research Question 2; if OEM outperforms EKF (or vice versa) then this method is better suited for SysID of GA aircraft from PED data.

3.3 Effect of Sensor Quality

Both OEM and EKF method rely on estimated aircraft states and controls to create the model. In general, these estimates come from processing sensor measurements through some filtering algorithm such as an EKF. In EKF SysID, the state estimates and model parameters are obtained simultaneously in the same filter. For OEM, state and control estimates are needed prior to execution of the minimization; therefore, some *a priori* model should be used in an EKF to estimate only states and controls. In a real-world application of OEM, this *a priori* model would likely be an initial guess from manufacturer data or have come from a previous OEM SysID routine. This initial guess would be used to generate state and control estimates, and those estimates post-processed using OEM to update the model. A similar routine will be employed here and is discussed in more detail in CHAPTER 4.

In either case, the SysID methods will depend on the quality of the measurement data. This is especially important for GA SysID using low-cost FDRs and PEDs because the measurements are of limited type and lower quality than the more robust FDRs typically used for flight testing SysID. The effect of measurement type on observability will be investigated in Experiment 1. However, the quality of measurements must also be assessed to determine feasibility of SysID in GA. Therefore, Research Question 3 must be answered:

Research Question 3

What requirements on sensor quality are needed to improve *a priori* model accuracy through System Identification?

Previous research has shown that low-cost FDR and PED sensors are accurate enough for data-driven safety efforts. However, the quality of measurements afforded by these devices has yet to be assessed in a SysID process. Additionally, applications for PEDs often recommend the inclusion of an additional AHRS or GPS unit to improve the quality of data [10] [24]. Given that these devices have been utilized as FDRs, it is likely that their use for SysID will provide adequate results. Therefore, the following hypothesis to address Research Question 3 can be constructed:

Hypothesis 3: *If measurements are obtained with only low-cost Flight Data Recorders or Personal Electronic Devices, improvement in an a priori model can be achieved using System Identification.*

To test this hypothesis, sensor data from these devices can be simulated for a given trajectory and used in the SysID methods discussed in the previous section. If improvements in the *a priori* model are obtained, then Hypothesis 3 will be validated. The results can also be compared to those of the previous experiment, in which near-perfect

sensors will be assumed. This forms the basis of Experiment 3, the results of which are discussed in Section 5.3.

It should be noted that to fully address Research Question 3, several cases would have to be conducted for varying sensor quality such that the relationship between sensor quality and SysID results could be quantified in more detail. However, the computational burden to carry this out is not trivial. As discussed in Section 4.3, filter performance is not only a function of sensor quality, but also of filter tuning. In general, filter tuning algorithms can be computationally expensive, not to mention the computation time needed to carry out SysID. Therefore, Experiment 3 will only assess two cases: the near-perfect sensors of Experiment 2, and PED sensors in Experiment 3. For the purposes of this study, it will be assumed that this is adequate to characterize the effect of sensor quality on SysID.

3.4 Robustness of Method to Inaccuracies in the Model

The last step in addressing the research objective deals with the robustness of the proposed processes. Experiments 1(a) and 1(b) will yield a model structure that can be used for Experiments 2 and 3; however, this model will include assumptions that may or may not be known or accurate. In cases where these assumptions break down, it is important to understand how this will affect the results of SysID.

Research Question 4

How sensitive are General Aviation aircraft System Identification results to assumptions made in the system model?

Assumptions that have been used in forming the model structure in Experiment 1(a) and 1(b) can be assessed by perturbing them with uncertainty and observing the effect on the SysID process. However, given that many real-world applications of SysID have been successful even under uncertainty, it is not unreasonable to predict that SysID results will be somewhat robust to the accuracy of assumptions in the model, so long as those assumptions are relevant for the operation considered. However, results will certainly change as the accuracy of these assumptions is varied.

Hypothesis 4: *If the assumptions in the system model are within reasonable limits under conditions typical of General Aviation operations, improvement in an a priori model can be achieved using System Identification.*

It is difficult to formulate a more concrete hypothesis and experimental procedure without first understanding what assumptions need to be investigated. Therefore, before the results of Experiment 4 are presented, the results of Experiment 1 will be used to revise Research Question 4 and Hypothesis 4. This discussion is included in Section 5.4.

CHAPTER 4. METHODOLOGY

The experiments discussed in the previous chapter were carried out using simulation in MATLAB/Simulink 2017b. A flight vehicle simulation was used to simulate aircraft motion and trajectories, and is described in Section 4.1, along with the atmospheric modelling used and the designed control inputs for SysID. Sensor simulations were used to simulate measurements from an FDR or PED as well as some additional sensors. The equations used to simulate sensor output are described in Section 4.2. Two different SysID methods were then implemented: Output Error Method (OEM) and Extended Kalman Filter method (EKF). For OEM, a state-estimation process using a separate EKF was utilized to filter the measurements from the sensor simulation, similar to the "subspace" SysID method in [57]. This is described in Section 4.3. Section 4.4 provides the details on both the OEM and EKF SysID implementation. Lastly, Section 4.5 discusses the construction of the observability/identifiability test. The simulation architecture is shown below in Figure 8.

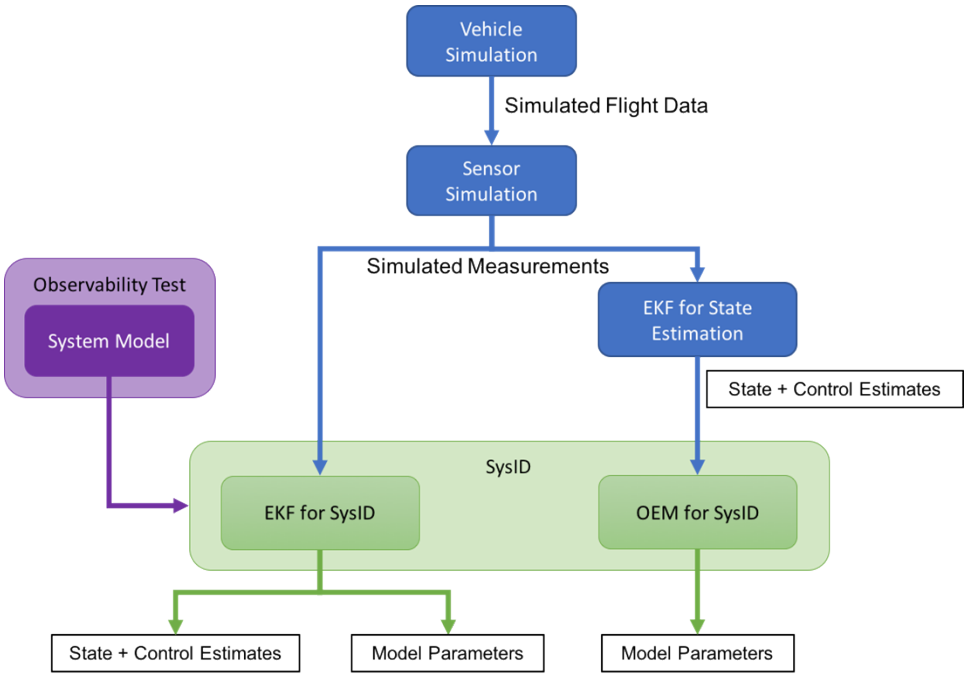

Figure 8. Simulation Architecture

4.1 Vehicle Simulation

4.1.1 Aircraft Model

The aircraft model used in this work is based on a Cessna 172P. Data from Flight Gear Desktop Simulator's (FGDS) nonlinear Cessna model [48] and Scott and Selig's simplified constant-coefficient model [49] was used to create the simulation. Pertinent aircraft geometry and weight characteristics were taken from FGFS are shown in the three-view in Figure 9 and summarized in Table 3 and Table 4 below:

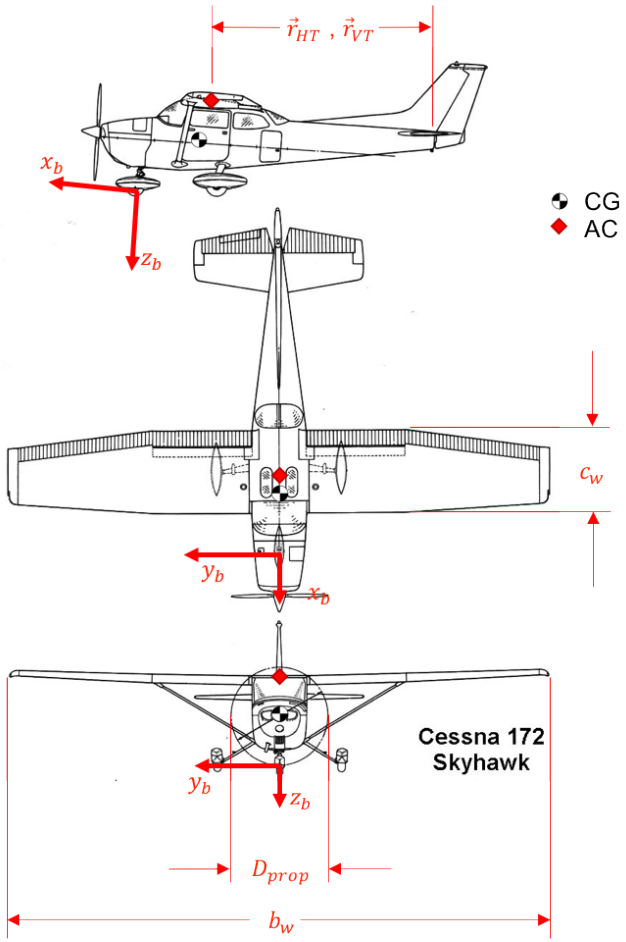

Figure 9. Cessna 172 Three-View

Table 3. Cessna 172P Geometry

Parameter	Value	Units	Description
S_w	174	ft^2	Wing reference area
b_w	35.8	ft	Wingspan
c_w	4.9	ft	Mean aerodynamic chord
S_{HT}	21.9	ft^2	Horizontal tail reference area
S_{VT}	16.5	ft^2	Vertical tail reference area
$\vec{r}_{CG}$	-	in	Center of gravity (CG) location

Table 3 (Continued). Cessna 172P Geometry

$\vec{r}_{AC}$	$\vec{r}_{xAC}$	-40.6	in	Aerodynamic center (AC) location
	$\vec{r}_{yAC}$	0	in	
	$\vec{r}_{zAC}$	-59.4	in	
$\vec{r}_{HT}$		15.7	ft	Distance between horizontal tail and AC
$\vec{r}_{VT}$		15.7	ft	Distance between vertical tail and AC
D_{prop}		75	in	Propeller diameter

Table 4. Cessna 172P Weight and Balance

Component	**Weight (lb)**	$\vec{r}_x$ **(in)**	$\vec{r}_y$ **(in)**	$\vec{r}_z$ **(in)**
Empty Aircraft	1467	-39.06	0	-36.5
Pilot	180	-36	-14	-24
Copilot	180	-36	14	24
Left Passenger	0	-70	-14	-24
Right Passenger	0	-70	14	-24
Bags	0	-95	0	-24
Initial Fuel	240	-56	0	-59.4

Empty Inertia		
I_{xx} **($slug \times ft^2$)**	I_{yy} **($slug \times ft^2$)**	I_{zz} **($slug \times ft^2$)**
948	1285	1906

Modelling of the mass properties assumes each component is a point mass. This is similar to the formulation in FGDS. However, FGDS models fuel as a distributed mass, whereas in this work, this is simplified as a point mass. The weight and balance configuration given in Table 4 above was used throughout this study. Moments of inertia were calculated from the point masses using Equation (52), where $\vec{r}_{cg_i}$ is the vector from each component to the center of gravity:

$$I_{tot} = I_{empty} + \sum m_i \vec{r}_{cg_i}^2 \tag{52}$$

The aerodynamic model used is a combination of constant-coefficients from Scott and Selig [49] and nonlinear lift and drag characteristics from FGFS [48]. In reality, no model will ever completely duplicate a real system; since the "real system" in this work is itself a model, it was deemed necessary to include higher-order nonlinearities in certain variables to approximate this effect. The coefficients utilized in the aerodynamic force buildups are the same as in Equations (12) through (17), duplicated below. The corresponding values for the coefficients for the are shown below in Table 5. Note that no values are specified for K_{CL}, C_{L_0}, and C_{L_α}. These are the nonlinear terms from FGDS [48], and are plotted as functions of AoA in Figure 10.

Drag
$$C_D = C_{D_0} + K_{C_L}(C_L - C_{L_0})^2 + C_{D_\beta}\beta + C_{D_{\delta_e}}\delta_e \tag{12}$$

Side-force
$$C_Y = C_{Y_\beta}\beta + C_{Y_p}p\left(\frac{b_w}{2V_\infty}\right) + C_{Y_r}r\left(\frac{b_w}{2V_\infty}\right) + C_{Y_{\delta_r}}\delta_r \tag{13}$$

Lift
$$C_L = C_{L_0} + C_{L_\alpha}\alpha + C_{L_{\dot\alpha}}\dot\alpha\left(\frac{c_w}{2V_\infty}\right) + C_{L_q}q\left(\frac{c_w}{2V_\infty}\right) + C_{L_{\delta_e}}\delta_e \tag{14}$$

Roll
$$C_L = C_{L_\beta}\beta + C_{L_p}p\left(\frac{b_w}{2V_\infty}\right) + C_{L_r}r\left(\frac{b_w}{2V_\infty}\right) + C_{L_{\delta_a}}\delta_a + C_{L_{\delta_r}}\delta_r \tag{15}$$

Pitch
$$C_M = C_{M_0} + C_{M_\alpha}\alpha + C_{M_{\dot\alpha}}\dot\alpha\left(\frac{c_w}{2V_\infty}\right) + C_{M_q}q\left(\frac{c_w}{2V_\infty}\right) + C_{M_{\delta_e}}\delta_e \tag{16}$$

Yaw
$$C_N = C_{N_\beta}\beta + C_{N_p}p\left(\frac{b_w}{2V_\infty}\right) + C_{N_r}r\left(\frac{b_w}{2V_\infty}\right) + C_{N_{\delta_a}}\delta_a + C_{N_{\delta_r}}\delta_r \tag{17}$$

Table 5. True Aircraft Parameters

Drag	C_{D_0}	.027	**Roll**	C_{L_β}	-0.092
	K_{C_L}	-		C_{L_p}	-0.47
	C_{D_β}	0		C_{L_r}	0.096
	$C_{D_{\delta_e}}$(rad)	0.06		$C_{L_{\delta_a}}$(rad)	-0.178
	-	-		$C_{L_{\delta_r}}$(rad)	0.0147
Side-Force	C_{Y_β}	-0.31	**Pitch**	C_{M_0}	-0.015
	C_{Y_p}	-0.037		C_{M_α}	-0.89
	C_{Y_r}	0.21		$C_{M_{\dot{\alpha}}}$	-5.2
	$C_{Y_{\delta_r}}$(rad)	0.187		C_{M_q}	-12.4
	-	-		$C_{M_{\delta_e}}$(rad)	-1.28
Lift	C_{L_0}	-	**Yaw**	C_{N_β}	0.065
	C_{L_α}	-		C_{N_p}	-0.03
	$C_{L_{\dot{\alpha}}}$	1.7		C_{N_r}	-0.099
	C_{L_q}	3.9		$C_{N_{\delta_a}}$(rad)	-0.053
	$C_{L_{\delta_e}}$(rad)	0.43		$C_{N_{\delta_r}}$(rad)	-0.0657

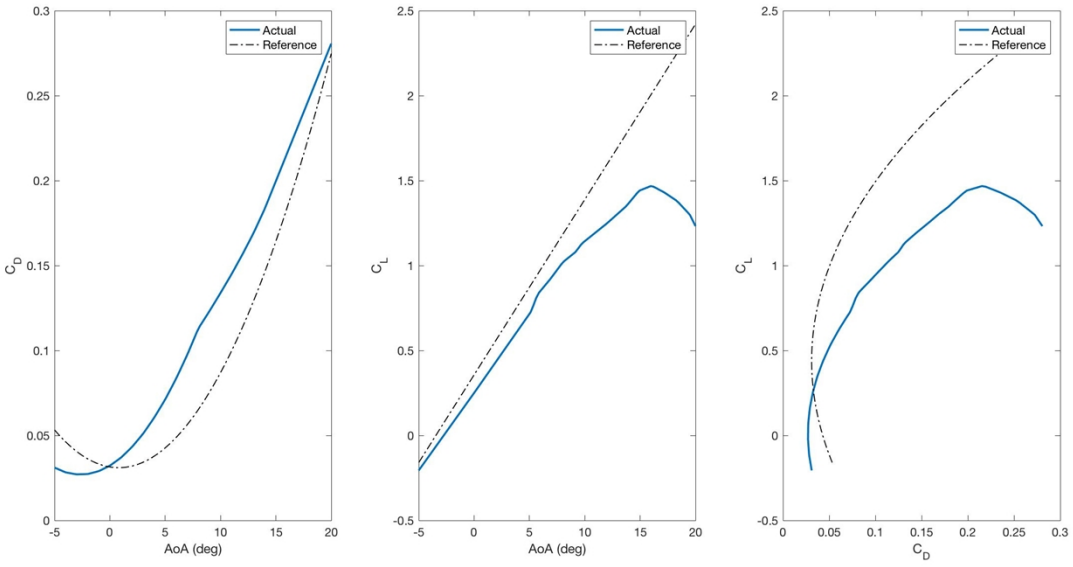

(a) (b) (c)

Figure 10. True Aircraft Lift and Drag Curves

In addition to the true aircraft, an approximation to the true aircraft was derived to simulate *a priori* knowledge of the vehicle dynamics. As discussed in CHAPTER 1, aircraft models may already exist for certain GA aircraft. These models may be estimates from the manufacturer, a similar aircraft, or calculated using analytical methods. In any case, these models may be subject to error. SysID seeks to obtain higher-accuracy models; hence, an *a priori* approximation to the true model can be used as a comparison to the results from SysID. This will be discussed in more detail in CHAPTER 5, but the parameters of the reference model are listed below in Table 6. These values were obtained by perturbing the true aircraft parameters by a positive 15% increment.

Table 6. Reference Aircraft Parameters

Drag	C_{D_0}	0.0311	**Roll**	C_{L_β}	-0.1058
	K_{C_L}	0.0621		C_{L_p}	-0.5405
	C_{D_β}	0		C_{L_r}	0.1104
	$C_{D_{\delta_e}}$	0.031		$C_{L_{\delta_a}}$	-0.0715
	-	-		$C_{L_{\delta_r}}$	0.0047
Side-Force	C_{Y_β}	-0.3565	**Pitch**	C_{M_0}	-0.0172
	C_{Y_p}	-0.0426		C_{M_α}	-1.0235
	C_{Y_r}	0.2415		$C_{M_{\dot{\alpha}}}$	-5.9800
	$C_{Y_{\delta_r}}$	0.0601		C_{M_q}	-14.2600
	-	-		$C_{M_{\delta_e}}$	-0.6422
Lift	C_{L_0}	0.3565	**Yaw**	C_{N_β}	0.0748
	C_{L_α}	5.9144		C_{N_p}	-0.0345
	$C_{L_{\dot{\alpha}}}$	1.9550		C_{N_r}	-0.1139
	C_{L_q}	4.4850		$C_{N_{\delta_a}}$	-0.0213
	$C_{L_{\delta_e}}$	0.2158		$C_{N_{\delta_r}}$	-0.0211

Note that the true aircraft control derivatives take deflections in terms of radians, whereas the reference model uses normalized control inputs. In the true aircraft model,

normalized inputs are scheduled using the following control deflection scheduling from FGDS [48]:

Table 7. True Aircraft Control Input Scheduling

Control	Minimum (-1) (deg)	Maximum (+1) (deg)
δ_a	-20	20
δ_e	-28	23
δ_r	-16	16

Lastly, both a true-aircraft and a reference-aircraft propulsion model were developed. The true-aircraft propeller power and thrust were replicated from the FGDS model [48] as a function of advance ratio, J. Normalized throttle inputs (0 to 1) were transformed into engine rpm (600 to 2700). Advance ratio is calculated from the component of airspeed in the body x direction, rpm, and propeller diameter:

$$J = \frac{u_\infty}{(rpm/60)D_{prop}} \tag{53}$$

For the true aircraft, thrust and power coefficients were determined from a lookup table as a function of advance ratio, J. These lookup tables were obtained from FGDS [48]. For the reference aircraft, a linear relationship was defined, shown in Equations (54) and (55). Both the true model and reference model are shown in Figure 11 below. For the true aircraft cruise speed and rpm, advance ratio is relatively low; these linear approximations work well for advance ratio between 0.5 and 1.5.

$$C_T = C_{T_0} + C_{T_J} J \tag{54}$$

$$C_P = C_{P_0} + C_{P_J} J \tag{55}$$

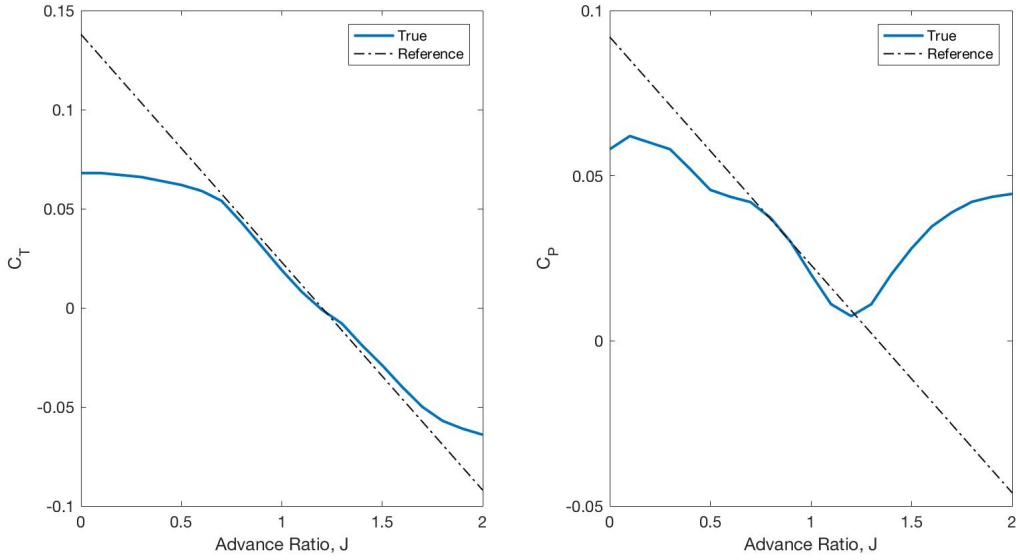

(a) (b)

Figure 11. Aircraft Thrust and Power Curves

From the coefficients, thrust, power, and torque can be calculated from Equations (56), (57), (58) respectively, where ω_{prop} is propeller rpm converted to radians per second:

$$T = C_T \rho \left(\frac{rpm}{60}\right)^2 D_{prop}^4 \tag{56}$$

$$P = C_P \rho \left(\frac{rpm}{60}\right)^3 D_{prop}^5 \tag{57}$$

$$\tau = \frac{P}{\omega_{prop}} \tag{58}$$

4.1.2 Atmospheric Model

Atmospheric conditions were modeled using MATLAB/Simulink's International Standard Atmosphere (ISA) and Dryden Wind Turbulence Model. Nonstandard temperature was used to correct the density output from the ISA function using the ideal gas law and the original pressure output. Only density is used in the simulation models, so this was deemed sufficient to simulate density fluctuations for nonstandard conditions. Winds aloft was specified using a wind speed, heading, and downdraft/updraft velocity. Wind velocities from the turbulence model were then added in. Most cases assume ISA with zero wind and no turbulence; in Experiment 4 however (Section 5.4), the effects of these phenomenon will be assessed.

4.1.3 Control Input Design

As discussed in Section 2.4, control inputs that adequately excite the dynamics to perform system identification. Several types of control inputs are used in aircraft SysID, including chirps, pulses, doublets, 2-1-1, 3-2-1-1, and optimally designed inputs, either square waves [71] or more sinusoidal [70] inputs. Comparisons of these inputs have been conducted to determine their suitability. 3-2-1-1 inputs are often used when optimal control inputs are not feasible, such as in non-automated systems or when dynamics are not known

well enough to perform input design [71]. Doublets (throttle only) and 3-2-1-1 pulses will be used in this work. Typically, 3-2-1-1 pulses are designed by matching the 2 pulse to the frequency of the dominant oscillatory mode. However, this requires *a priori* knowledge of dynamics. Therefore, in this work, 3-2-1-1 pulses will be scaled into seconds: 3 seconds, 2, 1, 1, similar to the application by Grillo and Fernando [56]. This also makes the control inputs easily implemented by a GA pilot, and therefore more representative of the scope of this work. Additionally, for the Cessna 172 model discussed above, both the short-period and Dutch roll frequencies are close to 0.5 Hz, making this approximation nearly ideal anyhow.

Control inputs were first staggered to allow the SysID process to individually determine the dynamics in each axis. A full sequence of inputs (throttle, elevator, aileron, rudder) will be referred to as a maneuver. Three maneuvers were performed, each with less staggering time than the previous. The last maneuver uses coincident inputs. Doublet inputs for throttle used 5-seconds of full-scale magnitude. Other control inputs had a magnitude of 5% control authority. This sequence was shown to produce an observable trajectory (see Section 5.1), required no closed-loop control to stabilize, and allowed repeatable SysID results to be obtained (see Section 5.2). The maneuver sequence and resulting trajectory are shown below in Figure 12 and Figure 13 and are used throughout the rest of the study.

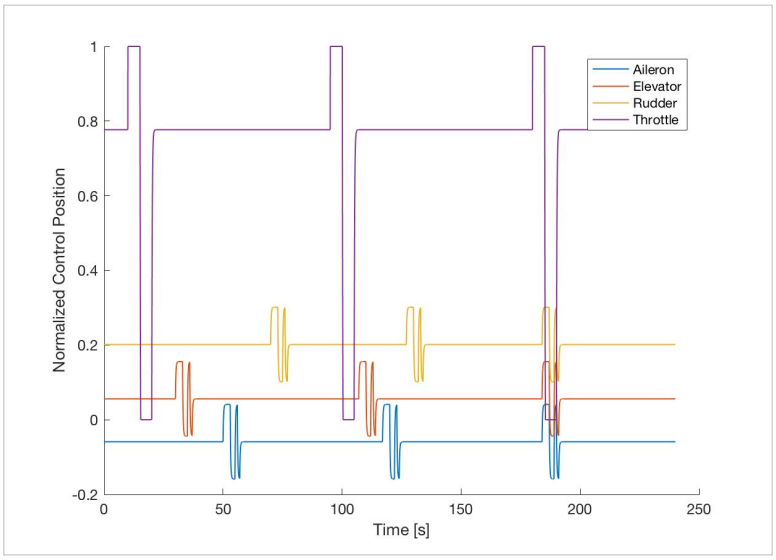

Figure 12. System Identification Control Input Sequence

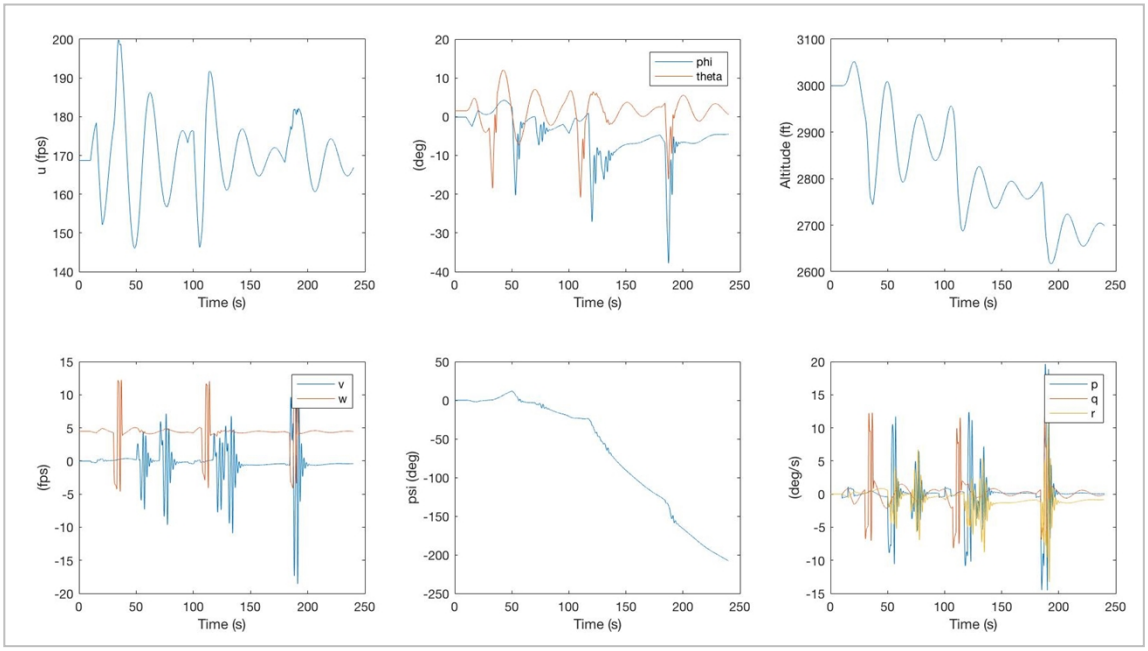

Figure 13. Aircraft Trajectory

4.2 Sensor Modelling

Sensor models were used to simulate measurements from a PED. The sensors considered were GPS, accelerometer, gyroscope, and magnetometer [15] [17]. Sensor quality was simulated using update rate, or frequency, and accuracy, or noise. Sensor noise was assumed to be zero-mean Gaussian white noise. In reality, other effects such as bias and scale-factor can cause erroneous measurements. However, these effects can often be calibrated out, especially for short timescales [43]. Therefore, for the purposes of this study, only noise was utilized. For the same reason, it has been assumed that the sensor location and mounting is perfectly known, allowing easy transformation of the measurements into the aircraft body-fixed reference frame.

GPS, gyroscope, altimeter, and magnetometer measurements are all direct measurements of the aircraft state (position, altitude, rotation rate, and orientation, respectively). Accelerometers, however, measure both the aircraft body linear acceleration and centripetal, in addition to the centripetal, Coriolis, and Euler accelerations due to the measurement device being offset from the aircraft CG. The total acceleration measured by an accelerometer offset from the CG by $\vec{r}_{cgk}$ is therefore:

$$\overrightarrow{a_k} = \dot{V}_k + (\omega_k \times V_k) + (\omega_k \times \omega_k \times (\vec{r}_{cgk})) + (\dot{\omega}_k \times \vec{r}_{cgk}) + 2\left(\omega \times \dot{\vec{r}}_{cg_k}\right) + DCM_{e2b}(\phi_k, \theta_k, \psi_k) \begin{bmatrix} 0 \\ 0 \\ g \end{bmatrix} \quad (59)$$

4.3 State and Control Estimation

An EKF-based state estimation algorithm was implemented to filter sensor measurements and provide calculations of state variables that are not directly measured, such as velocity. EKFs are commonly implemented for such tasks, especially in navigation [19] [55]. The EKF algorithm itself is discussed in more detail in Section 2.2.3. This section will discuss the implementation and tuning procedure used for the aircraft state estimation problem.

Aircraft states include NED position, aircraft body-fixed linear velocity and acceleration, Euler angles, rotation rates and acceleration, and $\vec{r}_{cgk}$and $\dot{\vec{r}}_{cg_k}$ from Equation (59) above, due to its effect on accelerometer measurements. This leads to a total of 24 states in the state estimation problem. EKF also requires a process model (or dynamic model) to perform state estimation. The reference aircraft model (not true model) was used to perform this filtering; this model approximates the true aircraft model, and is meant to simulate the *a priori* known dynamics before SysID is performed.

In addition to the state estimates, unknown control inputs can also be estimated using the reference aircraft model, as noted by Harrison [39]. Using the aircraft reference model as the process model in the EKF state estimation will allow a simultaneous estimation of the aircraft states and control actions by appending the unknown controls as additional states in the state vector. Using the observability test described in Section *4.5*, it can be shown in Figure 14(a) that this estimation problem is valid and that all 28 quantities (24 states and 4 control inputs) are not only globally identifiable, but also locally observable along the trajectory. Atmospheric data (wind and density) can also be appended as additional states; however, this system is only globally identifiable, and not locally

observable, as seen in Figure 14(b). Therefore, only states and control inputs will be included in the filter estimation. These results are discussed in more detail in Section *5.1*.

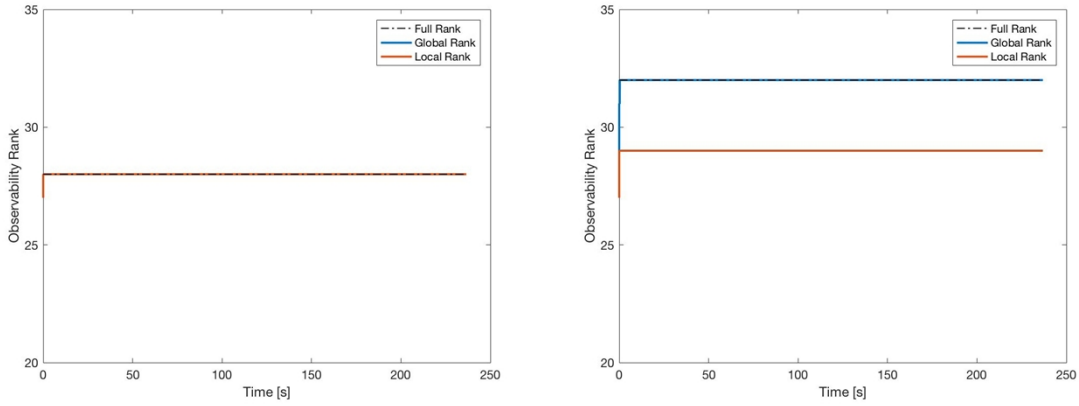

(a) (b)

Figure 14. Observability of Controls and Air Data

An example of the control estimation and its effect on state estimates is shown below in Figure 15 and Figure 16. Note that the lateral controls are estimated well, whereas the longitudinal control estimates are significantly different from the true values. This is due to the inaccuracy of the reference model being higher in the longitudinal states due to the presence of nonlinearities in lift, drag, thrust, and power that are not captured by the reference model, which assumes linear air reactions.

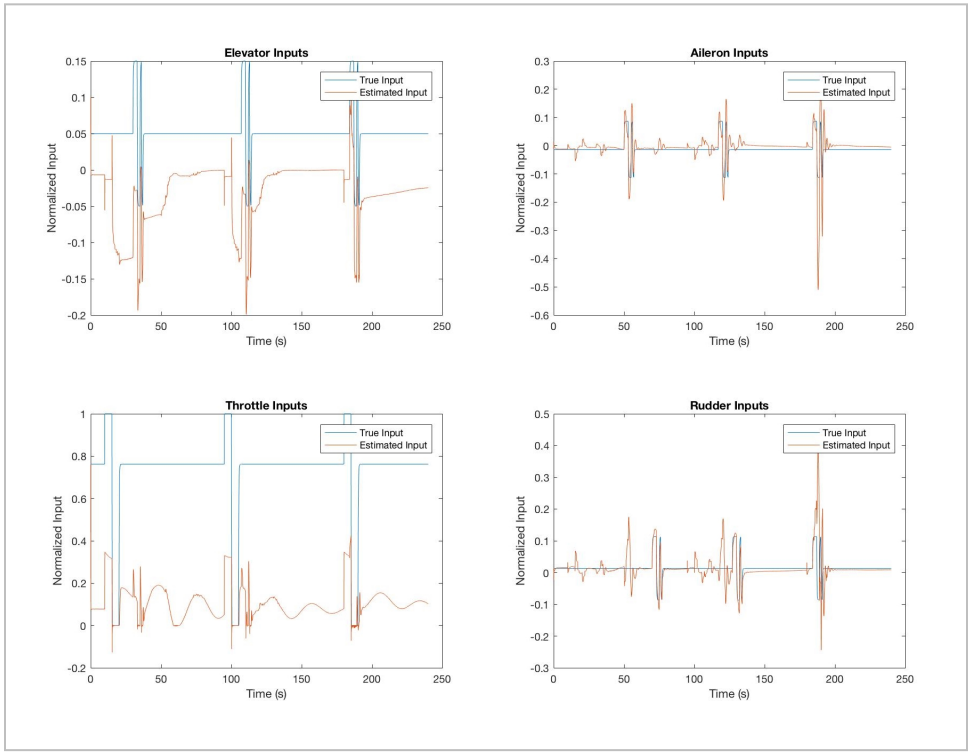

Figure 15. Estimated Controls Using EKF

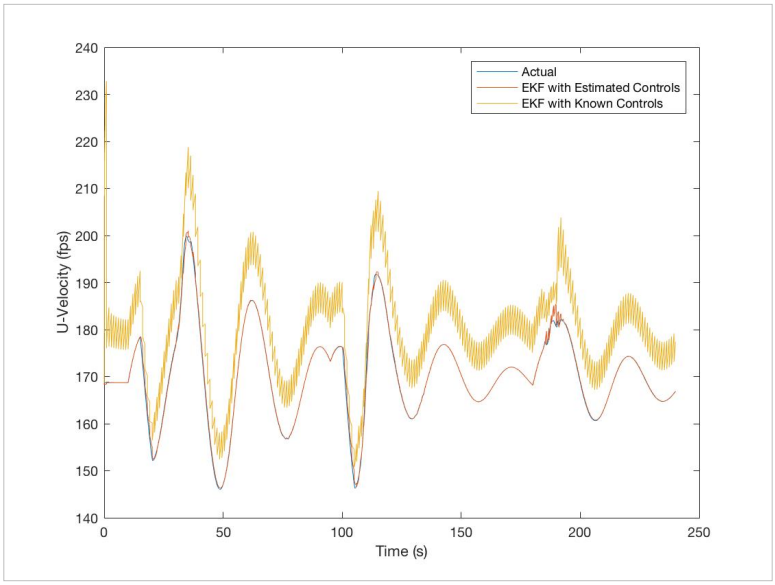

Figure 16. Effect of Control Estimation on State Estimates

Figure 16 shows a comparison of estimated body-fixed u-velocity in two different EKFs: the first (in red) shows the state estimates when controls are concurrently being estimated (corresponding to the control estimates in red in Figure 15). The second (yellow) is an EKF where control inputs are assumed known and only the states are estimated. The true value is shown in blue; the red and blue curves match well enough that this may be difficult to see. Both filters were tuned with the same procedure, discussed in the following paragraphs. Note that even though the control estimates in Figure 15 are inaccurate, the resulting state estimates are much more accurate than in the case of known controls. This is due to the error in the reference model. It was discussed in *CHAPTER* 1 that Kalman filters with biases are prone to significant error [43]. In this case, the reference model used in the EKF has a constant bias of 15% on all parameters; without compensation, this causes the state estimates to be inaccurate. However, estimating the controls in conjunction with the states allows the filter to "adjust" the controls to compensate for these biases and produce more accurate state estimates. This is similar in principal to including inertial sensor biases as additional states in an estimation process, as in [43]. The result is higher-fidelity estimates of state variables, at the expense of the control estimates. It is possible that introducing additional bias variables may free the controls to also be estimated more accurately, but this was not explored in this work.

Measurement and process noise must also be specified. Both time-varying and/or non-additive process noise can be used. In this work, the noise was assumed constant and is not a function of the state variables (additive). Measurement noise was taken as the sensor noise, given for each sensor simulation (see Section *5.3* for examples). It was assumed to be a diagonal matrix and is equivalent in each axis the sensor measures. The

initial covariance estimate was taken to be a diagonal matrix in which each element was equal to 15% of the corresponding state (in other words, the initial state is accurate to within 15%). Process noise was then used to tune the filter. Several tuning algorithms exist in the literature, but most commonly, filters are tuned by hand [56] [61]. Chen et. al. [60] discusses the use of consistency tests for filter tuning. Under the assumption of process and measurement noise being zero-mean Gaussian, the estimation error of a consistent filter should be χ^2 distributed. A cost function can be formulated as a function of both estimation error and deviation from χ^2 distribution (statistical hypothesis testing techniques) to design a filter that is both consistent and optimal. Oshman and Shaviv [59] note that the filter obtained with this method is not unique; there is a family of filters that minimize the consistency-error cost. In their work, a Genetic Algorithm is used to optimize a population of filters to achieve consistency and minimal error. However, the computational expense to perform this tuning is significant.

The tuning method implemented in this work uses a combination of manual tuning and optimization of process noise. The process noise was formulated as a function of a single positive scalar variable, q_x. Process noise was calculated by multiplying the (true) initial state vector by this value to obtain the diagonal elements of noise matrix Q_k. This variable then represents a "percentage" error in the process model. For example, $q_x = 0.1$ means that the process model (in this case, the reference aircraft model) can predict new states within +/- 10%. An initial q_x was found via trial and error; once a stable filter was found, MATLAB's optimizer `fminsearch` was used to refine this estimate and determine q_k in that neighborhood to minimize the error in state estimates. An example of

the results of this tuning procedure is shown below in Figure 17. This produced adequate results for the purposes of this study, but is still limited by the following assumptions:

1. Process noise in all states scales equivalently
2. Off-diagonal elements of Q_k are zero (no correlation of noise between states)
3. Only process noise was used as a tuning variable; other variables such as the initial covariance P_0 also affect filter performance [61]

Therefore, performance of the methods discussed could likely be improved by a more robust tuning process.

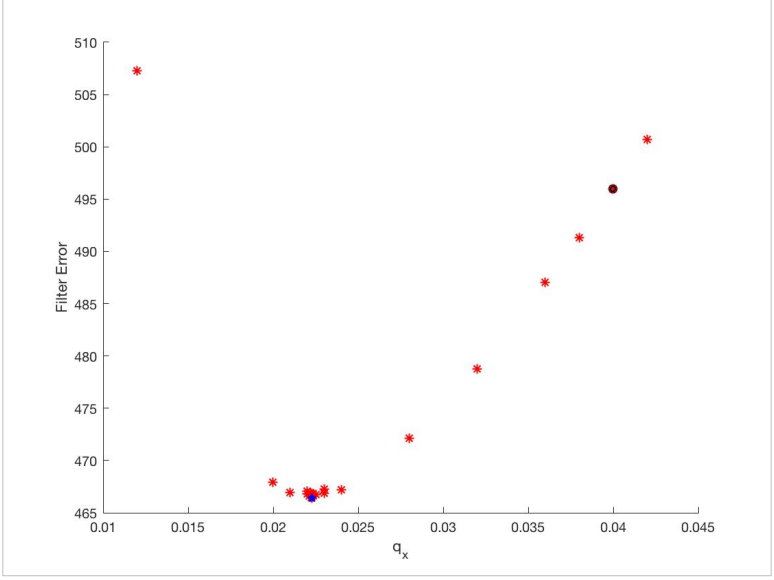

Figure 17. Example EKF Tuning Results

4.4 System Identification Implementation

4.4.1 Output Error Implementation

Output error method (OEM) utilized a modified formulation of OEM from Section 2.2.2. As discussed in the previous section, a state estimation EKF was used for initial measurement filtering and obtaining state estimates and control estimates. Cost was formulated as a pure sum of squares error in states, as opposed to a weighted sum of squares in measurements:

$$J(\Theta) = \sum_{k=1}^{N} (\hat{x}_k - x_k(\Theta))^T (\hat{x}_k - x_k(\Theta)) \tag{60}$$

The state simulated using the unknown parameters ($x_k(\Theta)$) is calculated by propagating the first state estimate, $\hat{x}_0$, through the dynamic model of Equation (18) for the entire trajectory. The difference between the points along this trajectory and the "true" (EKF estimated) trajectory can then be computed and summed using Equation (60). To minimize this cost, MATLAB's `fminunc` was used, which uses a quasi-Newton minimization procedure. Results are shown in Section 5.2.

As opposed to Filter Method SysID, OEM is incapable of simultaneously estimating states, controls, air data, and parameters. OEM assumes the parameters under estimation are constants; any variables under estimation that change frequently (such as controls and air data) must be estimated prior to application of OEM. This is the reason behind the EKF for state estimation discussed in the previous section.

4.4.2 Filter Method Implementation

Filter method SysID was implemented using an EKF. Measurements and measurement functions were the same as those in section 4.2. The process model utilized the aircraft dynamics formulations from Section 2.1 to propagate aircraft states. Other quantities under estimation, such as stability and control coefficients, control inputs, etc. were propagated with no change ($C_{D_{0k+1}} = C_{D_{0k}}$, for example). Filter tuning was conducted with the same approach used for tuning the state-estimation EKF, discussed in 4.3. Results of SysID using this approach are discussed in Section 5.2.

4.5 Observability Determination

The observability condition for nonlinear systems described in Section 2.3 was implemented to help determine appropriate model structures for SysID. This condition is an extension of the linear observability rank condition which dictates that the system is observable if and only if the observability matrix Q_o has full rank. For nonlinear systems, this can be extended using Q_{stack}, formed by appending each consecutive linear observability matrix (calculated from the Jacobians of the system model and measurement models evaluated at that time step). If this matrix is full rank, then each variable in the state has a unique effect on the output, and is therefore structurally observable.

The aircraft dynamics as discussed in Sections 2.1 and 4.1 and measurement functions can be written as a function of the current state (x_k) , controls (u), atmospheric

data (A), weight and balance (W), and the unknown parameters (Θ). Appending these together (X_k) yields

$$X_{k+1} = f(X_k) \tag{61}$$

$$y_k = h(X_k) \tag{62}$$

For a given trajectory, input sequence, atmospheric condition (density and wind), loading condition, and parameter set, the Jacobian of these functions can be approximated using finite differencing: each variable is perturbed a small amount away from its current value, the new state vector and measurement vector are calculated, subtracted from the initial value, and the deviation divided by the initial perturbation. With the Jacobians F_k and H_k, the local linear observability matrix at time-step k can be calculated as in equation (50), repeated here, where N is the dimension of the appended vector X_k:

$$Q_{ok} = \begin{bmatrix} H_k \\ H_k F_k \\ H_k F_k^2 \\ \vdots \\ H_k F_k^{N-1} \end{bmatrix} \tag{50}$$

The global observability matrix can then be created by appending all Q_{ok} along the given trajectory. Note that this method assumes the availability of known trajectory, control inputs, atmospheric data, weight and balance data, and parameters. Therefore, this method determines the observability of the true trajectory only; it is entirely possible that even if the true trajectory is observable, an estimated trajectory (from an EKF, for example), is not. Additionally, this condition only determines IF all variables are observable over a

trajectory, but does not characterize WHEN or how often. Therefore, it does not provide any indication of practical observability. Zhen Yao et. al. [67] developed a method for characterizing the observable and unobservable variables for a given observability matrix. Analyzing the local linear observability matrix Q_{ok} in this way could potentially determine which variables are observable/unobservable at each time step. After implementation, however, it was found that this method was extremely sensitive to the cutoff value used in the algorithm [67]. Therefore, only the local and global observability rank conditions were used – no determination of practical identifiability was conducted. However, rather than compute the global observability matrix over the entire trajectory, a "stepping" approach was used, such that the global observability matrix is "built up" along the trajectory, and its rank assessed. In this way, additional information was gained about when rank increases/decreases occurred along the trajectory. Examples of the results for this study are discussed in Section 5.1.

CHAPTER 5. SYSTEM IDENTIFICATION RESULTS

5.1 Experiment 1: Identifiability of Aircraft Model

This experiment seeks to answer research questions 1(a) and 1(b) repeated here:

Research Question 1(a):

Which quantities in the parameterization of General Aviation aircraft dynamics are locally observable using measurements obtained from a low-cost Flight Data Recorder or Personal Electronic Device?

Research Question 1(b):

What parameterizations of General Aviation aircraft dynamics are globally identifiable using measurements obtained from a low-cost Flight Data Recorder or Personal Electronic Device?

Parameterizing the information above could lead to potentially infinite models to test. The parameters used in this work are therefore limited to the following, as discussed in Section 4.1:

Aircraft State:

$$X = \begin{bmatrix} x_N, x_E, x_D, \\ u, v, w, \\ \dot{u}, \dot{v}, \dot{w}, \\ \phi, \theta, \psi, \\ p, q, r, \\ \dot{p}, \dot{q}, \dot{r}, \\ r_{cgx}, r_{cgy}, r_{cgz}, \\ \dot{r}_{cgx}, \dot{r}_{cgy}, \dot{r}_{cgz}, \end{bmatrix}^T \tag{63}$$

Stability and Control Derivatives:

$$\Theta = \begin{bmatrix} C_{D_0}, C_{D_K}, C_{D_\beta}, C_{D_{\delta_e}}, \\ C_{Y_\beta}, C_{Y_p}, C_{Y_r}, C_{Y_{\delta_r}}, \\ C_{L_0}, C_{L_\alpha}, C_{L_{\dot{\alpha}}}, C_{L_q}, C_{L_{\delta_e}} \\ C_{L_\beta}, C_{L_p}, C_{L_r}, C_{L_{\delta_a}}, C_{L_{\delta_r}} \\ C_{M_0}, C_{M_\alpha}, C_{M_{\dot{\alpha}}}, C_{M_q}, C_{M_{\delta_e}} \\ C_{N_\beta}, C_{N_p}, C_{N_r}, C_{N_{\delta_a}}, C_{N_{\delta_r}} \\ C_{T_0}, C_{T_J}, C_{P_0}, C_{P_J} \end{bmatrix}^T \quad (64)$$

Control Inputs:

$$u = [\delta_a, \delta_e, \delta_r, \delta_T]^T \quad (65)$$

Air Data:

$$P = [u_w, v_w, w_w, \rho]^T \quad (66)$$

Weight and Balance Data:

$$\Omega = [W_{pilot}, W_{copilot}, W_{pass_{LT}}, W_{pass_{RT}}, W_{bags}, W_{fuel}] \quad (67)$$

Experiments 1(a) and 1(b) to address the above research questions will determine the local and global observability of each of these parameters, respectively. Locally observable variables can be estimated using a standard EKF or other filters. Variables that are globally identifiable but not locally observable can be estimated using regression techniques such as OEM only if assumed constant (time-independent) over a batch of data. Variables that are neither locally nor globally identifiable must be removed or assumed known to obtain an observable system; otherwise the proposed estimation and SysID problem does not have a unique solution.

Although each experiment deals with only one type of observability (local or global), both conditions are computed for all cases and allow additional information to be obtained from the results.

5.1.1 Experiment 1(a) – Local Observability

The first experiment with observability deals with the local observability of the state, controls, and air data. The hypothesis for this experiment is reiterated below:

Hypothesis 1(a): *If only Personal Electronic Device sensor data is used, Aircraft State, Control Inputs, and Air Data will be locally observable.*

This hypothesis can be tested by computing the local observability matrix for the state, state and controls, state and air data, and all three together at each point in the trajectory. The results are shown in Figure 18 below. Case (a) shows observability of the state, (b) for the state and controls, (c) for the state and air data, and (d) for the state, air data, and controls together.

For the aircraft state alone, all 24 values are everywhere locally observable along the trajectory. The same is true for both cases (b) and (c) with state + controls and state + air data, respectively (both rank 28 systems). Case (d) however, shows that only 29 of the 32 quantities are locally observable, but that all parameters are globally identifiable. This means that both controls and air data cannot be estimated concurrently in real time; one or the other must be assumed known or assumed constant for a time and estimated with a different technique. Of the two types of information, air data is more easily assumed; either a standard atmosphere with no wind can be assumed, or wind aloft and air density can be

assumed constant and estimated with OEM. In either case, the remaining parameters (state and control inputs) will be locally observable and can therefore be estimated using a filtering approach such as an EKF.

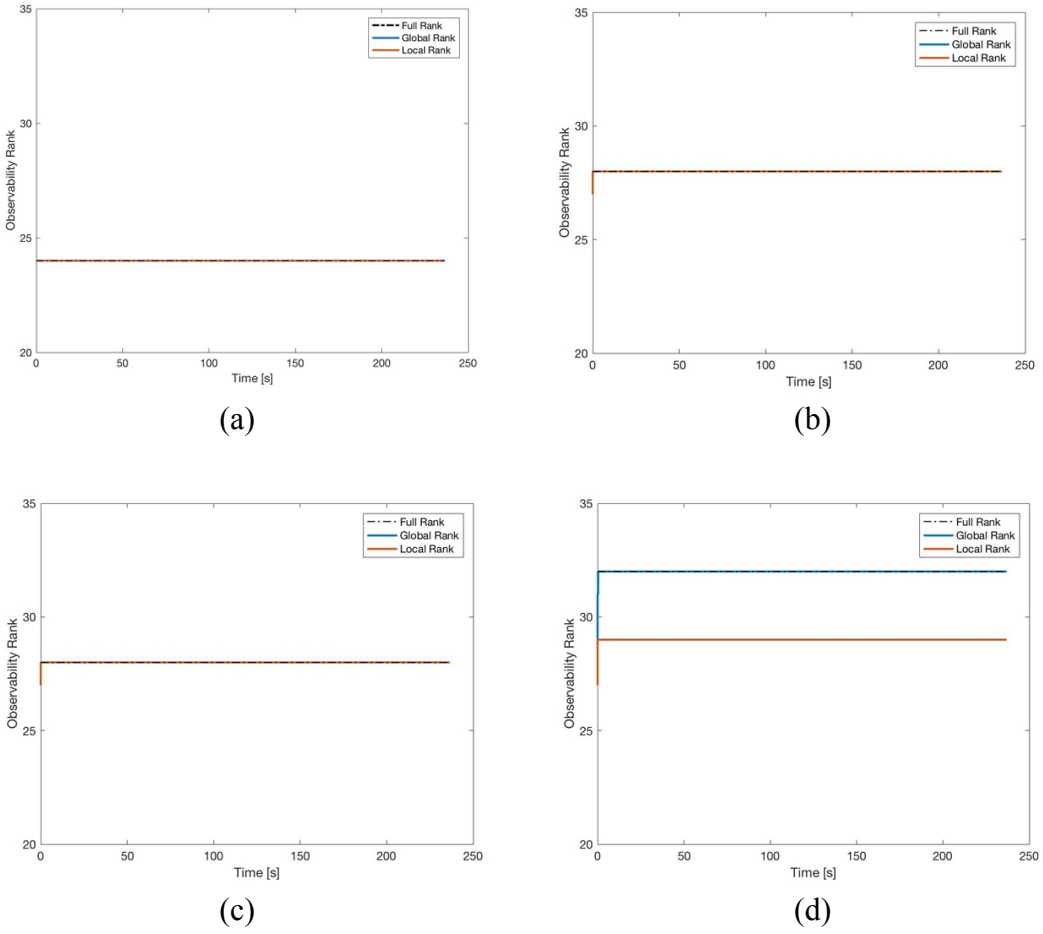

Figure 18. Local Observability of System

This result partially invalidates hypothesis 1(a), which proposed that all three quantities would be together locally observable. This hypothesis was drawn from the results of other studies in which controls [39] or air data quantities [4] [5] were estimated in real time. However, in none of these were both controls and air data estimated

concurrently. For the dynamics formulation proposed here, it appears that this estimation cannot be carried out. Additionally, for air data in [4] and [5] only angle of attack and angle of sideslip were the parameters considered. These quantities were not estimated so much as constructed directly from inertial measurements by assuming no ambient wind and applying equations (8) through (10). The results here have proven that assumption necessary (construction of angle of attack and sideslip is only possible under the assumption of known winds). Therefore, the assumption of no wind and standard atmosphere will be carried forward for the remaining experiments.

Hypothesis 1(a) has therefore been partially invalidated, answering research question 1(a). Note that the results shown here pertain only to the parameterization of the dynamics discussed in Section 4.1. Different dynamics formulations (linear dynamics, frequency domain models, etc.) may yield different results, but will also come with their own set of assumptions.

5.1.2 Experiment 1(b) – Global Identifiability of Parameters

Hypothesis 1(b) to address research question 1(b) is reiterated here:

Hypothesis 1(b): *If only Personal Electronic Device sensor data is used, weight and balance data and stability and control derivatives will not be together globally identifiable. However, if one is assumed known, the other will be globally identifiable.*

This hypothesis can be tested by applying the global observability rank condition to the full system first with 24 states, 4 controls, and 32 stability and control parameters, and subsequently with the additional 6 configuration parameters. The results of the first case are shown below in Figure 19. The local rank of the system remains at most 30; this is to be expected, as the 24 states and 4 controls were shown to be locally observable in the previous experiment. The global rank increases in steps until reaching full rank (rank 60) at 70 seconds. The stepping behavior in Figure 19 is due to the staggered control input sequence as described in Section 4.1.3 and shown again in more detail below in Figure 20. As each control surface is perturbed, the stability and control derivatives for that axis of motion become identifiable, increasing the global rank condition until full rank is achieved.

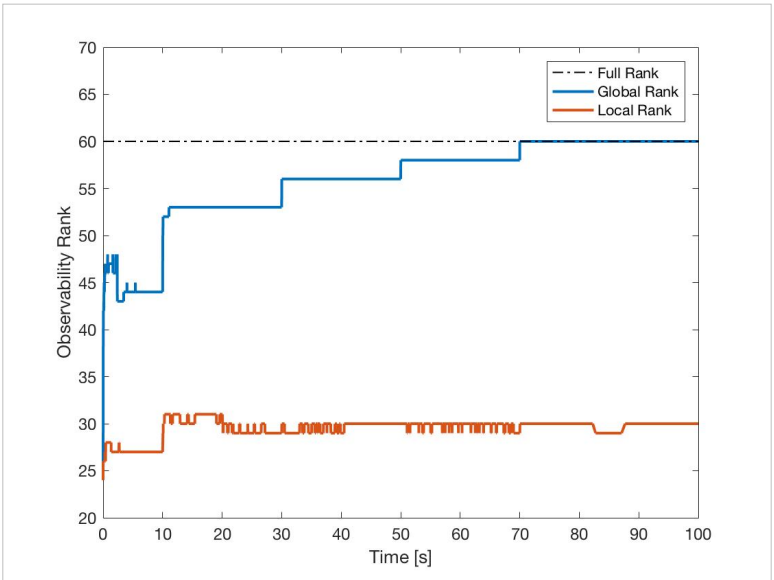

Figure 19. Global Observability of State, Controls, and Parameters

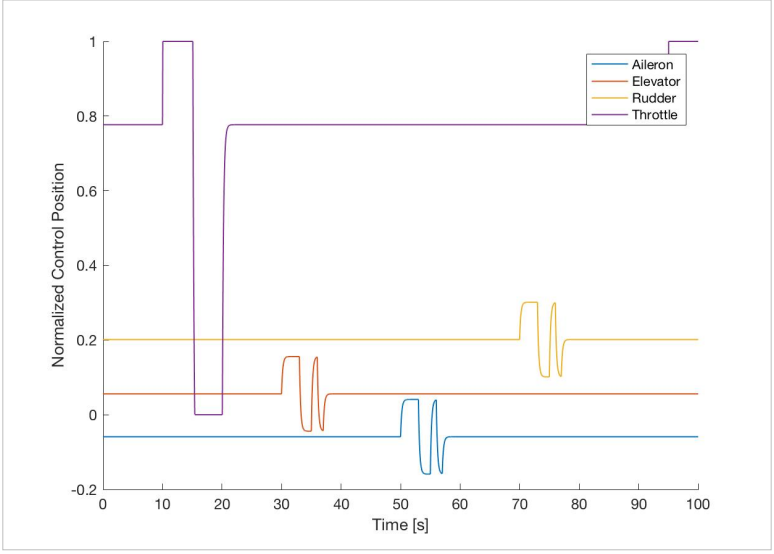

Figure 20. Control Inputs for Observability Study

Results for the second case in which the six weight and balance parameters are included are shown below in Figure 21. Note that the local observability has not changed; the additional 6 parameters are not locally observable. Additionally, the system never achieves global observability; full rank is 66 but only 64 parameters are observable. Therefore hypothesis 1(b) has been confirmed: when estimated together, the unknown parameters and weights are not together observable, but estimated alone, the unknown parameters are observable. However, some of the weight parameters may be identifiable. In fact, Equation (68) below demonstrates how fuel weight can be directly calculated from the other parameters if they are assumed known. In this equation, $W_{tot_{subFuel}}$ and $r_{cg_{subFuel}}$ are the weight and balance calculations with fuel excluded; these parameters are assumed known. The estimated CG location, $r_{cg_{est}}$, is included in the 24 aircraft states (see Equation (63) above) which was shown to be locally observable in Experiment 1(b). The location of the fuel tanks, r_{fuel}, is assumed known from the aircraft geometry in Table 4.

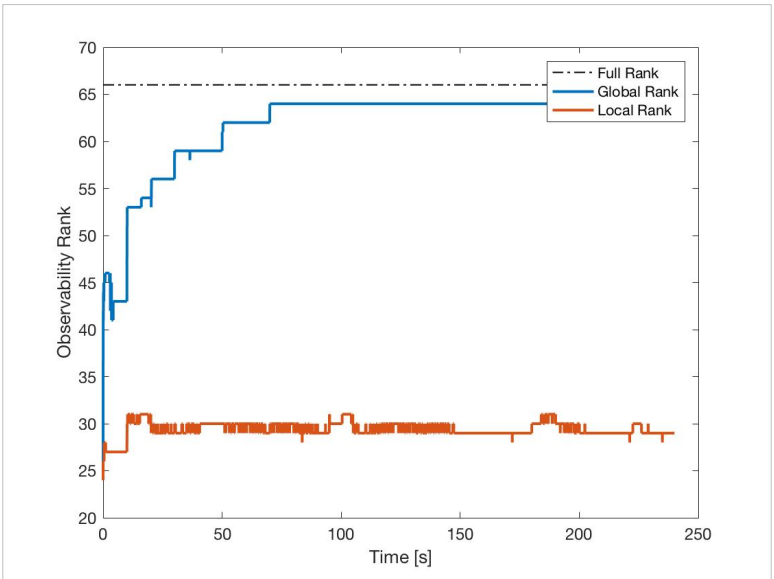

Figure 21. Observability of State, Parameters, Controls, and Weights

$$W_{fuel} = \frac{(r_{cg_{est}} - r_{cg_{subFuel}})W_{tot_{subFuel}}}{(r_{cg_{subFuel}} - r_{fuel})} \tag{68}$$

The results of this experiment demonstrate that the weights and parameters cannot be estimated concurrently, although important parameters such as fuel weight can be calculated directly from other quantities. It is therefore likely that the non-identifiable parameters are simply redundant; these can be calculated directly from other parameters in the estimation process, and therefore their effect is not "unique", hence, not identifiable. However, for simplicity, only fuel weight was estimated in this manner. It was then assumed that the other weight and balance parameters were known such that the stability and control derivatives remain globally identifiable. These parameters are the typical focus of aircraft SysID. It is also often assumed in typical aircraft SysID that weight and balance is known. The results here have proven that assumption necessary; for the remainder of the experiments it will be assumed that weight and balance is known. The accuracy of this assumption will be perturbed and its effect on SysID analyzed in Experiment 4. The resulting system model is globally identifiable; the results are the same as those in Figure 19, and are not repeated here.

5.1.3 Conclusion of Observability Study

The results of experiment 1 tested hypotheses 1(a) and 1(b), and answered research question 1(a) and 1(b) respectively. State and control variables were determined to be locally observable, and the stability and control parameters in the equations of motion from Sections 2.1 and 4.1 were shown to be globally identifiable. Air data parameters (wind velocity in NED-frame and ambient density) were shown to be globally identifiable, but not locally observable. These parameters could therefore be estimated using batched data; global rank for this case is achieved rapidly, indicating that only a few data points would be necessary to estimate these quantities. Near-real-time estimation could therefore likely be achieved. However, for the purposes of this study, a zero-wind and standard atmosphere assumption will be carried forward. All weight and balance data will be assumed known, with the exception of fuel weight which can be estimated in real time, as the results indicated that these parameters are not identifiable. Using these assumptions, all remaining quantities are observable either locally or globally. Therefore, the system model is well constructed, and the SysID problem using this system is guaranteed to have a unique solution. However, it is important to note that this condition does not guarantee that the methods being utilized will be able to find the solution, only that the solution, in theory, exists. Performance of SysID will depend on the methods used and the quality of measurement data, which are the subjects of Experiments 2 and 3, respectively.

Improvements to Experiment 1 could be made to provide more information about the system. No effort was spent to characterize which specific variables were unobservable. For example, only two of the six weights appear to be unobservable, but which two these are remain unknown. Similarly, with air data; one of the four parameters was locally

observable. Characterizing the observable and unobservable subspaces of the system could maximize the potential of a SysID process. Additionally, Southall et. al. [66] and Zhen Yao et. al. [67] discuss how the global identifiability rank condition can be used to determine the minimum amount of measurements needed for a specific variable. Therefore, experimental design (in this case, control input design) could be carried out by further analysis of the global rank condition. In the experiments of this study, no determination on number of measurements was made; a globally identifiable system could result even if global observability occurs at only a single point. Therefore, expanding this condition to account for quantity and quality of measurements could yield additional information about the system and its usefulness for SysID.

Although outside the scope of the current work, the observability conditions described can also be used to investigate the impact of additional sensors. As discussed in Section 2.3, one of the ways to mitigate unobservable systems is to add measurements. An example is shown below in Figure 22 for local observability of the full 60-parameter system (state, controls, and stability and control derivatives). As sensors are added, the local rank of the system increases, meaning more quantities are locally observable at each time step. For example, adding a pitot probe increases the local observability rank by 4 by providing airflow measurements that can be used to estimate the 4 airflow parameters (three-axis wind speed and air density). Pitot probes are often used to measure airflow, specifically dynamic and static pressure, and are often used in aircraft SysID problems. Additionally, many FDRs in GA have capability to tap into existing aircraft pitot-static system, or an externally mounted pitot probe. While this study is concerned with only PED data, this increase of observability could be used to make a case for installing a system that

is capable of capturing this data. Another example is given by including a direct throttle measurement. FDRs or PEDs can use audio or visual [15] [74] to estimate engine\rotor\propeller RPM. Adding an RPM measurement allows throttle position to be measured directly, increasing the observable parameters by one.

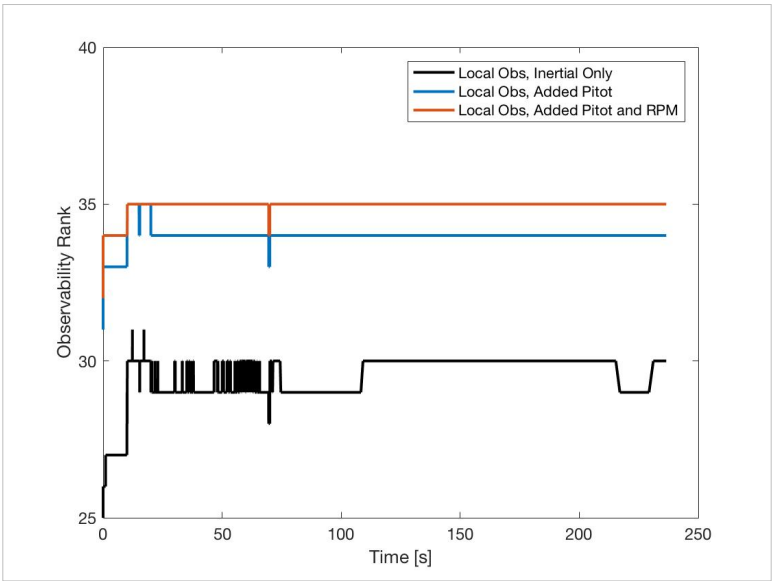

Figure 22. Local Rank Comparison for Added Sensors

5.2 Experiment 2: Comparison of OEM and EKF System Identification

Experiment 2 was designed to address Research Question 2 and its associated hypothesis:

Research Question 2

Which method of System Identification is best suited for accurately determining a 6-Degree-of-Freedom model of a General Aviation aircraft from low-cost Flight Data Recorder or Personal Electronic Device data?

Hypothesis 2: *Post-processing data using Output Error System Identification will provide higher accuracy for stability and control parameters than online estimation using Extended Kalman Filter System Identification*

To test this hypothesis, two experiments were developed to assess the quality of estimates obtained through OEM and EKF SysID. Experiment 2(a) is a validation of the methods using perfectly known states, controls, air data, and weight and balance data. This represents the theoretical "best" that can be obtained from the given trajectory data using these methods. Experiment 2(b) deals with the more realistic GA SysID problem: state and control estimates are obtained using an EKF and sensor data (for EKF SysID this estimation is in the same filter as the parameter estimation). Cases are summarized below in Table 8. Both experiments used the same trim point and sensor characteristics. These are listed in Table 9.

Table 8. Experiment 2 Cases

	State	Controls	Air Data	Config	Sensors
Experiment 2(a)	Known	Known	Known	Known	Perfect
Experiment 2(b)	Estimated	Estimated	ISA	Known	Perfect

Table 9. Conditions of Experiment 2

Trim Conditions	
VTAS	100 KTAS
Altitude	3000 ft
Vertical Speed	0 ft/min
Roll	0 deg
Atmospheric Conditions	
Wind	None
Turbulence	None
Temperature	Standard
Sensor Characteristics	
GPS Frequency	1 Hz
GPS Accuracy	1e-9 ft
Accelerometer Frequency	30 Hz
Accelerometer Accuracy	1e-9 ft/s^2
Gyroscope Frequency	30 Hz
Gyroscope Accuracy	1e-9 deg/s
Magnetometer Frequency	30 Hz
Magnetometer Accuracy	1e-9 deg

Several performance metrics were used to compare the methods. The first is a sum of squares error between the true accelerations at each point in the trajectory, and those calculated using the reference model and identified model. This is a point-wise mapping; given a point on the true trajectory, each model will predict the accelerations which can be compared to the true values. This is repeated at each point in the trajectory, and the sum of squares of the errors recorded. This provides a "big-picture" indication of how well the

model fits the true trajectory and gives an indication of suitability of the model for use in an EKF, but taken alone is insufficient to understand how well the SysID process performed. The second metric is a direct comparison between each individual parameter of the true model, reference model, and system identified model. The third metric is the lift and drag curves and drag polar; these values are useful for performance evaluation and planning, such as range and endurance. This comparison therefore provides insight into how useful the identified model might be in practice. Lastly, the stability modes can be computed for the trim point and compared again between the true model, reference model, and identified model. The purpose of the above comparisons is to determine the accuracy and usefulness of the identified model and compare to an *a priori* model (reference model). For each metric, a percent improvement figure was calculated using Equation (69). This figure represents the difference in accuracy between the reference model and the identified model. Positive improvement means the identified model is closer to the true value than the reference model.

$$\%_{improvement} = 100 \times \left(1 - \left|\frac{SysID - True}{Ref - True}\right|\right) \tag{69}$$

5.2.1 Experiment 2(a) – System Identification of Known Data

Experiment 2(a) was conducted as a validation study to determine the applicability of the methods given perfectly known data, and to ensure that the methods were constructed properly. The observability study in Section 5.1 showed that the problem is at least structurally sound; that is, the parameters are all identifiable given an infinite amount of

data. However, this does not guarantee that the methods under consideration will perform well on the data for the specific trajectory. This experiment seeks to quantify the ability of the methods in the absence of inaccuracies from sensors or assumptions. OEM was investigated first, and EKF method will be discussed after.

Table 10 below shows the sum of squares error for both the reference model and the identified model obtained through OEM for Experiment 2(a). Significant improvement over the reference model was obtained which indicates that the OEM model can more closely match the true trajectory than the reference model can.

Table 10. OEM Performance Metrics of Experiment 2(a)

OEM Performance	
SSE_{REF}	79927583.9694
SSE_{OEM}	2438.5720
Improvement	99.99 %

A more complete picture can be obtained by examining the individual parameter accuracy, shown in Figure 23. Most parameters identified through OEM show improvement over those in the reference model (+/- 15% of true model). However, several parameters show significant deviation, namely drag coefficients, thrust and power coefficients, and the zero-lift moment coefficient. Inaccuracies in these parameters could be the result of several causes. In this experiment, perfect trajectory, controls, atmospheric, and weight and balance data were all used. Therefore, inaccuracies in the provided data cannot be the culprit of this deviation. One potential cause is inadequacy of the postulated model. Recall that the true aircraft drag, lift, thrust, and power were modelled using

nonlinear lookup tables. However, for SysID, these forces and moments have been parameterized as linear relationships; the resulting discrepancy could therefore be due to an inability to find an adequate linear model to represent these forces properly while still minimizing error in the forces and moments computation.

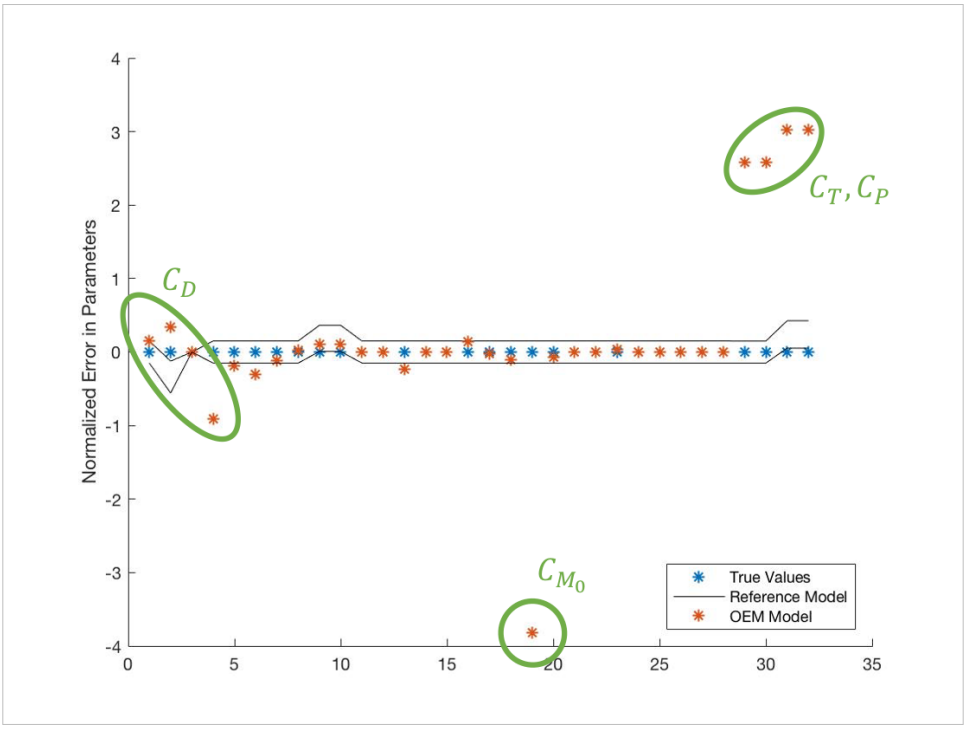

Figure 23. OEM Parameters, Experiment 2(a)

The last potential cause of these inaccuracies is practical observability. Note that drag, thrust, and power operate primarily along the aircraft body-fixed x-axis. In fact, the only difference between the line of action of drag and thrust is angle of attack (AoA), which can be presumed to be relatively small. In fact, for the trajectory analyzed, the AoA reaches a maximum value of only 3.87 degrees, and a minimum of -1.34 degrees; it is highly likely, therefore, that this small variation in AoA is insufficient to fully

distinguish thrust and drag, making them together practically unidentifiable. Both drag and thrust seem to be overestimated, essentially balancing each other out while still allowing a good fit to the trajectory as described in Table 10.

Lastly, the zero-lift moment coefficient seems to be an outlier in this estimation. Note however from Table 5 (true aircraft parameters) that C_{M_0} is smaller in magnitude than any other moment coefficient by at least an order of magnitude. Specifically, $C_{M_{\delta_e}}$, which appears four to the right of C_{M_0} in Figure 23, is slightly overestimated, but the correct value is two orders of magnitude higher than C_{M_0}. Therefore, it is entirely possible that these two parameters have also been confounded and are not practically identifiable; a small deviation in $C_{M_{\delta_e}}$ could be compensated for a large deviation in C_{M_0} while still matching the trajectory well. Accuracy in these parameters, and drag and thrust in the previous example, could therefore be improved by using flight data from different flight conditions and maneuver sequences. However, for the remainder of the studies, the same trajectory and maneuver will be compared. The results here therefore correspond to the "best achievable" parameter values for the model and trajectory considered.

The next two results provide insight into the potential usefulness of the model by quantifying aerodynamic performance and characterizing the stability modes of both the reference model and identified model. Lift to drag ratio (L/D) was used as the metric in Table 11, and the lift, drag, and drag-polar curves are plotted in Figure 24. L/D ratio was calculated for a cruise trim condition (initial state of trajectory) and for the Cessna 172P's best-glide speed of 65 KTAS [75]. The L/D ratio at cruise (the trim point in this case) is used to calculate endurance and range and is therefore a useful metric. The L/D ratio at

best glide is also useful as it is often used to compute glide range in the case of an engine failure.

Table 11. OEM Lift/Drag Ratio Experiment 2(a)

	True Value	Reference Model	OEM Model	Improvement %
Lift/Drag Ratio at Trim	9.2227	15.2828	11.1524	68.2 %
Lift/Drag Ratio at Best Glide	8.5311	16.1957	9.6358	80.2 %

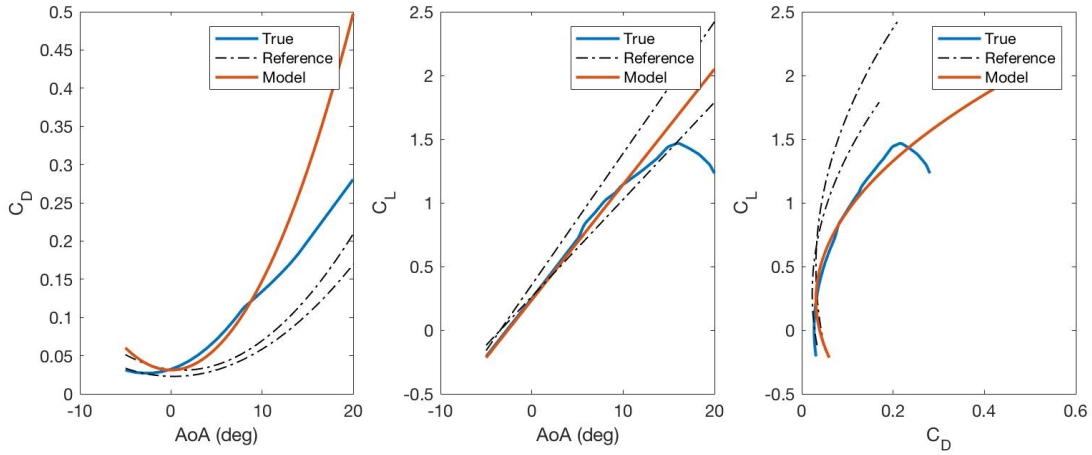

(a) (b) (c)

Figure 24. OEM Lift and Drag Curves, Known Data, Experiment 2(a)

Both Table 11 and Figure 24 show that the identified model has significantly improved the lift and drag estimates compared to the reference model. Just like above, more flight data in other regimes is likely to continue to refine these estimates and improve the accuracy of aerodynamic performance calculations.

Lastly, the dynamic modes of the aircraft models at the initial trim point were calculated and compared. These are useful for understanding stability margins, designing or tuning autopilots, and estimating LOC envelope boundaries as in [39]. Values are shown below in Table 12 and Figure 25:

Table 12. OEM Dynamic Modes Experiment 2(a)

	True Values	Reference Model	OEM Model	Improvement %
Longitudinal Modes	-2.5675 + 3.5551i	-2.8810 + 4.0505i	-2.5231 + 3.5472i	92.3 %
	-2.5675 - 3.5551i	-2.8810 - 4.0505i	-2.5231 - 3.5472i	92.3 %
	-0.0310 + 0.2193i	-0.0062 + 0.1580i	-0.0292 + 0.2205i	96.8 %
	-0.0310 - 0.2193i	-0.0062 - 0.1580i	-0.0292 - 0.2205i	96.8 %
Lateral Modes	-10.0239	-11.1796	-9.7969	80.4 %
	-0.5870 + 2.6918i	-0.6932 + 2.9001i	-0.5873 + 2.7072i	93.4 %
	-0.5870 - 2.6918i	-0.6932 - 2.9001i	-0.5873 - 2.7072i	93.4 %
	-0.0187	-0.0237	-0.0170	65.9 %

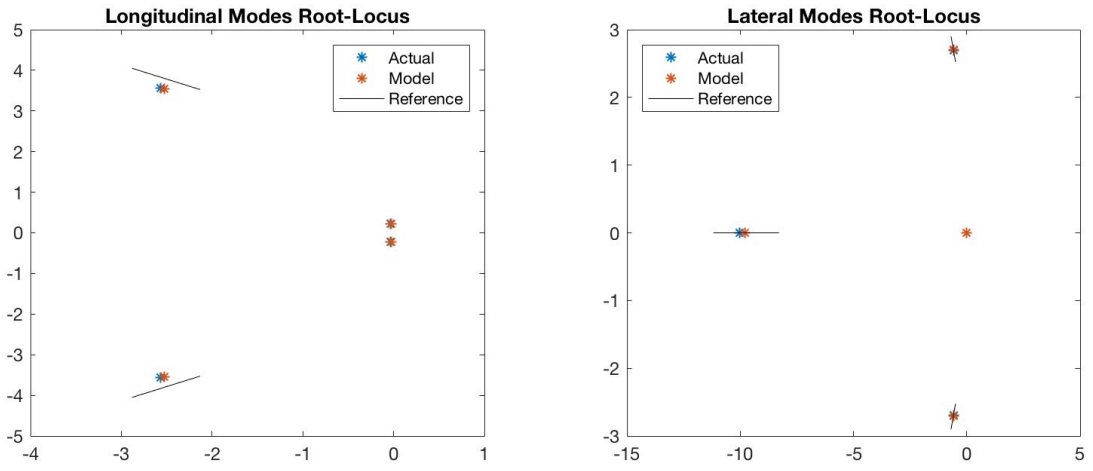

(a) (b)

Figure 25. OEM Root Locus Plots, Known Data, Experiment 2(a)

Once again, the identified model shows significant improvement from the reference model. All longitudinal and lateral-directional modes were nominally 90% closer to the true value.

The conclusion from the above results is that OEM works well for identifying the aircraft model along the trajectory examined. Some deficiencies in model parameters (namely drag and thrust) were identified, and the cause determined to be a combination of inadequate practical identifiability along the trajectory, as well as inadequate modelling of these nonlinear forces and moments. These inaccuracies are therefore not a result of the method itself being flawed.

The next step in answering Research Question 2 is to compare the performance of the OEM method discussed above with an EKF SysID process under the same assumptions: all controls, air data, and weight and balance data are assumed perfectly known. For an EKF, known quantities cannot be directly assumed; rather, near-perfect sensors were utilized for filtering, resulting in near-perfect trajectory estimates.

The first metric is the total error in model-calculated accelerations and is shown below in Table 13:

Table 13. EKF Performance Metrics of Experiment 2(a)

EKF Performance	
SSE_{REF}	79927583.9694
SSE_{EKF}	10728386.8856
Improvement	86.5 %

EKF SysID appears to have improved the model by 86.5%. As suspected in Hypothesis 2, the EKF method showed less improvement and accuracy than OEM for the same case. However, just like for the OEM case, this value does not necessarily mean that individual metrics and parameters are accurate. Figure 26 below shows the estimates for each parameter obtained through EKF SysID, and Table 14 shows the calculated L/D ratio at trim. Both indicate that EKF performed significantly worse than OEM method, even for this case in which perfect sensors were utilized. This is no doubt due to the local observability of the system; EKFs linearize the system at each time step to perform estimation, and at most 30 of the 56 values under estimation are locally observable at any time step. For OEM, which assumes constant parameters over the trajectory, this is not an issue. However, it significantly limits the performance of EKF method SysID in this case.

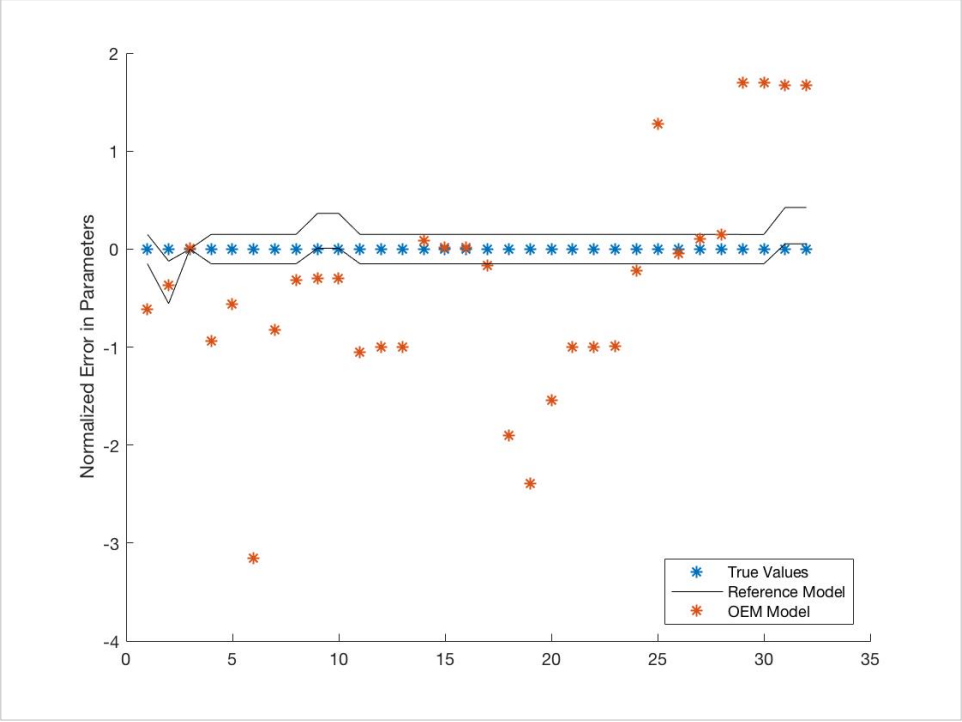

Figure 26. EKF Parameters, Experiment 2(a)

Table 14. EKF Lift/Drag Ratio, Experiment 2(a)

	True Value	Reference Model	EKF Model	Improvement %
Lift/Drag Ratio at Trim	9.2227	15.2828	49.28	-561 %

For the sake of brevity, the other performance metrics for EKF SysID are not shown here. Without further investigation, it can be concluded that OEM method does indeed provide more accurate results than EKF for the situation considered. Therefore, Hypothesis 2 has been validated. For the remaining studies, only OEM SysID will be considered. While it is possible that EKF SysID could still have success, this would no doubt require an alteration to the methods proposed. Lowering the dimensionality of the problem, increasing the amount of known data through assumptions or additional measurements, improving the control inputs and resulting trajectory, and/or more robust filter tuning could potentially lead to a solution using EKF SysID. Additionally, an EKF that utilizes multiple measurements or "batches" to update would likely be able to more directly take advantage of global observability [66]. Formulation of a frequency-domain model may also have more success due to the implicit "memory" of the discrete Fourier transform [1]. However, these were deemed outside the scope of the current work.

The results above are valid only under the assumption of perfectly known data. This is not representative of the GA SysID problem, in which controls and air data especially are unknown. Therefore, the performance of OEM will also be assessed through Experiment 2(b) which removes the assumption of known states and controls.

5.2.2 Experiment 2(b) – Estimating Control Inputs

Experiment 2(b) explores OEM SysID using state and control estimates instead of true data. The estimates were obtained using EKF state estimation, as described in Section 4.3. The tuning of the filter is described in Table 15 below along with the SSE of both the reference model and OEM model that resulted from this experiment. Note that a significant improvement in model capability was obtained through OEM. This is confirmed by the parameter comparison shown in Figure 27 and Figure 28:

Table 15. Performance Metrics of Experiment 2(b)

Filter Performance	
Process Noise Parameter, q_x	0.0064
SSE_{EKF}	776.8
OEM Performance	
SSE_{REF}	79927583.9694
SSE_{OEM}	11652357.2722
Improvement	85.4 %

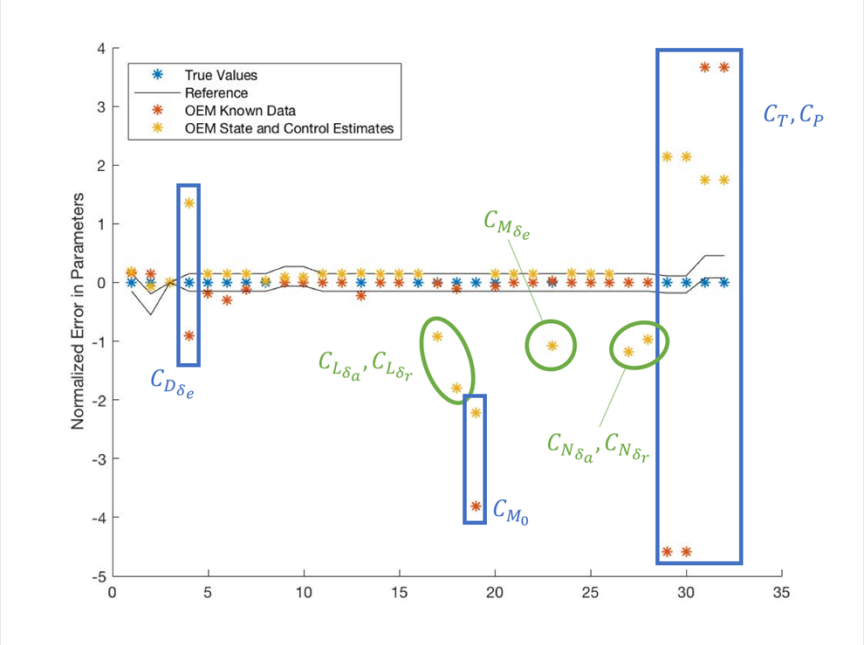

Figure 27. OEM Parameters, Experiment 2(b)

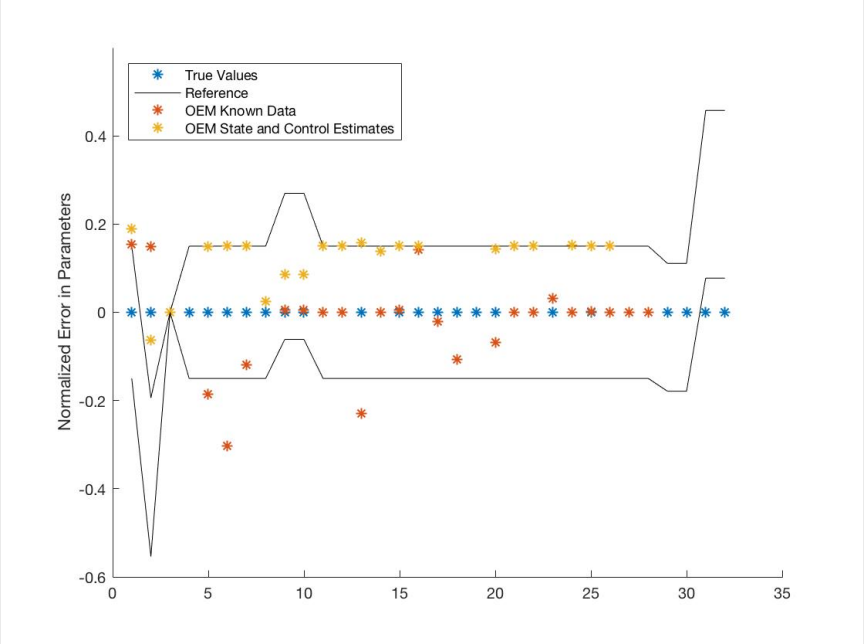

Figure 28. OEM Parameters, Experiment 2(b) Zoomed

Figure 27 and Figure 28 show the parameter results of both Experiment 2(a) and 2(b) compared with the true values and reference model. In Figure 27, parameters that were inaccurate in both experiments are boxed in blue, whereas inaccurate parameters specific to Experiment 2(b) are circled in green. For those that were inaccurate in both cases, it was discussed previously in Experiment 2(a) that this was likely caused by practical identifiability and/or inadequacy of the proposed linear model to fit the nonlinear drag and thrust data. Experiment 2(a) represents the theoretical "best case" that can be achieved by this method given perfect data; therefore, it is no surprise that these same parameters have error in Experiment 2(b).

For the erroneous parameters unique to Experiment 2(b), it can be observed that they are all control derivatives. It was discussed in Section 4.3 that the control estimation in the EKF prior to OEM was inaccurate. However, accurate state estimates were still obtained and the identified stability derivatives either match or improve upon those of the reference model (this is most easily seen in Figure 28). The most notable improvements are those of the lift and drag coefficients. The resulting drag, lift, and drag polar curves are much closer to the true model as shown in Figure 29, and the L/D ratios for both trim and best glide (listed below in Table 16) show significant improvement as well:

Table 16. Lift/Drag Ratio Experiment 2(b)

	True Value	Reference Model	OEM Model	Improvement %
Lift/Drag Ratio at Trim	9.2227	15.2828	10.6550	76.4 %
Lift/Drag Ratio at Best Glide	8.5311	16.1957	7.1618	82.1 %

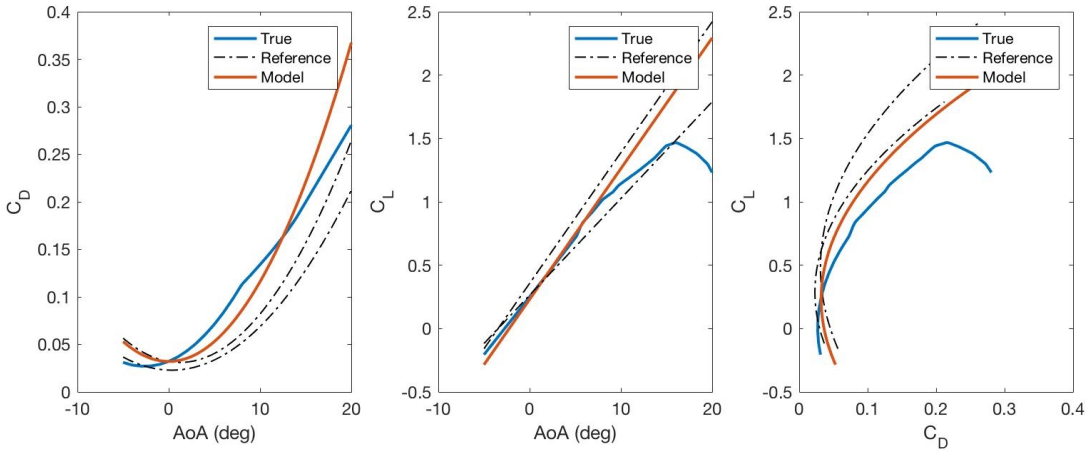

(a) (b) (c)

Figure 29. OEM Lift and Drag Curves, Experiment 2(b)

It is interesting to note that the identified lift and drag curves and improvement in L/D ratios are comparable to the improvement obtained in Experiment 2(a), despite significantly less information being known about the aircraft's trajectory in this case.

Most of the stability derivatives besides lift and drag remained relatively close to the reference model. Improvement in the longitudinal modes was likely due mostly to the lift and drag improvement, and very little change was seen in the lateral dynamic modes. However, all changes were positive, as shown by Table 17 and Figure 30:

Table 17. Dynamic Modes Experiment 2(b)

	True Values	Reference Model	OEM Model	Improvement %
Longitudinal Modes	-2.5675 + 3.5551i	-2.8810 + 4.0505i	-2.8863 + 3.9373i	15.1 %
	-2.5675 - 3.5551i	-2.8810 - 4.0505i	-2.8863 - 3.9373i	15.1 %
	-0.0310 + 0.2193i	-0.0062 + 0.1580i	-0.0016 + 0.2299i	52.8 %
	-0.0310 - 0.2193i	-0.0062 - 0.1580i	-0.0016 - 0.2299i	52.8 %
Lateral Modes	-10.0239	-11.1796	-11.1793	<0.1 %
	-0.5870 + 2.6918i	-0.6932 + 2.9001i	-0.6928 + 2.9002i	<0.1 %
	-0.5870 - 2.6918i	-0.6932 - 2.9001i	-0.6928 - 2.9002i	<0.1 %
	-0.0187	-0.0237	-0.0231	13.3 %

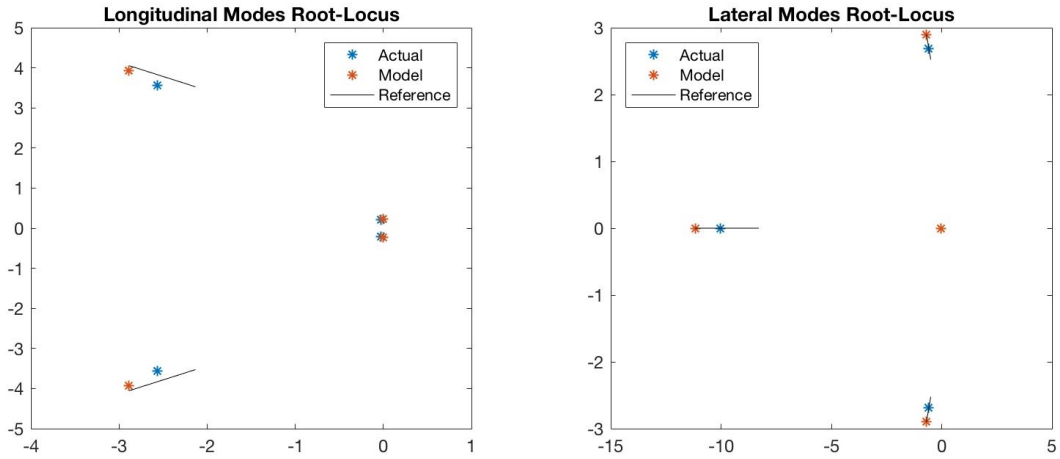

(a) (b)

Figure 30. OEM Root Locus, Experiment 2(b)

f

The lack of improvement in the lateral-directional parameters is likely due again to the error in control estimation; erroneous control inputs and control derivatives may have conspired to represent most of the lateral dynamics, leaving the other lateral-directional derivatives as practically unobservable. Improvements in the control input estimation

would therefore likely improve the ability to estimate these other parameters. It is also possible that the lack of improvement in the lateral-directional modes is due to the relatively small time-scale for which those modes are present. For example, the phugoid mode, which had the greatest improvement, has longer period and less damping than the other modes; phugoid oscillations persist for the majority of the trajectory. However, Dutch Roll, for example, is damped out within a few seconds of the lateral-directional excitations. Therefore, the error which OEM seeks to minimize is more heavily "weighted" towards the phugoid mode; error in the phugoid mode oscillations is likely to dominate error over the trajectory.

5.2.3 Conclusion of Experiment 2

The intent of this experiment was to answer Research Question 2 by comparing the performance of EKF vs OEM SysID. In Experiment 2(a), these methods were compared using perfect known data and results showed that EKF estimation for this case is infeasible due to the large number of unobservable/unidentifiable quantities at each time step. Therefore, OEM is most suited to the GA SysID problem. However, further experimentation was still needed to validate the use of OEM when perfect data is not available, and hence, Experiment 2(b) was conducted.

Important trends in the identified parameters can be identified. First, if Experiment 2(a) estimated a parameter with large error, the same occurred for Experiment 2(b). This is because the OEM process of Experiment 2(a) is the theoretical "best" that can be achieved with OEM for the trajectory studied. More maneuvers, flight conditions, or sensors would

be needed to refine the estimates for these parameters. Therefore, error in these parameters in the other experiments can be attributed to this effect.

Second, OEM with estimated data and controls was still able to improve the reference model despite relying on state estimates and erroneous control estimates from an EKF based on the reference model. The main exception to this result is the estimates for control derivatives. Similar to the state estimation discussed in Section 4.3, the control estimates seem to have "absorbed" error, allowing more accurate estimation of the other parameters such as lift and drag at the expense of decreased knowledge of control derivatives. However, even despite the erroneous control derivatives, all identified models decreased the total SSE compared to the reference model. It is possible, therefore, that replacing the reference model in the initial EKF with the new identified model could increase the fidelity of state and control estimates yet again. Also, as discussed above, further improvements in the model could likely be achieved through more flight data from other maneuvers, other flight conditions, or additional sensors.

Despite the inaccuracies incurred in some parameters, especially control derivatives, the identified model showed improvement over the reference model for the metrics considered. These are summarized in Table 18 below. The conclusion is therefore that, for the current model and trajectory, OEM SysID method as implemented here is better suited to the GA aircraft SysID problem than a standard EKF method, validating Hypothesis 2, answering Research Question 2, and demonstrating the potential of these methods for GA aircraft SysID.

Table 18. Summary of Experiment 2 Results

Metric	All Known Data (Experiment 2(a))	Estimated States and Controls (2(b))
	% Improvement	% Improvement
SSE	99.9 %	85.4 %
L/D at Trim	68.2 %	76.4 %
L/D at Best Glide	80.2 %	82.1 %
Phugoid Mode	92.3 %	15.1 %
Short Period Mode	96.8 %	52.8 %
Roll Mode	80.4 %	<0.1 %
Dutch Roll Mode	93.4 %	< 0.1 %
Spiral Mode	65.9 %	13.3 %

5.3 Experiment 3: Effect of Sensor Quality on System Identification

The previous experiment utilized the assumption of perfect sensors. PEDs and low-cost FDRs are likely to have limited sensor accuracy and noisy measurements. This experiment therefore seeks to answer Research Question 3 and associated hypothesis:

Research Question 3

What requirements on sensor quality are needed to improve *a priori* model accuracy through System Identification?

Hypothesis 3: *If measurements are obtained with only low-cost Flight Data Recorders or Personal Electronic Devices, improvement in an a priori model can be achieved using System Identification.*

From the results of Experiment 2, only OEM will be considered. Sensors with the characteristics described below in Table 19 were simulated for the same trajectory/control sequence as described previously. Sensor characteristics are representative of a smartphone PED; frequency and noise (accuracy) were compiled from data in [76] [77] [78]. The resulting conditions of Experiment 3 are shown below:

Table 19. Conditions of Experiment 3

Trim Conditions	
VTAS	100 KTAS
Altitude	3000 ft
Vertical Speed	0 ft/min
Roll	0 deg
Atmospheric Conditions	
Wind	None
Turbulence	None
Temperature	Standard
Sensor Characteristics	
GPS Frequency	1 Hz
GPS Accuracy	16 ft
Accelerometer Frequency	30 Hz
Accelerometer Accuracy	0.01 ft/s^2
Gyroscope Frequency	30 Hz
Gyroscope Accuracy	0.01 deg/s
Magnetometer Frequency	30 Hz
Magnetometer Accuracy	7 deg

The results from this experiment will be compared with Experiment 2(b), which is the same in all aspects except sensor quality (Experiment 2(b) assumes near-perfect sensors). The same performance metrics as in the previous experiments will be used. The

EKF tuning procedure described in Section 4.3 was implemented and its results, along with total SSE of the model and reference, are shown below in Table 20:

Table 20. Performance Metrics for Experiment 3

Filter Performance	
Process Noise Parameter, q_x	0.0001
SSE_{EKF}	3060.4
OEM Performance	
SSE_{REF}	79927583.9694
SSE_{OEM}	10839328.8664
Improvement	86.4 %

Note the difference between the process noise parameter in this experiment and that of Experiment 2(b); process noise is lower here because sensor quality is poor, and therefore the EKF must "trust" the process model more. Despite the significant drop in sensor quality, adequate state estimates can still be obtained with this tuned EKF, as shown by SSE_{EKF}.

The identified model from OEM shows significant improvement in total SSE, and is comparable to Experiment 2(b). The parameter estimates also show similarities, as shown in Figure 31 below. Most of the parameter estimates were close to one another between the cases. Additionally, all parameters that deviated significantly from the true values did so in both cases.

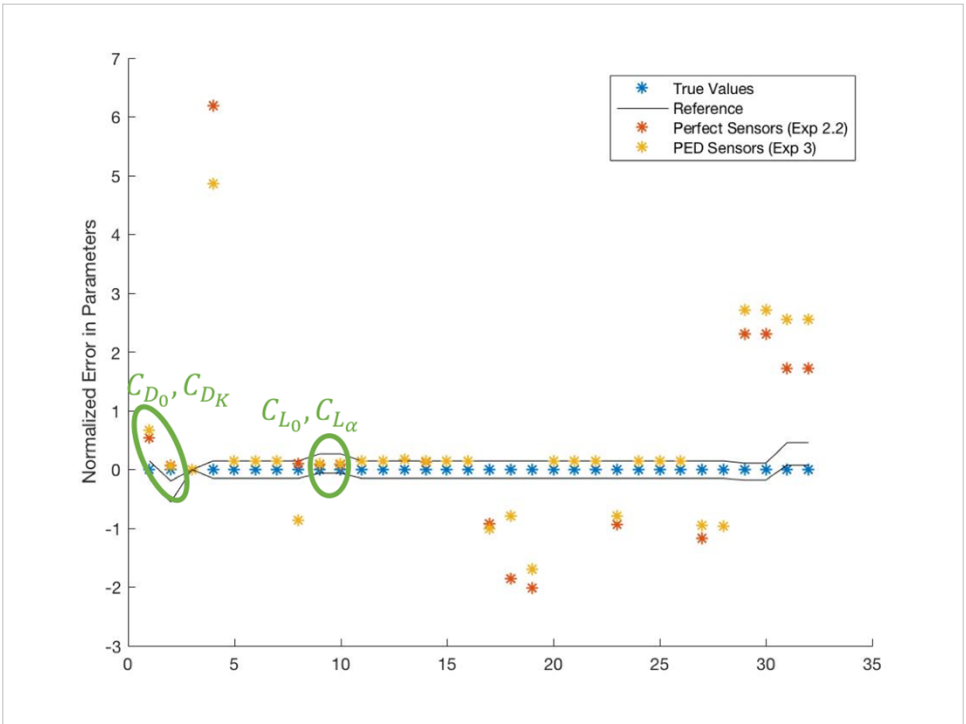

Figure 31. OEM Parameters from PED Data

The most significant improvement in both cases was in the lift coefficients C_{L_0} and C_{L_α}. However, zero-lift drag and induced drag were both overestimated, which can be seen in Figure 32 below.

Table 21. Lift/Drag Ratio from PED Data

	True Value	Reference Model	OEM Model	Improvement %
Lift/Drag Ratio at Trim	9.2227	15.2828	7.5329	72.1 %
Lift/Drag Ratio at Best Glide	8.5311	16.1957	4.2339	43.9 %

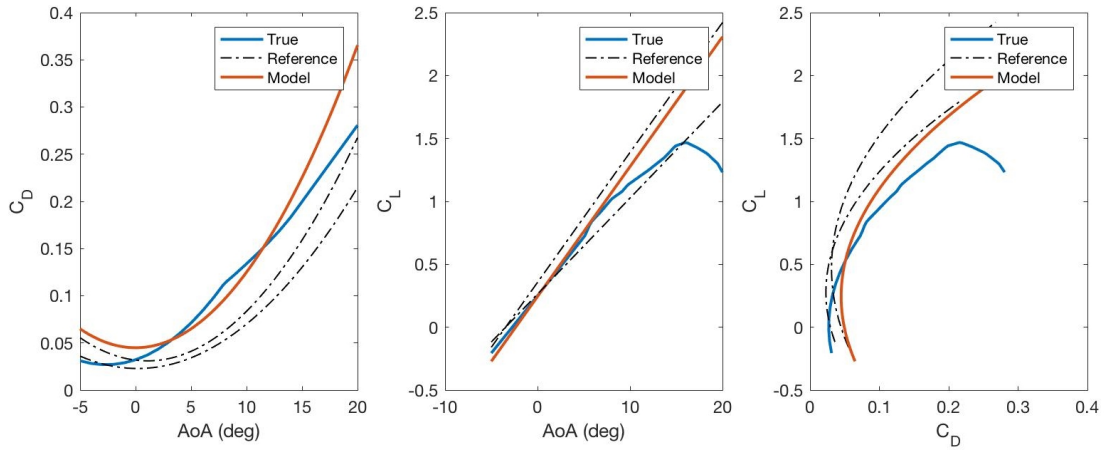

(a) (b) (c)

Figure 32. Lift and Drag Curves from PED Data

Because drag was over estimated, both the L/D ratio at the trim condition and at best glide speed of 65 KTAS was lower than the true model. However, in both cases, this estimate was closer to the true value than that predicted by the reference model, therefore showing an improvement in L/D estimation. Examination of the curves in Figure 32 confirms that better fits were obtained with the identified model. Stability modes show similar trends; almost all modes improved significantly with the identified model, as shown below in Table 22 and Figure 33. Once again, improvement was most notable in the longitudinal modes, especially phugoid mode, which is heavily dependent on lift and drag estimates.

Table 22. Dynamic Modes from PED Data

	True Values	Reference Model	OEM Model	Improvement %
Longitudinal Modes	-2.5675 + 3.5551i	-2.8810 + 4.0505i	-2.8905 + 3.9613i	11.5 %
	-2.5675 - 3.5551i	-2.8810 - 4.0505i	-2.8905 - 3.9613i	11.5 %
	-0.0310 + 0.2193i	-0.0062 + 0.1580i	-0.0107 + 0.2202i	69.3 %
	-0.0310 - 0.2193i	-0.0062 - 0.1580i	-0.0107 - 0.2202i	69.3 %
Lateral Modes	-10.0239	-11.1796	-11.1792	<0.1 %
	-0.5870 + 2.6918i	-0.6932 + 2.9001i	-0.6886 + 2.8953i	2.7 %
	-0.5870 - 2.6918i	-0.6932 - 2.9001i	-0.6886 - 2.8953i	2.7 %
	-0.0187	-0.0237	-0.0232	10.8 %

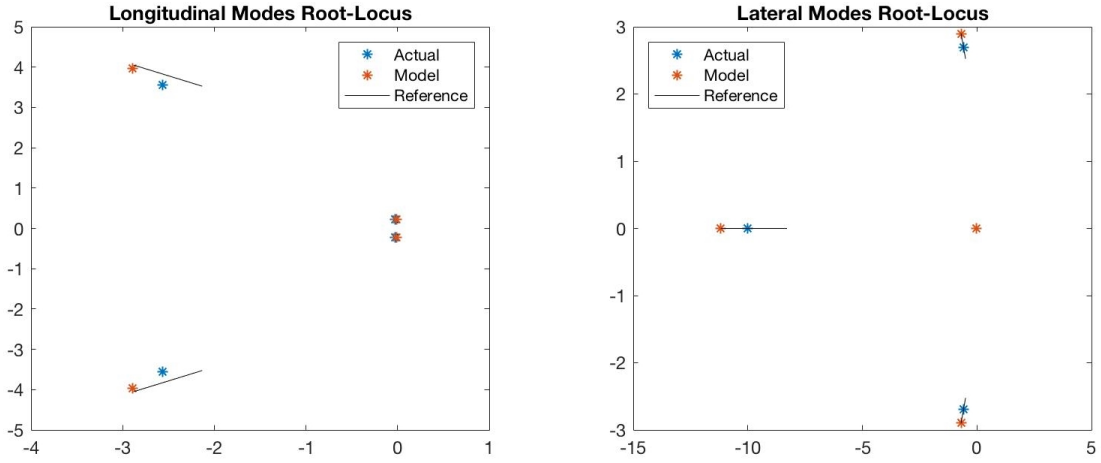

(a) (b)

Figure 33. Root Locus from PED Data

Table 23 summarizes the comparison between Experiment 2(b) and Experiment 3. Note that the results of both indicate that improvements were made from the reference model, and that the amount of change is comparable in both cases. Despite the lower sensor quality afforded by PEDs, similar levels of improvement were obtained. Note also that the percentage improvement is slightly higher for certain metrics when PED data was used.

However, the increased performance is marginal compared to the decrease in performance for other metrics and can be assumed to be caused by the random noise characteristics of the sensors. Ideally, several sets of measurement data could be used for SysID and a distribution of improvements obtained, rather than a single value. However, the computational expense needed to tune the filter and conduct OEM makes this difficult. Therefore, only a single case was tested. However, improvement in each metric was still obtained, leading to the conclusion that PEDs provide accurate enough data to improve the *a priori* model. This confirms Hypothesis 3 and answers Research Question 3.

Table 23. Experiment 3 Summary

Metric	Perfect Sensors (Experiment 2(b))	PED Sensors (Experiment 3)
	% Improvement	% Improvement
SSE	85.4 %	86.4 %
L/D at Trim	76.4 %	72.1 %
L/D at Best Glide	82.1 %	43.9 %
Phugoid Mode	15.1 %	11.5 %
Short Period Mode	52.8 %	69.3 %
Roll Mode	<0.1 %	<0.1 %
Dutch Roll Mode	< 0.1 %	2.7 %
Spiral Mode	13.3 %	10.8 %

5.4 Experiment 4: Robustness of Method to Inaccuracies in System Model

The last set of experiments in this study seeks to understand the effect of inaccurate assumptions in the model. In particular, atmospheric conditions have thus far been assumed as standard from ISA, with no wind or turbulence. It was shown in Sections 4.3 and Section 5.1.1 that estimating air data with a standard EKF was impractical under the current

methodology, and therefore this assumption was necessary. However, if nonstandard and windy conditions exist (as they often do), errors in SysID will likely be introduced.

Similarly, an assumption has been made that an accurate weight and balance of the aircraft has been carried out. This assumption was proven necessary from the results of Experiment 1(b) in Section 5.1.2. This is generally a reasonable assumption; pilots are required to understand the weight and balance of the aircraft before taking off. However, these calculations are rough estimates, and it is therefore important to understand how uncertainties in weight estimates affect SysID. Research Question 4 can then be restated and elaborated upon with sub-questions 4(a) and 4(b). New hypotheses for these research questions must also be developed and tested in Experiment 4.

Research Question 4

How sensitive are System Identification results to assumptions made in the system model?

- **Research Question 4(a):** Under the assumption of a standard atmosphere with no wind, how will nonstandard atmospheric conditions, wind, and turbulence affect the output of System Identification?
- **Research Question 4(b):** How will inaccuracies in weight and balance data affect the results of System Identification?

Hypothesis 4: *If the assumptions in the system model are within reasonable limits under conditions typical of General Aviation operations, improvement in an a priori model can be achieved using System Identification.*

- **Hypothesis 4(a):** *If wind velocity is known within +/- 5 knots and temperature known within +/- 10 degrees Celsius, then improvement in an a priori model can be achieved using System Identification.*
- **Hypothesis 4(b):** *If all assumed component weights are accurate within 10 pounds, then improvement in an a priori model can be achieved using System Identification.*

The standard atmosphere and zero wind assumptions are unlikely to ever be completely true. However, aviation weather services can supply the pilot with nonstandard temperature corrections as well as current and forecast average wind velocity and direction. Many PED applications obtain this information automatically and use it to correct glide range estimates [21] [24] [41]. This is equivalent to assuming known wind and density. Therefore, to test inaccuracies in this data it is sufficient to perturb the system from a standard atmosphere and zero wind condition. Additionally, it would be unreasonable to assume very large inaccuracies in these assumptions due to the availability of weather reporting. Therefore, perturbations of +/- 10 ft/s (approximately 6 knots) and +/- 10 degrees Celsius will be used to simulate the "worst case" for these inaccuracies. Experiment 4(a) will be conducted by adding 6 knots of wind and +10 degrees Celsius to the true conditions while maintaining the model's assumption of standard atmosphere and no wind.

Turbulence from Simulink's Dryden turbulence model will also be added. Results from the SysID process can then be compared to those of Experiment 3 to assess the impact of these assumptions on SysID and address Hypothesis 4(a) and Research Question 4(a). If improvements in the *a priori* model are still achieved under these inaccuracies, then Hypothesis 4(a) will be validated.

Similar logic can be used for Hypothesis 4(b) and Experiment 4(b): weight and balance calculations are a standard step in GA preflight processes. It can therefore be assumed that these quantities are known within a certain accuracy for a given loading condition. The weight and balance parameters used in this study are all pilot, passenger, baggage, or fuel weights, which can be assumed known within 10 pounds. Therefore, experiment 4(b) will perturb the true weights by +/- 10 pounds while the model retains the original assumed values. Once again, results from SysID can be compared from this case to Experiments 3 and 4(a) to address Hypothesis 4(b) and Research Question 4(b). If improvements are still achieved, Hypothesis 4(b) will be validated.

It is important to note that more experiment cases could be used to determine probability distributions relating the accuracy of assumptions and the accuracy of SysID. However, the computational cost to perform these cases using OEM is not insignificant, and therefore only these two cases will be tested. The conditions for Experiment 4 are listed below in Table 24:

Table 24. Conditions for Experiment 4

Trim Conditions	
VTAS	100 KTAS
Altitude	3000 ft
Vertical Speed	0 ft/min
Roll	0 deg
Atmospheric Conditions	
Wind	10 ft/s @ 045°
Turbulence	Dryden Model
Temperature	Standard +10°C
Sensor Characteristics	
GPS Frequency	1 Hz
GPS Accuracy	16 ft
Accelerometer Frequency	30 Hz
Accelerometer Accuracy	0.01 ft/s^2
Gyroscope Frequency	30 Hz
Gyroscope Accuracy	0.01 deg/s
Magnetometer Frequency	30 Hz
Magnetometer Accuracy	7 deg

5.4.1 Experiment 4(a) - Nonstandard Atmosphere

Experiment 4(a) was conducted to evaluate the effect of inaccurate assumptions regarding air data. The same tuning procedure as in previous experiments was used to tune the EKF for Experiment 4(a) after nonstandard temperature, wind, and turbulence were added into the model. The resulting tuning parameters shown in Table 25 indicate that state estimates remained accurate.

Table 25. Performance Metrics for Experiment 4(a)

Filter Performance	
Process Noise Parameter, q_x	.000038
SSE_{EKF}	2160
OEM Performance	
SSE_{REF}	51725205.6688
SSE_{OEM}	81840608.328
Improvement	36.8 %

The performance improvement of the identified model is significantly lower in this case than in others, indicating that the ISA no-wind assumption does play a large role in the accuracy of the SysID process. However, improvement was still made. Direct comparison of parameters in Figure 34 shows similar trends as in Experiment 3.

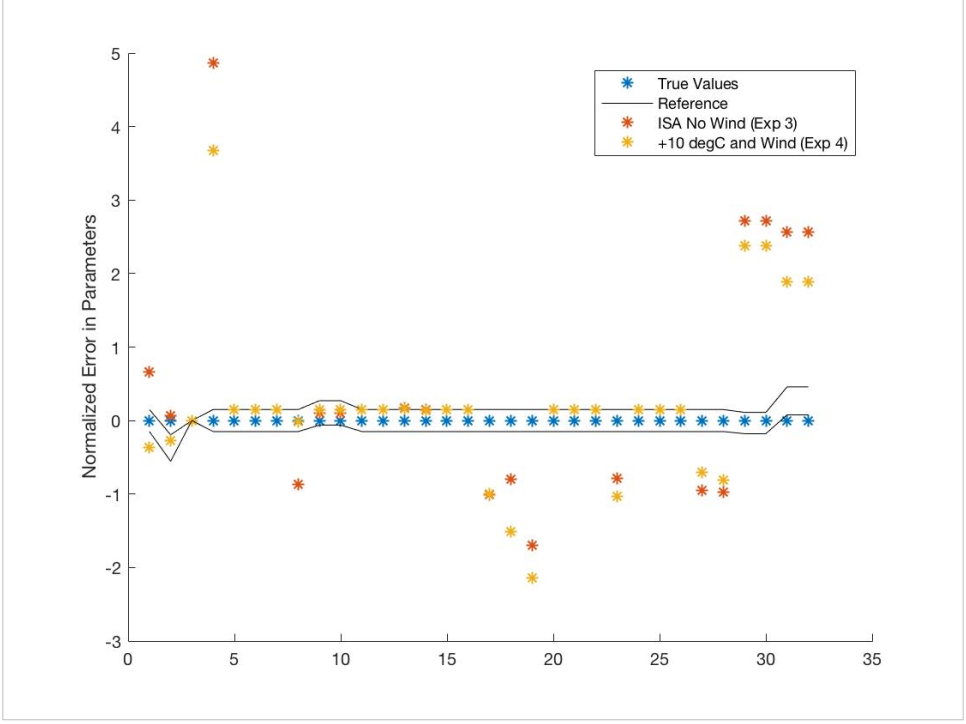

Figure 34. OEM Parameters Experiment 4(a)

Many parameters remained close to those obtained in Experiment 3. However, there are noticeable differences, especially in the control derivatives. The effects of these on aerodynamic calculations can be seen below in Table 26 and Figure 35:

Table 26. Lift/Drag Ratio Experiment 4(a)

	True Value	Reference Model	OEM Model	Improvement %
Lift/Drag Ratio at Trim	8.8926	14.2532	15.8840	-30.4 %
Lift/Drag Ratio at Best Glide	9.1891	16.5038	5.4258	48.6 %

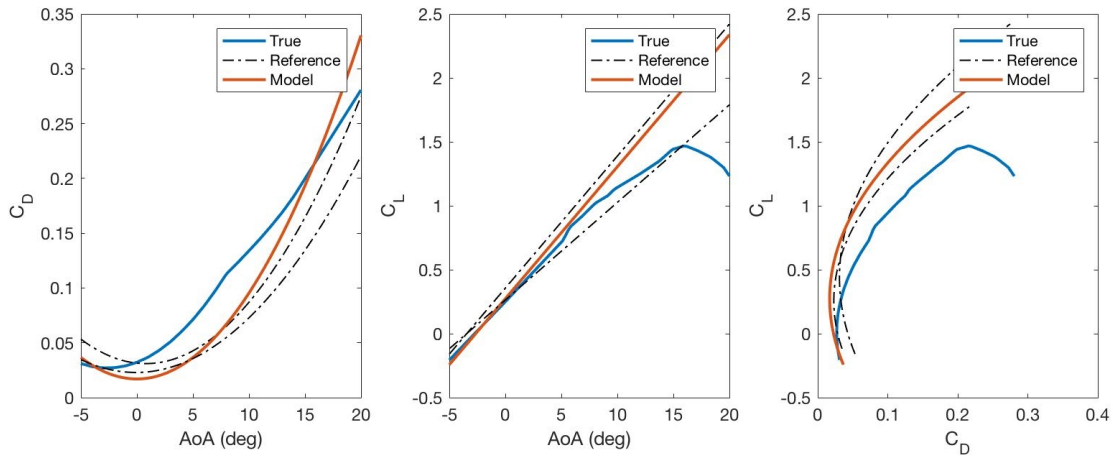

(a) (b) (c)

Figure 35. Lift and Drag Curves Experiment 4(a)

Improvement in the dynamic modes was mostly positive, though slightly reduced compared to that of Experiment 3. This can be seen below in Table 27 and Figure 36.

Table 27. Dynamic Modes Experiment 4(a)

	True Values	Reference Model	OEM Model	Improvement %
Longitudinal Modes	-2.5865 + 3.5885i	-2.9048 + 4.1196i	-2.9075 + 4.0474i	9.5 %
	-2.5865 - 3.5885i	-2.9048 - 4.1196i	-2.9075 - 4.0474i	9.5 %
	-0.0296 + 0.2104i	-0.0059 + 0.1462i	0.0043 + 0.2296i	43.0 %
	-0.0296 - 0.2104i	-0.0059 - 0.1462i	0.0043 - 0.2296i	43.0 %
Lateral Modes	-10.1173	-11.2835	-11.2833	<0.1%
	-0.5856 + 2.6992i	-0.6917 + 2.9078i	-0.6942 + 2.9100i	-1.3 %
	-0.5856 - 2.6992i	-0.6917 + 2.9078i	-0.6942 - 2.9100i	-1.3 %
	-0.0192	-0.0239	-0.0234	10.6 %

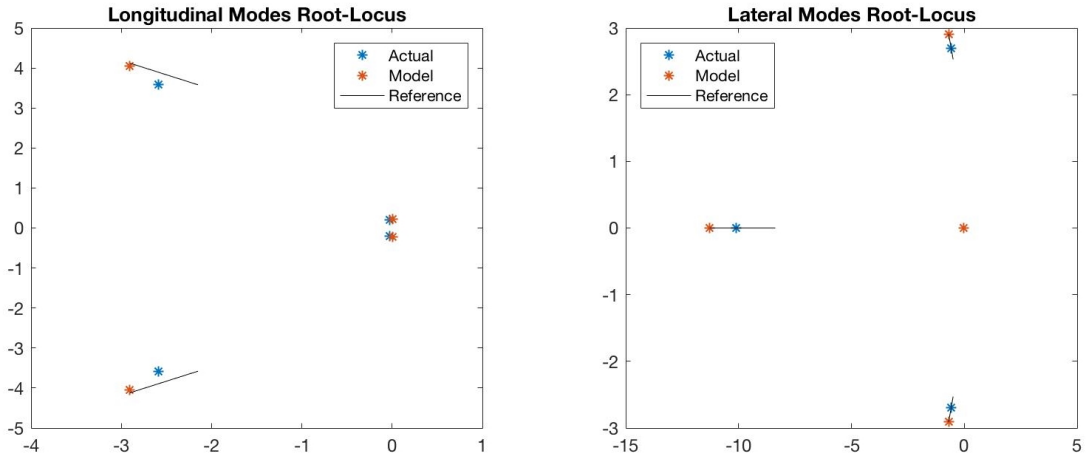

(a) (b)

Figure 36. Root Locus Experiment 4(a)

The results above show that increased error in the standard atmosphere no-wind assumption increased error in the SysID process. Improvements were still made from the reference model in most metrics, but performance was significantly reduced, and in some cases (lift to drag ratio at trim, for example) became much worse. This is similar to the results of Valasek and Chen [3] who documented the effects of prolonged wind gusts on

EKF SysID performance. However, most metrics show improvement and therefore Hypothesis 4(a) is validated. Further improvements could likely be obtained by estimating wind direction in conjunction with the unknown parameters in OEM (note that these quantities were shown to be together globally identifiable in Experiment 1). Comparison between experiment 3 and 4.1 is summarized below in Table 28.

Table 28. Experiment 4(a) Summary

Metric	ISA and No Wind (Experiment 3)	Nonstandard (Experiment 4(a))
	% Improvement	% Improvement
SSE	86.4 %	36.8 %
L/D at Trim	72.1 %	-30.4 %
L/D at Best Glide	43.9 %	48.6 %
Short Period Mode	11.5 %	9.5 %
Phugoid Mode	69.3 %	43.0 %
Roll Mode	<0.1 %	<0.1 %
Dutch Roll Mode	2.7 %	-1.3 %
Spiral Mode	10.8 %	10.6 %

5.4.2 Experiment 4(b) – Erroneous Weight and Balance

Experiment 4(b) was conducted to assess the impact of incorrect weight and balance assumptions on the SysID process. Inaccuracy in the air data assumptions was retained from Experiment 4(a). The true weights and assumed weights are shown below in Table 29.

Table 29. Weight and Balance Data for Experiment 4(b)

Component	True Weight (*lb*)	Assumed Weight (lb)
Pilot	170	180 (+10)
Copilot	190	180 (-10)
Left Passenger	0	0
Right Passenger	0	0
Bags	0	0
Initial Fuel	240	240

The error in the assumptions for pilot and copilot weights was set at 10 lb. This was assumed to be within the limits of a properly conducted weight and balance while still introducing error into the assumption. The total model improvement is given below in Table 30, followed by the parameter comparison in Figure 37.

Table 30. Performance Metrics for Experiment 4(b)

OEM Performance	
SSE_{REF}	82308089.0935
SSE_{OEM}	55576279.0799
Improvement	32.5 %

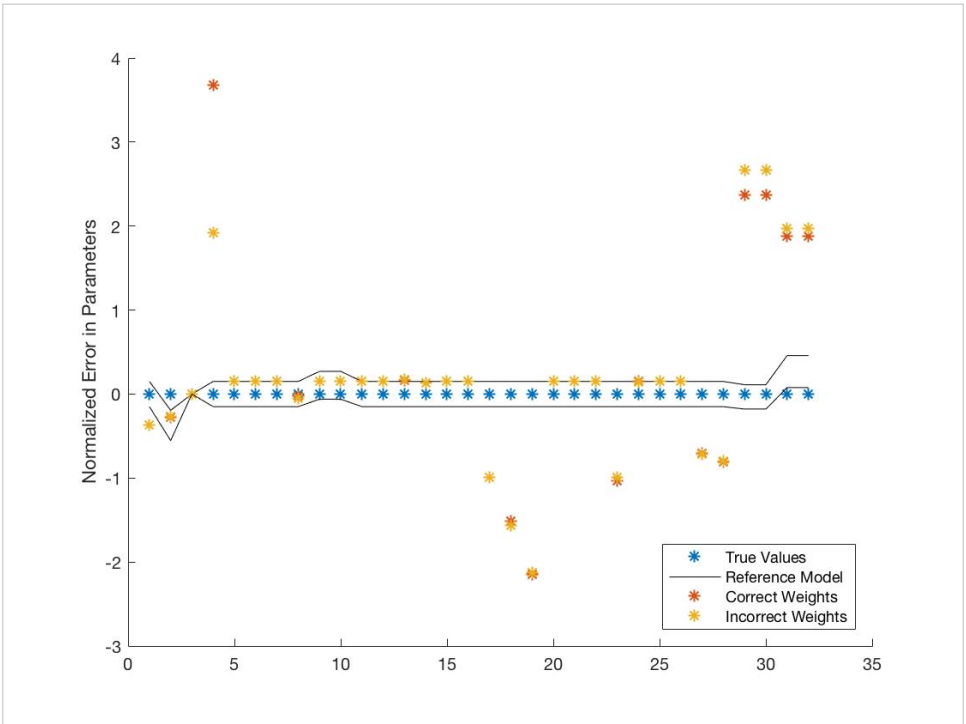

Figure 37. OEM Parameters Experiment 4(b)

Similar model improvement and individual parameters were obtained between Experiments 4(a) and 4(b). This is likely due to the relatively mild inaccuracies in weight and balance; a deviation of 10 lb. is a reasonable assumption for the accuracy of a weight and balance calculation, but represents only a small percentage of the total aircraft weight. However, noticeable changes occurred in both the engine parameters and the drag due to elevator deflection. Throttle and elevator are the primary control surfaces for trim, and their positions are highly dependent not only on total weight but also on the location of the center of gravity. Having inaccurate weight and balance could cause inaccurate estimation of these control deflections, which in turn causes inaccurate estimation of control derivatives.

The reduced drag from elevator deflection increased the lift to drag ratios compared to Experiment 4(a). For the first metric, this shift causes the estimate to become worse; in the second, it improves the estimate. This can be seen below in Table 31 and Figure 38:

Table 31. Lift/Drag Ratio Experiment 4(b)

	True Value	Reference Model	OEM Model	Improvement %
Lift/Drag Ratio at Trim	8.8927	14.2534	17.7459	-65.2 %
Lift/Drag Ratio at Best Glide	9.1891	16.5039	7.0851	71.2 %

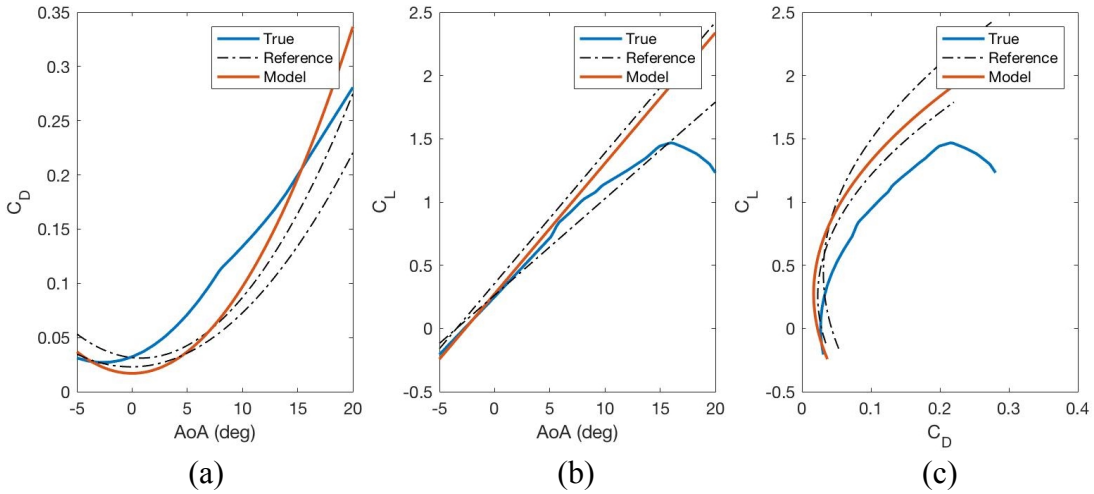

(a) (b) (c)

Figure 38. Lift and Drag Curves Experiment 4(b)

The improvement in longitudinal and lateral modes is similar to that of Experiment 4(a), as shown below in Table 32 and Figure 39. Again, this is likely due to the relatively mild perturbation in weight assumption.

Table 32. Dynamic Modes Experiment 4(b)

	True Values	Reference Model	OEM Model	Improvement %
Longitudinal Modes	-2.5866 + 3.5886i	-2.9048 + 4.1196i	-2.9066 + 4.0498i	9.3 %
	-2.5866 - 3.5886i	-2.9048 - 4.1196i	-2.9066 - 4.0498i	9.3 %
	-0.0296 + 0.2104i	-0.0059 + 0.1462i	0.0054 + 0.2261i	43.8 %
	-0.0296 - 0.2104i	-0.0059 - 0.1462i	0.0054 - 0.2261i	43.8 %
Lateral Modes	-10.1161	-11.2822	-11.2822	0 %
	-0.5856 + 2.6992i	-0.6917 + 2.9078i	-0.6946 + 2.9066i	< -0.1%
	-0.5856 + 2.6992i	-0.6917 - 2.9078i	-0.6946 - 2.9066i	< -0.1%
	-0.0203	-0.0251	-0.0249	3.6 %

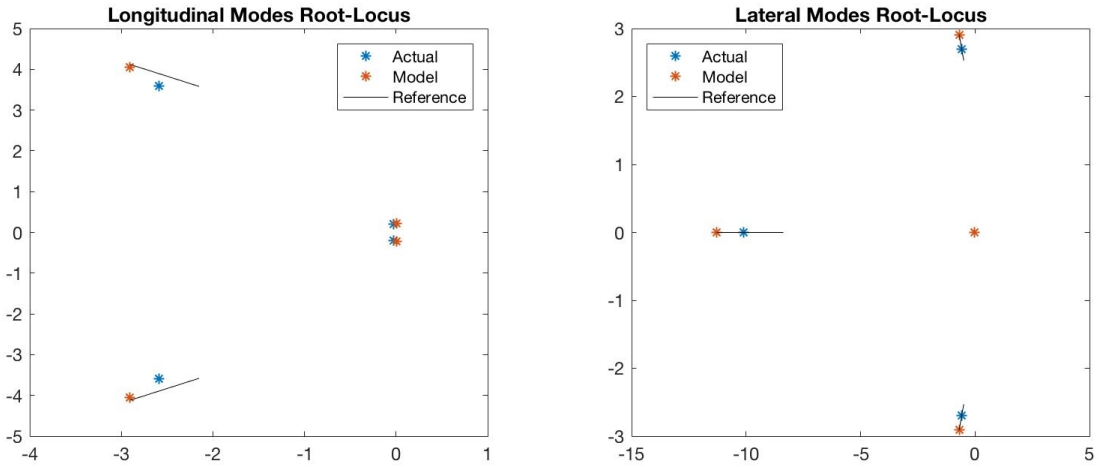

(a) (b)

Figure 39. Root Locus Experiment 4(b)

5.4.3 Conclusion of Experiment 4

In Experiment 4, the effects of inaccuracies in the assumptions of standard atmosphere and known weight and balance were quantified. It was shown that inaccurate

wind and density estimates have a much larger effect on the SysID performance than inaccurate weight and balance. However, both sources of inaccuracy caused degradation of the SysID process. Improvements in the model were still obtained, but the importance of accurate information for SysID was established. Therefore, both Hypothesis 4(a) and 4(b) were confirmed; improvements in model accuracy were still obtained despite the presence of inaccuracies. This in turn answers Research Questions 4(a) and 4(b).

More accurate wind and density information can likely be obtained by estimating these quantities instead of assuming them known from a standard atmosphere with no wind. In Experiment 1, these quantities were shown to be globally identifiable, meaning they can likely be estimated by processing several measurements at one time. Post-processing data using OEM can accomplish this if these parameters are added to the set of stability and control derivatives that OEM seeks to estimate. Another option is to construct a modified EKF in which measurements are processed in batches to perform updates. However, neither of these strategies was tested in this work.

CHAPTER 6. CONCLUSION

The overall research goal in this work is reiterated below. To accomplish this goal, research into previous SysID studies was conducted and several experiments were performed to test existing SysID methods.

Research Objective:

Determine the requirements, capabilities, and limitations of existing System Identification methods and their application to General Aviation aircraft flight data obtained through a low-cost Flight Data Recorder or Personal Electronic Device.

Several research questions were developed to address specific aspects of the SysID problem for GA. The first of these relates to the observability of the parameterized aircraft model. Using a PED as the measurement device on the aircraft results in "blind" SysID, in which no information about control deflections is available. In addition, there are no measurements of airflow such as airspeed or angle of attack. As these quantities are typically measured in aircraft SysID, it was important to understand how lack of these measurements affects SysID. In particular, confirming that the parameters of the dynamical model were observable and therefore able to be estimated. The first research questions posed were therefore:

Research Question 1(a):

Which quantities in the parameterization of General Aviation aircraft dynamics are locally observable using measurements obtained from a low-cost Flight Data Recorder or Personal Electronic Device?

Research Question 1(b):

What parameterizations of General Aviation aircraft dynamics are globally identifiable using measurements obtained from a low-cost Flight Data Recorder or Personal Electronic Device?

Experiment 1 sought to address these research questions by exploring parameterizations of aircraft dynamics through a global observability/identifiability condition. For the dynamics parameterization considered in this work, aircraft state and control deflections were determined to be locally observable, and therefore can be estimated "online" using a filter such as an EKF. Air data and the stability and control parameters of a nonlinear aircraft model were shown to be globally identifiable but not locally observable. These can therefore be estimated using regression techniques. For this work, only the stability and control parameters were estimated; air data was assumed from a standard atmosphere and zero wind. Weight and balance parameters were shown to be neither locally observable nor globally identifiable (though fuel weight can be directly calculated from other estimated quantities, and therefore estimated in real time). These must therefore be assumed known from preflight weight and balance calculations.

Research Questions 1(a) and 1(b) were therefore answered with regards to the models explored in this work.

It is important to note that the results from Experiment 1 are specific to the parameterization of aircraft dynamics that was used in this study. Different model structures (linear, for example) can be used in SysID. Choice of model structure and parameters of interest depends not only on observability/identifiability, but also the intent or purpose of the SysID process. For example, drag due to aileron deflection and rudder deflection was not modelled in the aircraft simulation utilized in this work, and was therefore also not included in the SysID parameterization. If it is desired to determine the effects of these variables, it should first be confirmed that these parameters are either locally observable or globally identifiable. If time-dependencies are of interest, such as transient aerodynamic effects, local observability must be confirmed. Otherwise, if it can be assumed that the parameters of interest are constant over a "batch" of data, then only global identifiability is needed. Therefore, the process documented in Experiment 1, while only applied to the parameterizations of this work, provides a means for ensuring that a SysID or any similar estimation process is constructed properly.

The observability/identifiability conditions used in Experiment 1 assess only structural identifiability. Practical identifiability relies on measurement quality and quantity. A system can be deemed structurally observable even if, for example, the parameters are only "observed" once. However, this is likely not sufficient to estimate the values of these parameters from noisy measurement data. Therefore, future exploration of a practical identifiability condition for aircraft SysID may prove more useful. For example, understanding practical observability/identifiability could inform selection of

measurement devices as well as design of maneuver sequences for SysID or other estimation problems.

Experiment 1 concluded with a model structure that was shown to be locally observable in time-dependent parameters (state and controls) and globally identifiable in time-independent parameters (stability and control derivatives). Therefore, the SysID problem for the trajectory, model parameterization, and SysID methods considered was confirmed to be well-posed and to have a unique solution. However, this does not guarantee that standard SysID estimation techniques will be successful in finding this solution, nor does it provide any indication about which of the many SysID techniques will perform best. Therefore, Research Question 2 was posed:

Research Question 2

Which method of System Identification is best suited for accurately determining a 6-Degree-of-Freedom model of a General Aviation aircraft from low-cost Flight Data Recorder or Personal Electronic Device data?

For the motivations discussed in CHAPTER 1, it was determined that a nonlinear model would be most suited, and therefore only nonlinear SysID methods (OEM and EKF) were investigated. Experiment 2 conducted a comparison of Output Error Method (OEM) and Extended Kalman Filter (EKF) SysID. Results indicated that EKF estimation was limited by observability of parameters, and therefore performed poorly. Due to the linear nature of the Kalman Filter equations, estimation using EKF is constrained by the local

observability condition as opposed to the global condition. OEM, on the other hand, could be used to identify parameters that are constant over the trajectory, but is unable to estimate time-dependent quantities, such as states and control inputs. Therefore, the estimation problem was divided into an online estimation using an EKF to estimate the locally observable states and unknown control inputs, and an offline estimation using OEM to estimate globally identifiable model parameters. This methodology was shown to improve upon the accuracy of the *a priori* model in most parameters. The answer to Research Question 2 is therefore that post-processing state and control estimates using OEM was best suited for the nonlinear model considered. However, this methodology and the resulting identified model could potentially be improved through several ways.

Parameter estimation using OEM is dependent upon the knowledge of control inputs used to excite the model. In this work, control inputs were estimated using an EKF and an *a priori* dynamic model. However, the control input estimation was shown to be noisy and inaccurate, a symptom of the known inaccuracy in the *a priori* model. Application of more robust filtering techniques may be able to achieve control estimation with higher accuracy. Additionally, poor modelling of throttle and power control inputs and their effect on the model contributed significant error. The effects of this modelling error were seen throughout, indicating that SysID processes are extremely sensitive to the accuracy of the proposed parameterization. This has important implications for SysID problems in which the dynamics are not fully understood *a priori*, such as for LOC events. The SysID methods examined in this work are only as good as the posited model structure; if an assumption of a linear model has been made even though the dynamics are highly nonlinear, the SysID process will be prone to error. However, methods such as ANN SysID, which do not rely

on any model structure could be useful for exploring possible parameterizations for unknown dynamics, such as LOC. The limitation of this approach is the loss of understanding of the obtained model itself; ANNs are purely mathematical and therefore the weightings obtained cannot easily be used to analyze physical relationships.

Another limitation to the approach in this work is the "circular" estimation of controls: inputs are estimated using an *a priori* model and then used in OEM to improve upon the same *a priori* model. Therefore, many of the identified parameters very closely resembled the *a priori* model; however, significant improvement in certain parameters, especially lift and drag estimation, were still observed. The results showed that it is still feasible to improve performance and stability estimates and modelling at the expense of error in the control estimation. However, refinement of the control estimation, or even ignoring control inputs altogether, may enable higher accuracy to be obtained.

The role of sensor quality in SysID processes was also investigated. The measurement quality afforded by a PED is significantly less than that of more robust FDRs, and introduces error into the SysID process. Research Question 3 was stated as follows:

Research Question 3

What requirements on sensor quality are needed to improve *a priori* model accuracy through System Identification?

For the purposes of this work, it was deemed sufficient to compare the results of SysID using near-perfect sensors to the results from using PED sensors, specifically GPS, accelerometer, gyroscope, and magnetometer. Ideally, a more robust investigation into sensor quality requirements would be conducted, but the computational expense for conducting such a study is nontrivial and therefore outside the scope of the current work. Experiment 3 used the same SysID process described in Experiment 2 with simulated PED measurements. The results were then compared to those of Experiment 2 which had assumed near-perfect sensors. The results demonstrated that although performance was mildly degraded, improvements to the *a priori* model when using PED data were similar to those obtained from near-perfect sensors so long as a tuning procedure was used to tune the EKF state and control estimation. Therefore, Research Question 3 was answered by concluding that the inertial sensors available on standard PEDs are adequate for improving aircraft model accuracy through SysID.

EKF tuning is not, in general, a simple task. In this work, a single parameter was used to scale process noise in the EKF and a simple optimization routine was employed to find a value for the tuning parameter that achieved local minimum of filter error. More robust tuning utilizing multiple parameters may result in increased performance. Additionally, no consideration was given to filter consistency (see Section 4.3 for a discussion of consistency-based tuning procedures). Robustness of the filter was also not considered; using bias-compensating techniques could improve performance especially for the control estimation as discussed in Section 4.3.

The last question that was addressed in this work pertains to the accuracy of the assumptions made in the proposed model for SysID. Aside from inaccuracies in model

structure (linear air reactions used to model nonlinear lift, drag, thrust, and power) discussed in Experiment 2, the parameterized model in this work also relied on the assumption of known wind velocities and air density from a standard atmosphere, as well as known weight and balance data. Inaccuracies in these assumptions will likely exist in a real SysID process, and therefore their effect on the results of SysID must be assessed:

Research Question 4

How sensitive are System Identification results to assumptions made in the system model?

- **Research Question 4(a):** Under the assumption of a standard atmosphere with no wind, how will nonstandard atmospheric conditions, wind, and turbulence affect the output of System Identification?
- **Research Question 4(b):** How will inaccuracies in weight and balance data affect the results of System Identification?

Experiment 4 perturbed true values of these quantities away from their assumed values and measured the impact on SysID results. Similar to Experiment 3, computational expense to fully investigate the effect of inaccuracies on SysID is nontrivial. Therefore, only two cases were tested for each research question: accurate assumptions and "worst case" inaccurate assumptions (see Section 5.4 for a more complete definition of "worst case" for air data and weight and balance assumptions). The results showed that inaccurate wind and density assumptions cause a significant decrease in the model improvement

obtained through SysID. However, model improvements were still possible, therefore answering Research Question 4(a). Inaccuracies in wind and density assumptions can still be detrimental to the SysID process. Fortunately, as discussed in Experiment 1, these quantities are globally identifiable and can therefore be estimated in OEM; however, this estimation was not carried out in this work.

Inaccuracies in weight and balance also degraded SysID performance but by a much smaller margin than in the previous case. Therefore, it was determined that the SysID process is robust to errors in weight and balance calculations so long as a proper weight and balance is conducted, therefore answering Research Question 4(b).

Table 33. Summary of Experiment Results

Metric	All Known Data (Experiment 2a)	Estimated States and Controls (Experiment 2b)	PED Sensors (Experiment 3)	Nonstandard Atmosphere & Wind (Experiment 4a)	Inaccurate Weight and Balance (Experiment 4b)
	Improvement %	Improvement %	Improvement %	Improvement %	Improvement %
SSE	99.9 %	85.4 %	86.4 %	36.8 %	32.5 %
L/D at Trim	68.2 %	76.4 %	72.1 %	-9.9 %	-65.2 %
L/D at 65 kts	80.2 %	82.1 %	43.9 %	59.5 %	71.2 %
Phugoid	92.3 %	15.1 %	11.5 %	9.5 %	9.3 %
Short Period	96.8 %	52.8 %	69.3 %	43.0 %	43.8 %
Roll	80.4 %	<0.1%	<0.1 %	<0.1 %	0 %
Dutch Roll	93.4 %	< 0.1 %	2.7 %	-1.3 %	< -0.1 %
Spiral Mode	65.9 %	13.3 %	10.8 %	10.6 %	3.6 %

Table 33 above shows that improvements from the *a priori* model were demonstrated in almost every case. These improvements demonstrate the ability of SysID to enable more accurate understanding of the dynamics of each individual GA aircraft. However, there are several limitations of the current work:

- Only one trajectory/maneuver sequence was analyzed. Results may be different for other trajectories/maneuver sequences performed at different flight conditions.
- Only time-domain estimation methods were examined. Frequency-domain methods have also been shown to be successful in aircraft SysID, especially online SysID, and therefore warrant further exploration.
- Different model forms (i.e. parametrizations of aerodynamics) may produce different results, and parameterizations that present the most benefit to GA could be explored.
- With regards to the unknown control estimation, accuracy of the estimation and subsequent OEM SysID process was highly sensitive to EKF performance. The tuning algorithm utilized in this work could be improved, possibly leading to more accurate results for state and control estimation and SysID.
- Control estimation was dependent on the existence and accuracy of an *a priori* model; in this study, an inaccurate model was purposefully used and potential improvement on the model was shown. A further study using the improved model in EKF state and control estimation may be able to demonstrate the usefulness of the obtained model to increase accuracy of control estimates. An iterative SysID process could therefore be envisioned in which an initial model is used in EKF to obtain state and control estimates, OEM is used to refine the model estimate, the new identified model is used to obtain new state and control estimates, and so on. It is possible that this process may increase

the improvements demonstrated in this work and be more representative of an operational application of SysID.

- Control inputs were designed specifically for SysID and are not representative of any actual GA flight. Additional investigation would be required to determine what action by the pilot beyond typical operations is needed, if any, in order to produce satisfactory data for SysID.
- OEM utilized a pure sum of squares over the entire trajectory, rather than a weighted sum of squares or a maximum likelihood estimation (MLE). As a result, most improvement was seen in longitudinal derivatives, likely due to the persistence of the phugoid mode. Error in longitudinal derivatives would likely dominate the error calculation due to the low damping and period of the phugoid mode, as opposed to the other dynamic modes whose response, and therefore error, would damp out relatively quickly. Analyzing subsets of the trajectory data (as opposed to the entire trajectory), or using a weighted sum of squares may allow "targeting" of specific parameters and could therefore increase accuracy of the estimation method.
- Only simulated data was used for this study. Actual flight data for GA aircraft using these devices has not been assessed.
- No assessment of computational power of PEDs or low-cost FDRs was conducted. It was assumed that the proposed methods were not limited by processing power; however, this is a necessary step before SysID using PEDs can be implemented for GA.

- ANN SysID was not explored beyond initial research into aircraft SysID using ANNs. However, because ANNs do not rely on *a priori* model structure, this method could prove useful in developing models for unknown aerodynamics, such as LOC

To carry out the above improvements, a methodology similar to the one used in this work can be adopted and utilized for exploring SysID in GA. An overview of this process is shown below in Figure 40. The first step is to understand the requirements and desired outcomes of the SysID process. In this work, the motivation for exploring SysID for GA was partially due to interest in LOC dynamics and performance planning. This motivation informed the decision to utilize a nonlinear aircraft model. Coefficients of interest were included in the model structure. However, it was necessary to then determine if, given the measurements available, the proposed system was observable and identifiable. In this work, it was found necessary to assume known weight and balance data in the model and to use a standard atmosphere assumption with no wind. This observability study can also reveal which parameters of interest in the model are locally observable and those that are only globally identifiable. For those that are locally observable, online estimation can be carried out. For those that are only globally identifiable, regression techniques must be used. If the desired locally observable and globally identifiable parameters are observable and identifiable in the model, then the online and offline estimations can be carried out and results analyzed. Otherwise, additional assumptions or measurements would be needed to produce meaningful results.

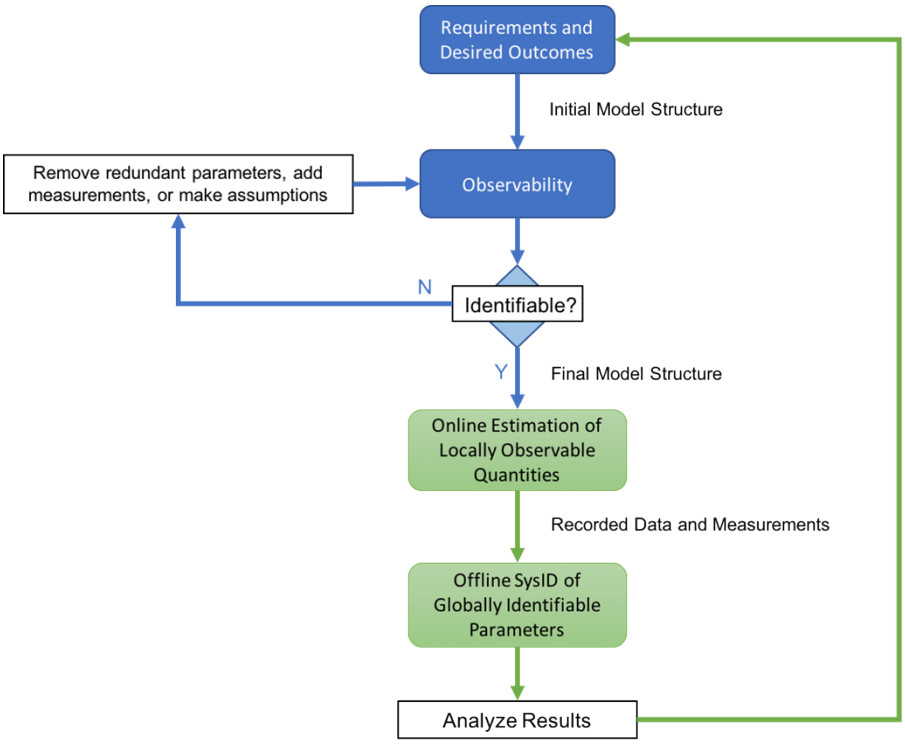

Figure 40. Overview of Experimental Process

In the introduction of this work, several potential benefits of SysID applied to GA were discussed, and are reiterated here. SysID in GA has potential to:

1. Assist efforts to introduce data-driven safety into GA by using identified models to increase fidelity in the definition and detection of relevant safety metrics for a wide range of operations and aircraft types
2. Increase understanding of LOC events through application to accident data
3. Assist efforts for LOC mitigation by providing models that can be used in the definition of safe sets, investigation of mitigation strategies, and increased simulator fidelity for upset conditions and upset recovery

4. Increase pilot situational awareness by providing estimates of unmeasured parameters such as AoA and fuel burn
5. Improve state-estimation, navigation, and performance calculations currently in-use on PEDs by increasing model fidelity used by such applications

Improvements over an assumed *a priori* model were demonstrated despite the limitations noted above, indicating that further development and refinement of the methods in this work could lead to the realization of these goals. Real-world implementation of the current methods in GA can be done in parallel with currently existing applications and systems for PEDs and low-cost FDRs. Real-time state and control estimation can be carried out using the sensors onboard a PED and uploaded to a database for post-processing, such as NGAFID [10] or CloudAhoy [20]. SysID using OEM can then be carried out, and the resulting models given to the pilot to be used for performance and dynamics calculations. As more data from more flights becomes available, the aircraft dynamic and performance model accuracy is likely to increase beyond what is demonstrated in this work.

The conclusion of this work is that SysID methods continue to show potential for improving GA operations and safety. This study serves as an initial investigation into the available methods and their applicability to the GA SysID problem. Results showed that it is possible to obtain a more accurate dynamic model through SysID using limited data from a PED. Further investigation into SysID methods, model parametrizations, control estimation algorithms, and applications of these to GA aircraft are likely to yield results that are useful and applicable to PED or FDR data for GA aircraft. The obtained models can then be used to assist efforts to improve GA safety and efficiency.

REFERENCES

[1] W. M. DeBusk, G. Chowdhary and E. N. Johnson, "Real-Time System Identification of a Small Multi-Engine Aircraft," in *AIAA Atmospheric Flight Mechanics Conference*, 2009.

[2] A. Noriega, *Observability and Confidence of Stability and Control Derivatives Determined in Real Time,* Embry-Riddle Aeronautical University, 2013.

[3] J. Valasek and W. Chen, "Observer/Kalman Filter Identification for Online System Identification of Aircraft," *Journal of Guidance, Control, and Dynamics,* vol. 26, no. 2, pp. 347-353, 2003.

[4] J. Sembiring, L. Drees and F. Holzapfel, "Extracting Unmeasured Parameters Based on Quick Access Recorder Data Using Parameter-Estimation Method," in *AIAA Atmospheric Flight Mechanics (AFM) Conference*, 2013.

[5] E. A. Morelli, "Real-Time Aerodynamic Parameter Estimation without Air Flow Angle Measurements," in *AIAA Atmospheric Flight Mechanics Conference*, 2010.

[6] Federal Aviation Administration, "Traffic Flow Management System Counts; Distributed OPSNET View," Federal Aviation Administration, 2018.

[7] National Transportation Safety Board, "2016 NTSB US Civil Aviation Accident Statistics," November 2017. [Online]. [Accessed October 2018].

[8] Federal Aviation Administration, "Advisory Circular 120-82: Flight Operational Quality Assurance," Federal Aviation Administration, 2004.

[9] S. E. Lowe, E. M. Pfleiderer and T. R. Chidester, "Perceptions and Efficacy of Flight Operational Quality Assurance (FOQA) Programs Among Small-Scale Operators," Federal Aviation Administration, 2012.

[10] M. McCollum, "General Aviation Pilots Get Their GAARD Up with New App," The MITRE Corporation, August 2015. [Online]. [Accessed October 2018].

[11] K. Mitchell, B. Sholy and A. J. Stolzer, "General Aviation Aircraft Flight Operations Quality Assurance: Overcoming the Obstacles," *IEEE Aerospace and Electronic Systems Magazine,* vol. 22, no. 6, pp. 9-15, 2007.

[12] Federal Aviation Administration, "Fact Sheet – Aviation Safety Information Analysis and Sharing Program," December 2017. [Online]. [Accessed October 2018].

[13] International Air Transport Association, "Flight Data eXchange (FDX)," 2018. [Online]. [Accessed October 2018].

[14] S. K. Lau, "General Aviation Flight Data Monitoring," CAPACG, LLC, 2007.

[15] B. C. Kuo, W.-l. Guan and P.-c. Chen, "In Search of General Aviation Flight Data Monitoring: Lightweight Recording System," in *17th AIAA Aviation Technology, Integration, and Operations Conference*, 2017.

[16] T. Puranik, *A Methodology for Quantitative Data-Driven Safety Assessment for General Aviation,* Georgia Institute of Technology, 2018.

[17] C. M. Gocha, *Data Acquisition for Flight Tests using Handheld GPS and Electronic Flight Instrument System,* California Polytechnic State University - Aerospace Engineering Department, 2012.

[18] S. Min, *A Proactive Safety Enhancement Methodology for General Aviation Using a Synthesis of Aircraft Performance Models and Flight Data Analysis,* Georgia Institute of Technology, 2018.

[19] L. J. Levy, "The Kalman Filter: Navigation's Integration Workhorse," *GPS World,* pp. 65-71, September 1997.

[20] CloudAhoy, "Flight Debrief in the Age of Technology," [Online]. [Accessed 2018].

[21] ForeFlight, "The Essential App for Aviation," [Online]. [Accessed 2018].

[22] Gyronimo, LLC, "Gyronimo for Aviators," 2013. [Online]. [Accessed 2018].

[23] AvPlan EFB, "AvPlan EFB – Electronic Flight Bag," [Online]. [Accessed 2018].

[24] A. Meyer, "Xavion," Xavion, 2013. [Online]. [Accessed 2018].

[25] D. Hirschman, "Avionics: When All Else Fails - An App That Helps You Glide to Safety," 2013. [Online]. [Accessed 2018].

[26] M. Leichtfried, C. Kaltenriner, A. Mossel and H. Kaufmann, "Autonomous Flight using a Smartphone as On-Board Processing Unit in GPS-Denied Environments," in *Proceedings of International Conference on Advances in Mobile Computing & Multimedia*, 2013.

[27] Federal Aviation Administration, "General Aviation and Part 135 Activity Surveys - CY 2016," 2017. [Online]. [Accessed 2018].

[28] C. Bonadonna, D. Brody and A. Lopez, "Design of a Low-Cost General Aviation Flight Data Recording and Analysis System," in *Systems and Information Engineering Design Symposium*, 2015.

[29] T. Berger, M. B. Tischler, S. G. Hagerott, C. Cotting, W. R. Gray, J. L. Gresham, J. E. George, K. J. Krogh, A. D'Argenio and J. D. Howland, "Development and Validation of a Flight-Identified Full-Envelope Business Jet Simulation Model Using

a Stitching Architecture," in *AIAA Modeling and Simulation Technologies Conference*, 2017.

[30] K. Krajček, D. Nikolić and A. Domitrović, "Aircraft Performance Monitoring from Flight Data," *Tehnicki vjesnik - Technical Gazette,* vol. 22, no. 5, 2015.

[31] Common Taxonomy Team, *Aviation Occurence Categories - Definitions and Usage Notes,* Commercial Aviation Safety Team and International Civil Aviation Organization, 2013.

[32] J. R. Chambers and H. P. I. Stough, "Summary of NASA Stall/Spin Research for General Aviation Configurations," in *AIAA General Aviation Technology Conference*, 1986.

[33] J. V. Foster, K. Cunningham, C. M. Fremaux, G. H. Shah, E. C. Stewart, R. A. Rivers, J. E. Wilborn and W. Gato, "Dynamics Modeling and Simulation of Large Transport Airplanes in Upset Conditions," in *AIAA Guidance, Navigation, and Control Conference and Exhibit*, 2005.

[34] P. Lichota and M. Lasek, "Maximum Likelihood Estimation for Identification of Aircraft Aerodynamic Derivatives," *The Archive of Mechanical Engineering,* vol. 60, no. 2, 2013.

[35] P. G. Hamel and R. V. Jategaonkar, "Evolution of Flight Vehicle System Identification," *Journal of Aircraft,* vol. 33, no. 1, 1996.

[36] P. C. Murphy and V. Klein, "Transport Aircraft System Identification Using Roll and Yaw Oscillatory Wind Tunnel Data," in *American Institute of Aeronautics and Astronautics*, 2017.

[37] L. R. Le Vie, "Review of Research on Angle-of-Attack Indicator Effectiveness," National Aeronautics and Space Administration - Langley Research Center, 2014.

[38] S. Scherer, *Development of an Active Flight Envelope Warning Method for General Aviation Aircraft,* The Ohio State University - Department of Mechanical and Aerospace Engineering, 2015.

[39] E. D. Harrison, *A Methodology for Predicting and Mitgating Loss of Control Incidents for General Aviation Aircraft,* Georgia Institute of Technology, 2018.

[40] Hilton Software LLC, "Proud developer of the award winning app WingX," 2017. [Online]. [Accessed 2018].

[41] Garmin Ltd., "Garmin Pilot: App for iPad and iPhone Devices," 2018. [Online]. [Accessed 2018].

[42] R. Kalman, "A New Approach to Linear Filtering and Prediction Problems," *Journal of Basic Engineering,* vol. 82, no. 1, pp. 35-45, 1960.

[43] R. Zanetti and R. H. Bishop, "Kalman Filters with Uncompensated Biases," *Journal of Guidance, Control, and Dynamics,* vol. 35, no. 1, pp. 327-335, 2012.

[44] D. Unsal and K. Demirbas, "Estimation of Deterministic and Stochastic IMU Error Parameters," in *IEEE/ION Position, Location and Navigation Symposium*, 2012.

[45] Y. M. Al-Rawashdeh, M. Elshafei and M. F. Al-Malki , "In-Flight Estimation of Center of Gravity Position Using All-Accelerometers," *Sensors,* vol. 14, no. 9, 2014.

[46] B. Etkin, Dynamics of Atmospheric Flight, Dover Publications, 2012.

[47] FlightGear, "FlightGear wiki," January 2018. [Online].

[48] FlightGear Developers, "Cessna 172P FlightGear Github," FlightGear, 2019. [Online]. Available: https://github.com/c172p-team/c172p. [Accessed February 2019].

[49] J. Scott and M. Selig, " Aircraft Dynamics Models for Use with FlightGear," UIUC Applied Aerodynamics Group, Dept. of Aerospace Engineering, University of Illinois

at Urbana-Champaign, 22 02 2002. [Online]. Available: https://m-selig.ae.illinois.edu/apasim/Aircraft-uiuc/cessna172-v1/. [Accessed 06 02 2019].

[50] E. Cetin, *System Identification and Control of a Fixed-Wing Aircraft By Using Flight Data Obtained from X-Plane Flight Simulator,* Middle East Technical University, 2018.

[51] E. A. Morelli, "In-Flight System Identification," in *23rd Atmospheric Flight Mechanics Conference*, 1998.

[52] R. R. Tanner and T. D. Montgomery, "Stability and Control Derivative Estimates Obtained from Flight Data for the Beech 99 Aircraft," NASA, 1979.

[53] M. Marwaha, J. Valasek and P. Singla, "GLOMAP Approach for Nonlinear System Identification of Aircraft Dynamics Using Flight Data," in *AIAA Atmospheric Flight Mechanics Conference and Exhibit*, 2008.

[54] R. E. Maine and K. W. Iliff, "Formulation of a Practical Algorithm for Parameter Estimation with Process and Measurement Noise," in *6th Atmospheric Flight Mechanics Conference*, 1980.

[55] G. Welch and G. Bishop, *An Introduction to the Kalman Filter,* University of North Carolina at Chapel Hill - Department of Computer Science, 1997.

[56] C. Grillo and F. Montano, "An Extended Kalman Filter-Based Technique for On-Line Identification of Unmanned Aerial System Parameters," *Journal of Aerospace Technology and Management,* vol. 7, no. 3, 2015.

[57] J. Evans, G. Elkaim, S. Lo and B. Parkinson, "System Identification of an Autonomous Aircraft using GPS," in *Proceedings of the 10th International Technical Meeting of the Satellite Division of The Institute of Navigation (ION GPS 1997)*, 1997.

[58] G. Chowdhary and R. Jategaonkar, "Aerodynamic Parameter Estimation from Flight Data Applying Extended and Unscented Kalman Filter," in *AIAA Atmospheric Flight Mechanics Conference and Exhibit*, 2006.

[59] Y. Oshman and I. Shaviv, "Optimal Tuning of Kalman Filters Using Genetic Algorithms," in *AIAA Guidance, Navigation, and Control Conference*, 2000.

[60] Z. Chen, C. Heckman, S. Julier and N. Ahmed, "Weak in the NEES?: Auto-tuning Kalman Filters with Bayesian Optimization," in *21st International Conference on Information Fusion*, 2018.

[61] S. Mohan M, N. Naik, R. Gemson and M. Ananthasayanam, "Introduction to the Kalman Filter and Tuning its Statistics for Near Optimal Estimates and Cramer Rao Bound," Indian Institute of Technology Kanpur, 2015.

[62] A. Roudbari and F. Saghafi, "Intelligent Modeling and Identification of Aircraft Nonlinear Flight," *Chinese Journal of Aeronautics,* vol. 27, no. 4, 2014.

[63] A. Raue, C. Kreutz, T. Maiwald, J. Bachmann, M. Schilling, U. Klingmüller and J. Timmer, "Structural and Practical Identifiability Analysis of Partially Observed Dynamical Models by Exploiting the Profile Likelihood," *Bioinformatics,* vol. 25, no. 15, 2009.

[64] M. Anguelova, *Observability and identifiability of nonlinear systems with applications in biology,* Department of Mathematical Sciences and Division of Mathematics, Chalmers University of Technology and Göteborg University, 2007.

[65] W. L. Brogan, Modern Control Theory, Prentice-Hall, 1991.

[66] B. Southall, B. F. Buxton and J. A. Marchant, "Controllability and Observability: Tools for Kalman Filter Design," in *British Machine Vision Conference*, 1998.

[67] K. Zhen Yao, B. M. Shaw, B. Kou, K. B. McAuley and D. W. Bacon, "Modeling Ethylene/Butene Copolymerization with Multi-site Catalysts: Parameter Estimability and Experimental Design," *Polymer Reaction Engineering,* vol. 11, no. 3, pp. 563-588, 2003.

[68] W. M. Haddad and V. Chellaboina, Nonlinear Dynamical Systems and Control: A Lyapunov-based Approach, Princeton University Press, 2008.

[69] Z. Bartosiewicz, P. Bialostocka and W. Bialystok, "Local Observability of Nonlinear Systems," *Systems & Control Letters,* 1995.

[70] N. K. Gupta and E. W. J. Hall, "Input Design for Identification of Aircraft Stability and Control Derivatives," National Aeronautics and Space Administration, 1975.

[71] E. A. Morelli, "Flight Test Validation of Optimal Input Design and Comparison to Conventional Inputs," in *22nd Atmospheric Flight Mechanics Conference*, 1997.

[72] E. Plaetschke, J. A. Mulder and J. H. Breeman, "Flight Test Results of 5 Input Signals for Aircraft Parameter Identification," *IFAC Proceedings Volumes,* vol. 15, no. 4, pp. 1149-1154, 1982.

[73] J. Linder, *Indirect System Identification for Unknown Input Problems,* 2017.

[74] Appareo, *Appareo FDM Brochure,* Appareo, 2019.

[75] Cessna, *Information Manual - Skyhawk Model 172P,* Cessna, 1982.

[76] F. van Diggelen and P. Enge, "The World's first GPS MOOC and Worldwide Laboratory using Smartphones," in *Proceedings of the 28th International Technical Meeting of the Satellite Division of The Institute of Navigation (ION GNSS)*, 2015.

[77] A. Kos, S. Tomažič and A. Umek, "Evaluation of Smartphone Inertial Sensor Performance for Cross-Platform Mobile Applications," *Sensors,* vol. 16, no. 4, 2016.

[78] Z. Ma, Y. Qiao, B. Lee and E. Fallon, "Experimental Evaluation of Mobile Phone Sensors," in *24th IET Irish Signals and Systems Conference (ISSC 2013)*, 2013.